

UDC 691.328:624.012.3:
061.3(480.1)

Keywords:
precast concrete, elements,
joints, meetings, Nordic
countries

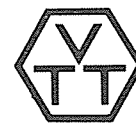
VTT SYMPOSIUM 62

**CONNECTIONS BETWEEN PRECAST
CONCRETE ELEMENTS**

Nordic seminar, Espoo, 12 March 1985

Edited by
Tapani Hakkarainen
Asko Sarja

Organized by the Technical Research Centre of Finland (VTT),
Concrete and Silicate Laboratory



VALTION TEKNILLINEN TUTKIMUSKESKUS
STATENS TEKNISKA FORSKNINGSCENTRAL
TECHNICAL RESEARCH CENTRE OF FINLAND
Espoo 1985

ISBN 951-38-2442-X

ISSN 0357-9387

Copyright © Valtion teknillinen tutkimuskeskus (VTT) 1985

JULKAISIJA – UTGIVARE – PUBLISHER

Valtion teknillinen tutkimuskeskus (VTT), Vuorimiehentie 5, 02150 Espoo
puh. vaihde (90) 4561, teleks 122972 vttha sf

Statens tekniska forskningscentral (VTT), Bergsmansvägen 5, 02150 Esbo
tel. växel (90) 4561, telex 122972 vttha sf


Technical Research Centre of Finland (VTT), Vuorimiehentie 5, SF-02150 Espoo, Finland
phone internat. + 358 0 4561, telex 122972 vttha sf

VTT, Betoni- ja silikaattiteknikan laboratorio, Betonimiehenkuja 5, 02150 Espoo
puh. vaihde (90) 4561

VTT, Betong- och silikattekniska laboratoriet, Betongblandargränden 5, 02150 Esbo
tel. växel (90) 4561

VTT, Concrete and Silicate Laboratory, Betonimiehenkuja 5, SF-02150 Espoo, Finland
phone internat. + 358 0 4561

VTT OFFSETPAINO, ESPOO 1985

Published by Technical Research Centre of Finland Vuorimiehentie 5 SF-02150 Espoo 15, Finland phone internat. + 358 0 4561 telex 122972 vttha sf		Name, number and report code of publication VTT Symposium 62 FI+VTTSYMP-85/62	
		Date November 1985	Project number 90212-0
Authors Hakkarainen, Tapani Sarja, Asko (Toim.)	Name of project Commissioned by		
Titel CONNECTIONS BETWEEN PRECAST CONCRETE ELEMENTS			
Abstract Nordic research cooperation entitled "Connection between precast concrete elements" has been under way over the last two years. The researchers and developers were asked to report their current research and development projects in a seminar held at the Technical Research Centre of Finland on the 12th Mars, 1985. The papers given in the seminar are presented in this publication.			
Activity unit Concrete and Silicate Laboratory, Betonimiehenkuja 5, SF-02150 Espoo, Finland			
ISSN and key name 0357-9387 VTT Symposium - Valtion teknillinen tutkimuskeskus			
ISBN 951-38-2442-X	Language English		
Class (UDC) 691.328:624.012.3: 061.3(480.1)	Key words precast concrete, elements, joints, meetings, Nordic countries		
Sold by Government Printing Centre P.O. Box 516 SF-00101 HELSINKI phone internat. +358 0 539011	Pages 170 p.	Price FIM 48	
Note			

compared to Rankweil, might depend on the higher cube strength, $f_{CC} = 40$ MPa in Luleå compared to $\beta_w = 25$ MPa in Rankweil. However, longer test periods are needed before any final conclusions can be drawn. The tests in Luleå and in Borås will therefore be carried on.

REFERENCES

1. Elfgrén, Lennart & Eriksson, Anders. Adhesive anchors, Progress report, June 1983. Borås 1983. National Swedish Testing Institute. Work report SP-A 83-14. 35 pp.
2. Granlund, Stig-Ola & Markström, Anders. Kemankare. Finit elementmodellering av last-deformations-egenskaper vid monotont ökande last. (In Swedish). Luleå 1984. Luleå University of Technology, Division of Structural Engineering, Skrift 84:04. 16 pp.
3. Helgevold, Håkan jr & Kirknes, Svein. Klebeanker i betong. Samband mellom laster og deformasjoner for forskjellige innlimingslengder. (In Norwegian). Luleå 1984. Luleå University of Technology, Division of Structural Engineering, Diploma work 1984:017E. 74 pp.
4. Formelsamling i hållfasthetslära. (In Swedish). Stockholm 1978. Kungliga Tekniska Högskolan, Institutionen för hållfasthetslära, Publikation nr 104. 379 pp.
5. Langzeitverhalten von HILTI-Verbundanker HVA M16, M8. (In German). Rankweil 1980. Höhere Technische Bundes-, Lehr- und Versuchsanstalt. 43 + 35 pp.
6. Longtime performance of HILTI HVA adhesive anchors, size M12. Rankweil 1978. Höhere Technische Bundes-, Lehr- und Versuchsanstalt. 30 pp.

FOREWORD

Construction with precast concrete elements is widely used and highly developed in the Nordic countries. Further development of quality and economy in industrialised prefabrication construction gives rise to a need for research and development of construction techniques. The development of connections is often highly necessary even for the development of mechanized production methods in element factories.

Nordic research cooperation entitled "Connections between precast concrete elements" has been under way over the last two years. The following institutes have taken part in the cooperation:

Chalmers University of Technology, Division of Concrete Structures, Sweden
Norwegian Precast Concrete Federation, Norway
Technical Research Centre of Finland, Finland.

The cooperation is organised by the leading group consisting of the following persons:

K. G. Bernander, Sweden, chairman
Björn Engström, Sweden, secretary
Asko Sarja, Finland
John Wilberg, Norway.

Many research scientists have taken part in the research projects in different countries.

The purpose of this seminar was to present and discuss the current aims and results of the cooperation in different countries. In addition, all other researchers and developers in research institutes and companies were asked to report their current research and development work. Discussions between participants were wanted in order to develop further the ideas of research and development projects.

English has been chosen as the main language of the seminar in order also to inform other countries of the Nordic research. In addition to English, the Scandinavian languages were also used in discussions and in some reports.

Asko Sarja
Professor
Technical Research Centre of Finland (VTT)
Concrete and Silicate Laboratory

CONTENTS	Page
FOREWORD	3
Stabilitet hos elementbygda stommar O. Krokstrand, Norway	5
Anslutningar av håldäckplattakonstruktioner A. Suikka, Finland	19
Diaphragm action in precast floor slabs - a pilot test series on precast hollow core slabs S. Svensson, Sweden	29
Resistance of locally damaged precast buildings - influence of the structural connections B. Engström, Sweden	41
Design of plain elastomeric bearing pads in precast concrete structures L. Vinje, Norway	60
Bolted beam-column connections for precast structures B. Engström, Sweden	71
Development of dry mechanical connections A. Sarja, Finland	88
Design of column corbels T. Hakkarainen, Finland	106
Column-to-base connection in a socket T. Hakkarainen, Finland	115
Adhesive anchors subjected to fatigue loading L. Elfgren et al., Sweden	124
Bæreevne af mørtelfuger mellem betonsøjjelementer H. Larsen, Danmark	138
Behaviour of mounted concrete corbels E. Thorenfeldt, Norway	147
Time-dependent deformations of adhesive anchors S.-O. Granlund, Sweden	163

From the longtime tests made in Luleå and others made at Höhere Technische Bundes-, Lehr- und Versuchsanstalt, Rankweil [5], [6], Austria, these parameters for adhesive anchors can be approximately evaluated. The strain velocity $\dot{\epsilon}$ [1/h] has been replaced with the displacement velocity $\dot{\delta}$ [m/h].

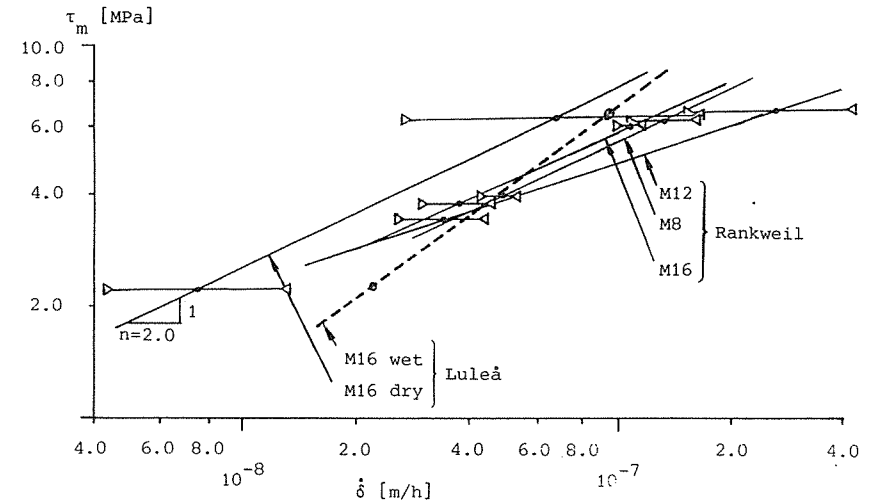


Figure 7. Relationship between the average shear stress τ_m and the displacement velocity $\dot{\delta}$.

The curves gives a similar gradient, $n = 2.0 - 2.2$, except M12 tested in Rankweil where $n = 3.0$. A rough expression for the time-dependent displacements can then be written as follows, $\bar{n} = 2.3$

$$\dot{\delta} = k\tau_m^{2.3}$$

The somewhat lower velocity in Luleå (except for wet samples),

Any obvious difference between the in- or outdoor placed adhesive anchors can not be seen. Water around the anchors, have however an accelerating effect on the displacements. The measured displacements are small for the load level 15 kN which corresponds to the permitted load for short time loading. The failure load for short time tests is approximately four time as high i.e. about 60 - 65 kN.

DISCUSSION

It is of great importance to know the time-depending displacements for different stress levels. For metals these are often modelled with Nortons creep function

$$\dot{\epsilon} = \frac{\dot{\sigma}}{E} + k \sigma^n$$

The creep term can here also be written as

$$\dot{\epsilon}_c = \frac{1}{\tau} \left(\frac{\sigma}{\sigma_c} \right)^n$$

where τ is a time parameter, usually 10^7 [h]. The material parameter σ_c is often mentioned as the creep limit. In material tables σ_c and n for various materials can be found. For adhesive anchors no such figures are available. The figure below shows how different temperatures effect the stress-strain velocity relationship for a metal.

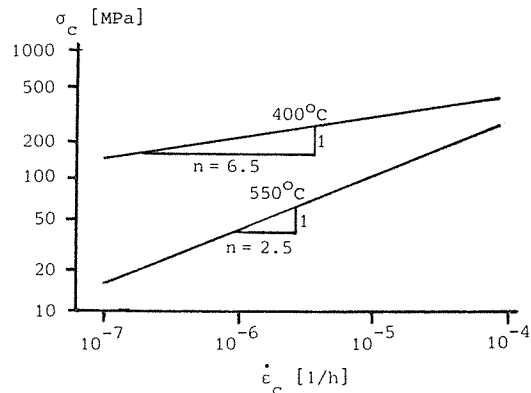


Figure 6. Stress-strain velocity curves for a metal (steel SIS 1330) according to data from [4].

STABILITET HOS ELEMENTBYGDA STOMMAR

Ole H. Krokstrand
ØSTLANDSKE SPENNBETONG A/S
Hønefoss, Norge

ABSTRACT

The paper outlines a method for load distribution to shear walls of various stiffness. It also gives an example on how to design a multy-story shear wall from precast concrete elements.

1 VERTIKALE SKIVER

Horisontale krefter blir overført til hver vertikal veggskive i henhold til veggens skjær og bøyestivhet.

De vertikale skiver kan bestå av:

- Enkeltstående veggelementer
- Sammensatte veggelementer
- Sjakter
- Stive rammer

1.1 Lastfordeling

For enkle bygg med symmetrisk plasserte veggskiver med lik stivhet er lastfordelingen også enkel.

Ofte er imidlertid veggskivene plassert usymmetrisk i forhold til horisontalkreftene og har ulik stivhet.

Dette må tas hensyn til for beregning av de enkelte skiver.

Vi skal her forsøke å gi en fremgangsmåte for en slik lastfordeling /1, 2, 3/:

1.2 Definisjoner

$$V_i = Q \frac{K_i}{\sum K} = \text{Last overført til veggskive "i"}$$

$$K_i = \text{Stivhet av vegg "i"} \quad \frac{1}{K_i} = \frac{1}{K_{si}} + \frac{1}{K_{bi}}$$

$\sum K$ = sum av stivheter av alle veggskiver som motstår horisontalbelastningen på dekkenivået under betraktning

Q = totale vindkrefter som opptrer i samme retning på dekkenivået under betraktning

K_{si} = skjærstivhet i vegg "i"
(Varierer i forhold til lastsituasjon.
Se tabell i fig 1.)

K_{bi} = bøyestivhet i vegg "i"
(Varierer etter lastsituasjon.
Se tabell i fig 1.)

Lasttilfelle		Stivhetstall	
		K _{bi}	K _{si}
1		$\frac{3E_i I_i}{h^3}$	$\frac{A_i E_i}{3h}$ *)
2		$\frac{8E_i I_i}{h^3}$	$\frac{A_i E_i}{1.5h}$ *)
3		$\frac{60E_i I_i}{11h^3}$	$\frac{A_i E_i}{2h}$ *)
4		$\frac{12E_i I_i}{h^3}$	$\frac{A_i E_i}{3h}$ *)

*) G_i = 0,4 E_i

Fig. 1. Stivhetstall for forskjellige lasttilfeller.

K_{xi} = stivhet av vegg i x-retning (se fig.2 og 3)

K_{yi} = stivhet av vegg i y-retning (se fig. 2 og 3)

Displacement

In the figures below the displacements for the adhesive anchors are shown at different load levels and environments. An increase in the load level from 15 kN to 45 kN gives an increase of the displacement.

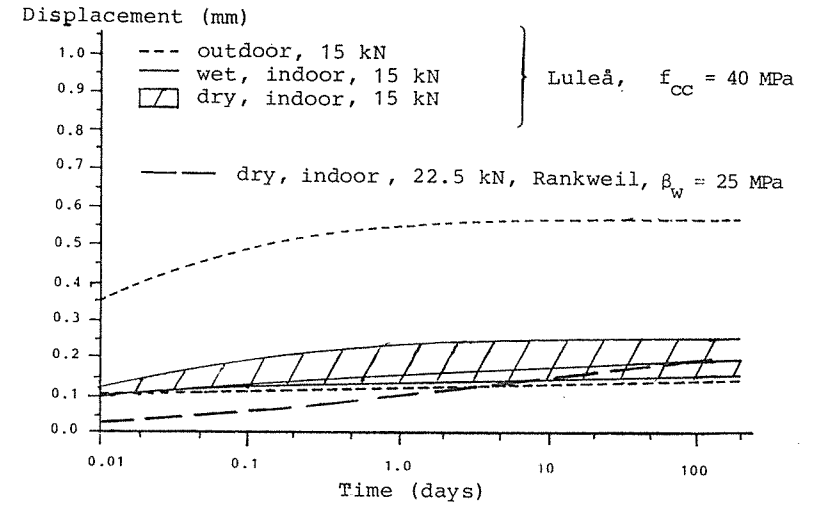


Figure 4. Time-displacement curves for adhesive anchors, at a loading level of 15 and 22.5 kN.

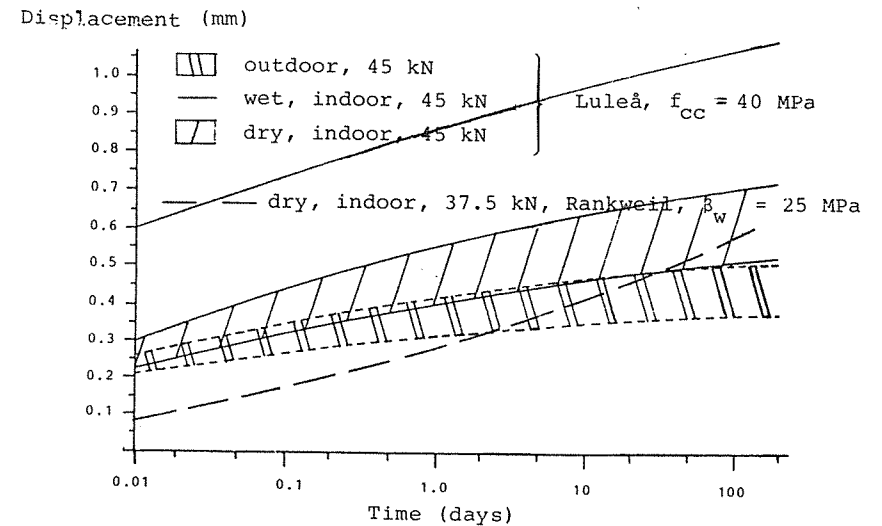


Figure 5. Time-displacement curves for adhesive anchors, at a loading level of 37.5 and 45 kN.

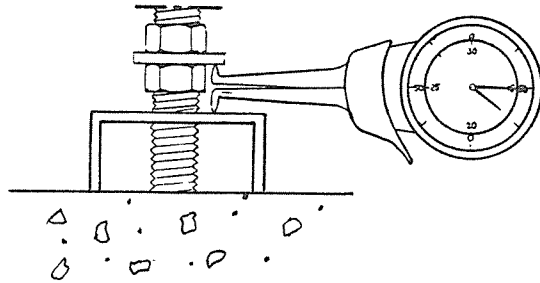


Figure 2. Displacement meter.

RESULTS

Failure

At one occasion failure occurred. This happened soon after loading (5 min). It was probably caused by a far too long mixing with the rotary hammer-drill. By turning too long the glue gets warm and the curing starts. If the turning goes on there will be failure in these parts, see Figure 3.

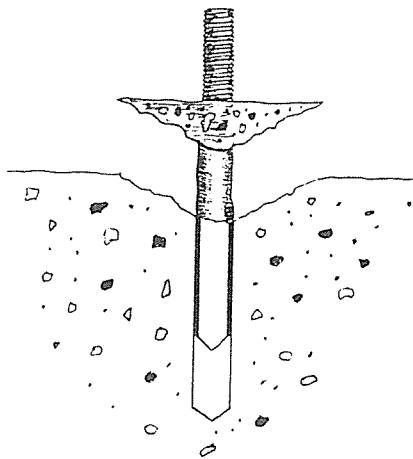


Figure 3. Failure of an adhesive anchor loaded with 45 kN.

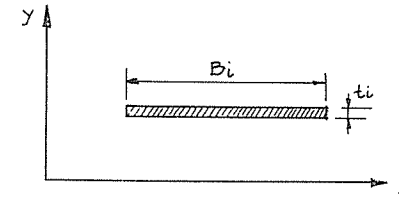


Fig. 2. Vegg parallell med X-aksen.
 Stivhet i X-retning = K_{xi}
 Stivhet i Y-retning = $K_{yi} = 0$

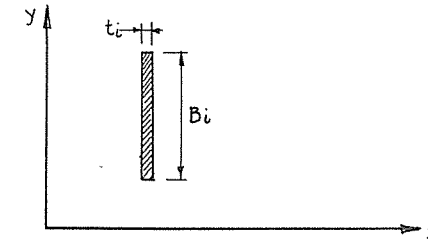


Fig. 3. Vegg parallell med Y-aksen.
 Stivhet i X-retning = $K_{xi} = 0$
 Stivhet i Y-retning = K_{yi}

G_i = skjærmodul av vegg "i" = 0,4 E for betong

A_i = arealet av vegg "i" som motstår belastningen
 (i lastens retning)
 (kun arealet av "steget") (= $B_i \cdot t_i$)

E_i = elastisitetsmodulen for vegg "i"

I_i = treghetsmomentet for vegg "i"

h = høyde på veggsegment under betraktning

1.3 Kombinert stivhet

Ovenfor viste vi at for en vegg er stivheten av vegg
avhengig av både veggens bøyestivhet og skjærstivhet
slik at

$$\frac{1}{K_i} = \frac{1}{K_{si}} + \frac{1}{K_{bi}} \quad (1)$$

Dette uttrykket (1) fremkommer fra formelen:

$$\Delta t = \Delta b + \Delta s \quad (2)$$

der Δb er utbøyning fra bøyestivheten og
 Δs utbøyning fra skjærstivheten.

For en utkraget vegg i fig. 4 er:

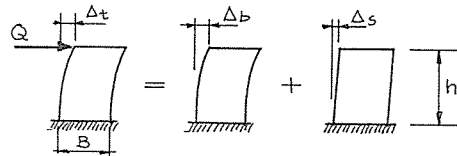


Fig. 4 Kombinert stivhet

$$\begin{aligned} \Delta t &= \frac{Qh^3}{3EI} + \frac{Q \cdot 3 \cdot h}{A \cdot E} \\ &= \left(\frac{h^3}{3I} + \frac{3h}{A} \right) \frac{Q}{E} \end{aligned} \quad (3)$$

$$I = \frac{B^3 \cdot t}{12} \quad A = B \cdot t$$

$$\Delta t = \left(\frac{h^3 \cdot 12}{B^3 \cdot 3} + \frac{3h}{B} \right) \frac{Q}{E \cdot t} \quad (4)$$

$$\frac{1}{K} = \left(4 \frac{h^3}{B^3} + \frac{3h}{B} \right) \frac{1}{E \cdot t} \quad (5)$$

Tilsvarende blir lastutbøyningen for en skive med jevnt
fordelt last:

$$\Delta t = \frac{Q \cdot h^3}{8EI} + \frac{Q \cdot 1,5h}{AE} \quad (6)$$

$$\frac{1}{K} = \left(\frac{h^3 \cdot 3}{2 \cdot B^3} + \frac{1,5h}{B} \right) \frac{1}{E \cdot t} \quad (7)$$

Specimens

The concrete samples are made of standard ready mixed
concrete K20T, with a maximum gravel-size of 16 mm. After
150 days it's concrete strength f_{cc} was 40 MPa (determined
on 150 mm cubes) and it's tension strength f_{ct} was 3.5 MPa.

In order to have adhesive anchors situated in an unaffected
area, the top 200 mm of the concrete sample is reinforced
only at the edges. How different environments affect the
displacements are studied by having different testing
conditions, according to Table 1.

Table 1. Load [kN] and number of samples in different
environments.

Load level [kN]	Indoors		Outdoors
	dry	wet	
15	2	1	2
45	3	1	2

Test process

The adhesive anchors of the mark HILTI are mounted
according to the manufacturers recommendations. In a
predrilled, well cleaned, borehole the glassphial
containing a two-component glue, is inserted. The steel
rod is attached to a rotary hammer drill, the ampoule is
crushed, the components are mixed and the curing starts.
The steel rod is rotated until it has reached the bottom
of the hole. After one day of curing the specimens were
loaded. The arisen displacements were mechanically
measured with a thickness gauge type INTERTEST, see
Figure 2.

TEST PROGRAM

General

The long-time behaviour is studied in corporation with the National Swedish Testing Institute in Borås and it is supported by the Swedish Council for Building Research.

To get an apprehension of the influence of the surrounding environment on the displacement and the strength, anchors are placed indoors and outdoors, under dry and wet conditions.

Test set up

A constant load on the adhesive anchors is applied with concrete weights, see Figure 1. With a lever arm the load from the weight is transferred to a force in the anchor. It is possible to check the load by attaching a load-cell to the anchor at the end of the steel rod. It can be interesting to see if the load has decreased due to rust.

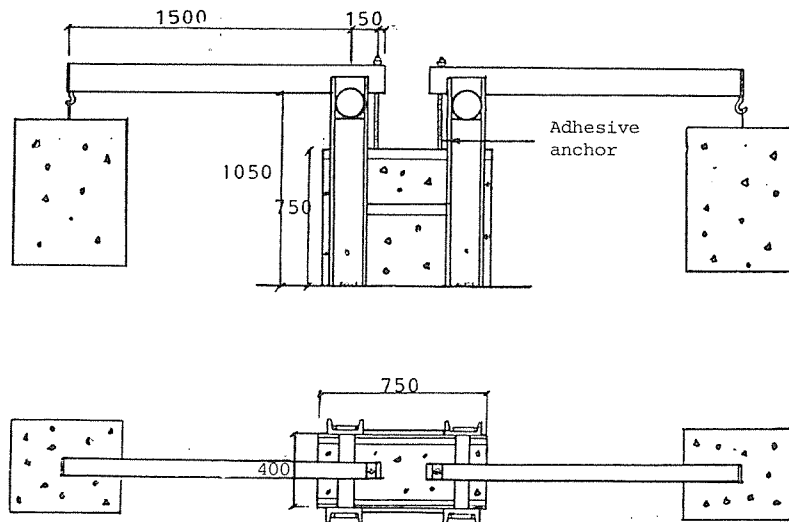


Figure 1. Test set-up.

1.4 Fordeling av krefter til vegger av forskjellig stivhet

Fordelingen av krefter til veggene utføres på samme måte som for en bolte- eller sveisegruppe:

Først finnes veggens nøytralakse i henholdsvis x- og y-retning således:

$$\text{Plassering av x-akse : } \bar{y} = \frac{\Sigma(K_x \cdot y)}{\Sigma K_x}$$

$$\text{Plassering av y-akse : } \bar{x} = \frac{\Sigma(K_y \cdot x)}{\Sigma K_y}$$

Krysningspunktet av de to akser kalles stivhetssenteret.

Nå kan kreftene fordeles i forhold til innbyrdes stivhet som følger: (Det forutsettes at veggene kun kan oppta krefter i veggens lengderetning)

$$V_{iy} = \div Q_y \frac{K_{yi}}{\Sigma K_y} + M_T \frac{K_{yi} \cdot x_i}{\Sigma(K_x \cdot y^2) + \Sigma(K_y \cdot x^2)} \quad (8)$$

$$V_{ix} = \div Q_x \frac{K_{xi}}{\Sigma K_x} + M_T \frac{K_{xi} \cdot y_i}{\Sigma(K_x \cdot y^2) + \Sigma(K_y \cdot x^2)} \quad (9)$$

x_i = avstand fra y-akse til veggskive "i" målt perpendikulært på veggens plan (husk fortegn)

y_i = avstand fra x-akse til veggskive "i" målt perpendikulært på veggens plan (husk fortegn)

M_T = påført vridningsmoment (positiv mot urviserns retning)

I Fig. 5 blir kraftfordelingen i veggene 1 og 2 som følger:

Kraft i vegg 1:

$$V_{1y} = \div Q_y \frac{K_{y1}}{\Sigma K_y} + M_T \frac{K_{y1} \cdot x_1}{\Sigma(K_x \cdot y^2) + \Sigma(K_y \cdot x^2)} \quad (10)$$

Kraft i vegg 2:

$$V_{2x} = \div Q_x \frac{K_{x2}}{\Sigma K_x} + M_T \frac{K_{x2} \cdot y_2}{\Sigma(K_x \cdot y^2) + \Sigma(K_y \cdot x^2)} \quad (11)$$

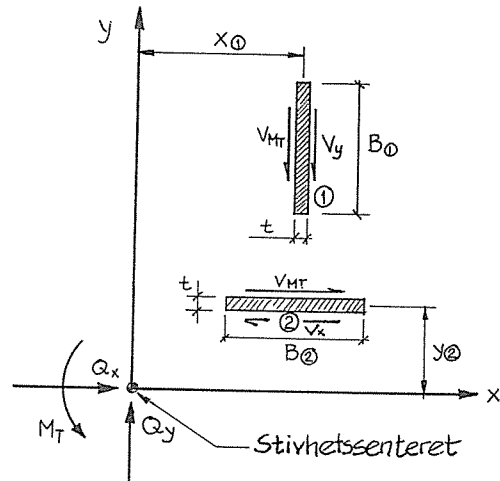


Fig. 5. Usymmetriske veggskiver (Kun to enkeltskiver er vist.)
 V_y = Kraft i vegg 1 fra Q_y
 V_{MT} = Kraft i vegger fra momentet M_T

For bygninger med rektangulære veggskiver og med høyde/lengde forhold mindre enn 0,3, kan bøyestivheten neglisjeres, og fordelingen kan således gjøres i forhold til veggens "stegtverrsnitt" A_i .

Dersom høyde/lengde er større enn 3, kan skjærstivheten neglisjeres, og fordelingen kan gjøres i henhold til treghetsmomentene.

(En tilsvarende analyse kan foretas der søyler og vegger virker sammen. Imidlertid er søylenes stivhet vanligvis svært liten i forhold til veggens, så søylene kan følgelig neglisjeres i denne sammenheng.)

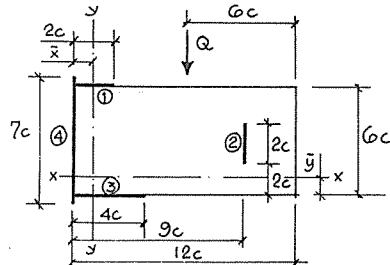


Fig. 6. Grunnplan i eksempelberäkning.

TIME-DEPENDENT DEFORMATIONS OF ADHESIVE ANCHORS

Stig-Ola Granlund
 Division of Structural Engineering
 Luleå University of Technology
 S-951 87 Luleå, Sweden

INTRODUCTION

The building industry today is using more and more anchors and other fixings. This is especially true for the sector that is repairing, rebuilding and renovating houses.

There are many types of anchors and fastenings, for example [1]:

- Anchor bolts embedded in concrete
- Anchor bolts grouted in recesses or drilled holes
- Expansion anchors
- Adhesive anchors

Adhesive anchors can be especially advantageous when an embedded anchor bolt has been placed in the wrong position and has to be replaced quickly. It is easy to install an adhesive anchor and it has a simple design. This makes it economically advantageous especially at larger dimensions.

In its country of origin, West Germany, adhesive anchors have been on the market for about 20 years. In spite of this, very few tests of the longtime behaviour have been performed. This has caused the building authorities to be somewhat restrictive in their admission of the use of adhesive anchors. Therefore it is of great interest to perform such tests, to determine its longtime behaviour. At Luleå University of Technology a project regarding adhesive anchors is carried out. It includes different types of tests as well as analytical modelling [2, 3].

Plane surface with cement paste

Specimen 1.4 was the only one which failed at a low load. A sudden deflection of 4 mm is not acceptable. The necessary friction coefficient at failure expressed by the ratio $P/(F_1+F_2)$ was approximately 0.65-0.85. This is what can be expected for smooth concrete/concrete friction without bond. Perhaps was the cement paste used not suitable for the purpose.

DESIGN SOLUTION

Choice of detailing for practical design will mainly be decided by further consideration of the practical problems in the production.

Several of the tested types seems to have sufficient strength for practical use.

REFERENCE

Muri, Terje & Eiterstraum, Ase Corbels with epoxy joint.
 Dragsholt, Geir & Myhre, Rune Corbels with indented joint.
 Trondheim, Norwegian University of Technology, Division for Concrete Structures (in Norwegian).

1.4.1 Eksempel

Dersom $0,3 < h/l < 3$, må vi fordele kreftene etter den kombinerte stivhet. (Vi antar utkraget skive med last i høyde h) Vi benytter grunnplanen i fig. 6 og setter $h = 2c$. Betongkvalitet = C45.

$$E = 5000 \cdot \sqrt{f_c} = 5000 \cdot \sqrt{45} = 33500$$

Fra avsnitt 1.2 ser vi at:

$$K_{si} = \text{skjærstivhet} = \frac{E_i \cdot A_i}{3 \cdot h} = \frac{33500 \cdot A_i}{3 \cdot 2c}$$

$$K_{si} = 5600 A_i/c$$

$$K_{bi} = \text{bøystivhet} = \frac{3 \cdot E_i \cdot I_i}{h^3} = \frac{3 \cdot 33500 \cdot I_i}{(2c)^3}$$

(Hvis vi antar at E er den samme for alle veggskiver, kan den settes lik 1)

$$K_{bi} = 12560 I_i/c^3$$

$$\frac{1}{K} = \frac{1}{K_s} + \frac{1}{K_b}$$

K_x :

Vegg nr.	A_x	I_{yy}	K_{sx}	K_{bx}	K_x
1	2c	0,67 c ³	11200	8375	4790
2	0	0	0	0	0
3	4c	5,33 c ³	22400	66990	16800
4	0	0	0	0	0

$$\sum K_x = 21600$$

K_y :

Vegg nr.	A_y	I_{xx}	K_{sy}	K_{by}	K_y
1	0	0	0	0	0
2	2c	0,67 c ³	11200	8375	4790
3	0	0	0	0	0
4	7c	28,58 c ³	39200	359000	35460

$$\sum K_y = 40250$$

Akseptlassering:

$$\bar{x} = \frac{\sum(K_{yi} \cdot xi)}{\sum K_y} = \frac{K_y(2) \cdot 9c + K_y(4) \cdot 0}{\sum K_y}$$

$$= \frac{4790 \cdot 9c + 0}{40250} = \underline{1,07 \text{ c}}$$

$$\bar{y} = \frac{\sum(K_{xi} \cdot yi)}{\sum K_x}$$

$$= \frac{4790 \cdot 6c + 0}{21600} = \underline{1,33 \text{ c}}$$

$$M_T = \div Qe = \div Q(6 - 1,07)c = \underline{\div 4,93 \text{ Qc}}$$

$$V_i = \div Q \cdot \frac{K_i}{\sum K} \pm \frac{M_T \cdot a_i \cdot k_i}{\sum(K \cdot a^2)}$$

Vegg	K	a	Ka	Ka ²
1	4790	4,67 c	22370 c	104470 c ²
2	4790	7,93 c	37895 c	301220 c ²
3	16806	-1,33 c	-22352 c	29370 c ²
4	35460	-1,07 c	-37942 c	40600 c ²

$$\sum Ka^2 = 476020 \text{ c}^2$$

$$V_{1x} = 0 + \frac{(\div 4,93 \cdot Qc) \cdot 22370c}{476020 \cdot c^2} = \underline{\div 0,23 \text{ Q}}$$

$$V_{2y} = \div \frac{(-Q) \cdot 4790}{40250} \div \frac{(\div 4,93Qc) \cdot 37895 \text{ c}}{476020 \text{ c}^2} = \underline{0,51 \text{ Q}}$$

$$V_{3x} = 0 + \frac{(\div 4,93Qc) \cdot (-22352c)}{476020 \cdot c^2} = \underline{+ 0,23 \text{ Q}}$$

$$V_{4y} = \frac{(-Q) \cdot 35460}{40250} - \frac{(-4,93Qc) \cdot (-37942c)}{476020 \cdot c^2} = \underline{+ 0,49 \text{ Q}}$$

Prestressing

Prestressing of the steel bolts reduces deflection and opening of vertical cracks, but have little influence on the failure load:

$$P_{f1.2}/P_{f1.3} = 0.331/0.315 = 1.05$$

High prestress will reduce the necessary friction coefficient or direct shearing strength of the contact surface especially when the load acts close to the column face. The amount of effective prestress is however uncertain because creep and shrinkage etc. may lead to considerable loss of prestressing in short bolts.

Indentation.

Indentation with 5 teeth and with epoxy on the compression faces has approx the same strength as fully glued plane surface:

$$P_{f2.3}/P_{f1.3} = 0.313/0.315 = 0.99$$

Dry mounting with 5 teeth reduced strength only slightly:

$$P_{f2.4}/P_{f2.3} = 0.307/0.313 = 0.98$$

Indentation with 2 teeth was less effective:

Compared to plane surface with epoxy:

$$P_{f2.1}/P_{f.1.1} = 0.258/0.271 = 0.95$$

$$P_{f2.2}/P_{f1.2} = 0.306/0.331 = 0.92$$

Compared to indented surface with 5 teeth, dry surface:

$$P_{f2.5}/P_{f2.4} = 0.253/0.307 = 0,82.$$

The effectiveness of a simple 20 mm recess with epoxy on the edge of the recess was the same as found for two teeth with epoxy:

$$P_{f1.5}/P_{f2.2} = 0.307/0.306 = 1.00$$

4 DISCUSSION

The following more detailed comparison between the different types of corbels is often based on single results.

The conclusions are therefore only indicative.

The maximum bearing strength of concrete corbels failing without yielding of the reinforcement is commonly described by the simplified formula:

$$p_f = P_f / f'_c w d = 0.3$$

The results seem to confirm that the strength of mounted corbels with plane contact surface glued with epoxy resin is approximately the same as corbels cast together with the column.

Epoxy resin has unfortunately very low resistance against high temperatures. A reserve strength is therefore necessary to cope with fire conditions.

Concrete strength

Bearing strength increases with concrete strength, but not proportional to the cylinder strength.:

$$P_{f1.1} / P_{f1.2} = 0.271 / 0.331 = 0.82$$

$$P_{f2.1} / P_{f2.2} = 0.258 / 0.306 = 0.84$$

$$P_{f1.6} / P_{f1.5} = 0.236 / 0.307 = 0.77$$

$$P_{f2.6} / P_{f2.5} = 0.217 / 0.253 = 0.85$$

The last two ratios are also influenced by stress concentration on the lower edge of the recess (series 1) or on the two concrete teeth with dry contact surface (series 2).

1.5 Sammensatte skiver

En veggskive er mest effektiv dersom flere betong-elementer sammenkoples. P.g.a. problemer med temperatursvingninger, svinn og kryp er det likevel ønskelig å kople færrest mulig slike elementer. Sammenkopling av vegger for å danne "T" eller "L"-vegger, øker bøyestivheten, men gjør lite for skjærstivheten.

Ved beregning av sammensatte veggskivers bøyestivhet kan effektiv flensbredde settes som vist i fig.7.

B' er minste verdi av 8 t eller 1/10 av høyden fra nivået under betraktning til topp av veggskive. /1/

Sammenkopling av hjørneelementer i bokskonstruksjoner kan ofte vise seg å være nødvendig for å sikre stabiliteten på slike bygg.

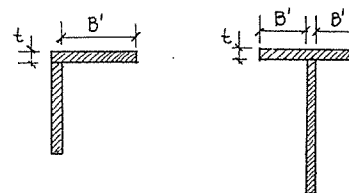


Fig. 7. Begrensninger for "T" og "L"-tverrsnitt.

1.5.1 Skjær i fuger

Skjærkapasiteten i utstøpte fuger kan beregnes etter uttrykket /5/:

$$V_d = v \cdot t' \cdot d$$

t' = fugestøpens bredde

$$v = v_c + \mu (\varphi f_s + \sigma_n)$$

Dersom $(\varphi f_s + \sigma_n) < 0,02 f_c$ blir:

$$v = \left(\frac{\varphi f_s + \sigma_n}{0,02 f_c} \right) (v_c + \mu \cdot 0,02 f_c)$$

Dersom $(\varphi f_s + \sigma_n) > 0,30 f_c$ er:

$$v = v_c + \mu \cdot 0,30 f_c$$

f_c = betongens dimensjonerende fasthet

f_s = armeringens dimensjonerende fasthet

$v_c = 0,06 f_c$ for fortannede eller ru fuger

= 0 for glatte fuger

μ = Friksjonskoeffisient

= 0,9 for fortannede fuger

= 0,7 for en ru fuge

= 0,5 for en glatt fuge

$$\varphi = \frac{A_s}{A_c}$$

A_s = Tverrsnittsareal av armeringen som krysser fugen over fugens utstrekning forutsatt at armeringen er tilstrekkelig forankret på begge sider av fugen.

A_c = Tverrsnittsareal av betongfugen

σ_n = trykkspenning i fugens trykksone dersom fugen er under påvirkning av trykkrefter ($\sigma_n = N_y/A_c$). Ellers settes $\sigma_n = 0$

For fortannede fuger regnes kun tannarealet ved beregning av $\varphi \cdot \sigma_n$ og v .

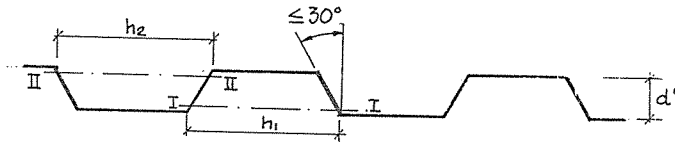


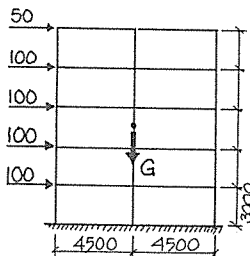
Fig. 8. Fortannet fuger.

En betongfuge kan regnes fortannet når tannhelningen er mindre eller lik 30° , og tanndybden $d' \geq 10$ mm. Tannarealet er definert som tverrsnittsarealet av tenner på samme side av fugen i et snitt parallelt med denne.

Snittet kan plasseres ved roten av de tenner som ønskes undersøkt. Tannarealet av tennene under fugen i fig. 8 er således tverrsnittsarealet av snitt I-I, mens arealet av tennene over fugen er tverrsnittareal av snitt II-II. Den effektive tannlengde h_1 eller h_2 kan ikke settes større enn $8d'$.

Fugen kan regnes ru når ruheten forekommer over hele flaten. Dybden skal være større enn 3 mm. Støpeflater støpt mot fornsider kan ikke regnes ru.

1.6 Eksempel



En veggskive er sammensatt av veggelementer på $4500 \times 3000 \times 180$ mm som vist i fig.9. Ved hver etasje virker en horisontal bruddlast på 100 kN. Ved taket en last 50 kN.

Fig. 9. Sammensatt skive.

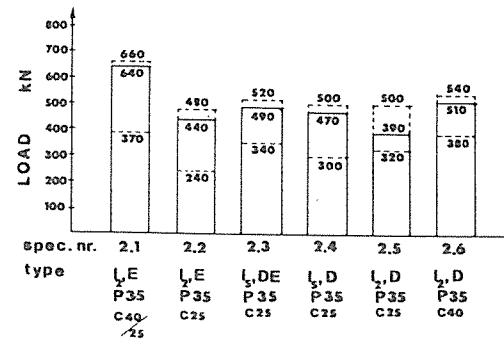
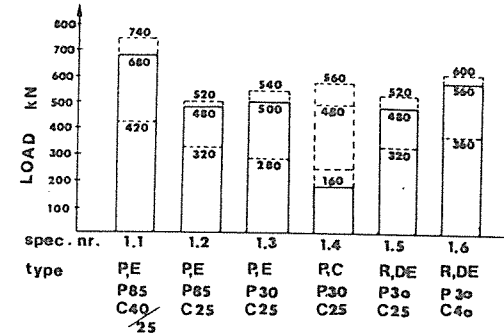


Figure 8. Charateristic load levels.

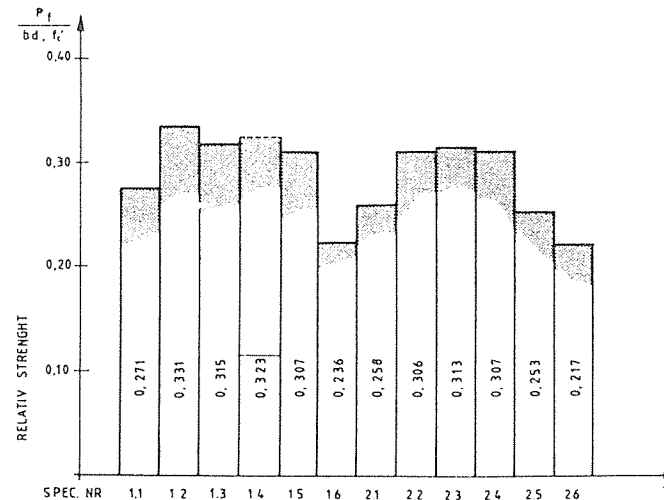


Figure 9. Relative strength p_f

Table 3. Characteristic load levels and relative strength.
SERIES 1

Number	1.1	1.2	1.3	1.4	1.5	1.6
Type	P, E P85 C40/25	P, E P85 C25	P, E P30 C25	P, C P30 C25	R, DE P30 C25	R, DE P30 C40
Max applied load P_u (kN)	740	500	540	560	520	600
Diagon. cracking load P_{cr} (kN)	420	320	280	240	320	360
Failure load P_f (kN)	680	480	500	(160) (500)	480	560
Relative failure strength $p_f = P_f/wd_1f'_c$	0,271	0,331	0,315	(0,323)	0,307	0,236

SERIES 2

Number	2.1	2.2	2.3	2.4	2.5	2.6
Type	I ₂ , E	I ₂ , E	I ₅ , DE	I ₅ , D	I ₂ , D	I ₂ , D
(All: P35)	C40/25	C25	C25	C25	C25	C40
Max applied load P_u (kN)	660	480	520	500	500	540
Diagon. cracking load P_{cr} (kN)	370	240	340	300	320	380
Failure load P_f (kN)	640	440	490	470	390	510
Relative failure strength $p_f = P_f/wd_1f'_c$	0,258	0,306	0,313	0,307	0,253	0,217

1.6.1 Dimensjonering av forankringer i bunnelementene (Fig. 10)

For disse vedkommende er

$$V_y = 4 \cdot 100 + 50 = 450 \text{ KN}$$

$$M_y = 100(3+6+9+12)+50 \cdot 15 = 3750 \text{ KNm}$$

$$N_y = G = 15 \cdot 0,18 \cdot 25 = 608 \text{ KN}$$

$$e = M_y/N_y = \frac{3750}{608} = 6,2 > 4,5$$

Må ha ekstra forankring:

Vi tar momentlikevekt om T:

$$M_y = S \cdot 8,4 + N_y \cdot 4,2$$

$$S = \frac{3750 - 608 \cdot 4,2}{8,4} = 142 \text{ KN}$$

Dersom vi benytter forankringsbolt i 8,8 kvalitet er $f_s = 556 \text{ MPa}$
Nødvendig $A_s = 142/0,556 = 256 \text{ mm}^2$
Benytt M24 bolt ($A_s = 353 \text{ mm}^2$)
Se fig. 14.

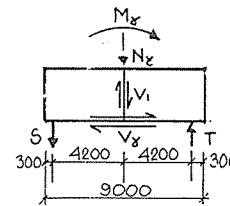


Fig. 10. Bunnelementer.

1.6.2 Kontroll av betongtrykket

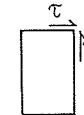
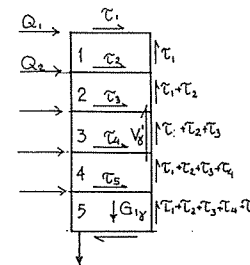
$$a = 300 \cdot 2 = 600$$

$$\sigma_m = \frac{N_y}{l \cdot a} \quad (t' = \text{betongfugens bredde} = 180-30=150 \text{ mm})$$

$$= \frac{608 \cdot 10^3}{150 \cdot 0,6 \cdot 10^3} = 6,75 < 12 \text{ MPa (C25 betong)}$$

1.6.3 Vertikal fuge (Fig. 11)

For et skivelement er skjærstrømmen langs ytterkantene like stor.



$$\text{Således er } \tau_1 = \frac{Q_1}{z} = \frac{50}{8,4} = 5,95 \text{ kN/m}$$

$$\tau_2 = \tau_3 = \tau_4 = \tau_5 = \frac{Q_2}{z} = \frac{100}{8,4} = 11,91 \text{ kN/m}$$

Fig. 11. Skjærstrøm på venstre skivelementer.

Skjær i vertikal fuge = $\Sigma \tau \cdot h$

Skjær i fuge i element nr. 5	= (5,95 + 4 · 11,91) · 3 = 161 kN
" " " " " " 4	= (5,95 + 3 · 11,91) · 3 = 125 kN
" " " " " " 3	= (5,95 + 2 · 11,91) · 3 = 89 kN
" " " " " " 2	= (5,95 + 11,91) · 3 = 54 kN
" " " " " " 1	= (5,95) · 3 = 17 kN

TOTALT $V_y' = 446$ kN

Kontroll: $S_y + G_y = 142 + 304 = 446$ kN

Vi dimensjonerer skjærforbindelsene i element 5 og 4 for 161 kN.

Dersom vi benytter sveiseforbindelser tilsvarer dette $161/0,48 = 335$, si 400 mm sveis

De resterende elementer gis en skjærforbindelse med kapasitet tilstrekkelig for å oppta 89 kN.

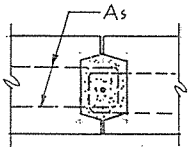


Fig. 12. Utstøpt fuge.

Dersom en velger å benytte en armert vertikalfuge (Fig. 12) istedet for sveisefester, - har fugen en skjærkapasitet tilsvarende av verdiene nedenfor: (Se avsn. 1.5, $\sigma_n = ()$)

$$\text{For } 0,02 f_c \leq \frac{A_s f_s}{h \cdot t'} \leq 0,3 f_c: V_{d1} = h t' \cdot v_c + \mu A_s f_s$$

$$\text{For } \frac{A_s f_s}{h t'} < 0,02 f_c: V_{d2} = (v_c + \mu \cdot 0,02 f_c) \frac{A_s f_s}{0,02 f_c}$$

$$\text{For } \frac{A_s f_s}{h t'} > 0,3 f_c: V_{d3} = h t' (v_c + \mu \cdot 0,3 f_c)$$

1.6.4 Horizontal fuge (Fig. 13)

Vi forutsetter en ru fuge.

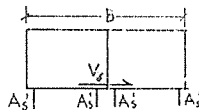


Fig. 13. Horizontal fuge.

Det er naturlig å gi hvert veggelement min. to forankringer. Disse gjøres like store. I vårt tilfelle er således det totale stålareal på tvers av fugen:

$$A_s = 4 A_s' = 4 \cdot 353 = 1412 \text{ mm}^2$$

$$f_s = 556 \text{ MPa}$$

$$\sigma_n = \frac{608 \cdot 10^3}{9000 \cdot 150} = 0,45 \text{ MPa}$$

$$f_c = 15/1,4 = 10,7 \text{ MPa} \quad (f_{cn}/\gamma_m)$$

$$\rho = \frac{A_s}{A_c} = \frac{1412}{B \cdot t'} = \frac{1412}{9000 \cdot 150} = 1,05 \times 10^{-3}$$

Typical crack patterns are shown in figure 6. Also the location of the crushing concrete zones are depicted.

Figure 7 shows typical development of tension in the steel bolts with increasing load. F_1 resp. F_2 is the sum of forces in two bolts at the same level.

In fig. 7 a) bolt forces in specimen 1.2 and 1.3 with different prestressing are compared.

Specimen 2.5 was loaded beyond the load-level where crushing of concrete occurred locally in the two concrete teeth. The reduced increase and slight reduction of forces in the lower pair of bolts is probably the result of the increasing compression zone in the corbel and transmission of shear forces by dowel action in the bolts.

3.2 Bearing strength

Observed bearing strength of the corbels are summarized i table 3.

Failure load was difficult to define exactly. It was usually associated with severe crushing of concrete and deflection of the corbel at the load axis about 3 - 4 mm. (P_f) Failure was also defined if the increase in observed bolt-forces was significantly reduced. (See figure 7 b)

The bearing strength was normally not fully exhausted at the defined failure load. This is mainly due to the dowel action of the high strength, large diameter bolts. Testing was terminated when dowel action was obvious. (P_u)

In addition to the failure load (P_f) and the maximum load at termination of the test (P_u), also the load at diagonal cracking (P_{cr}) is included in table 3.

The failure load is mainly dependent on the concrete strength. The relative failure strength $p_f = P_f / w d_1 f'_c$ is therefore included in the table. (w = width, d_1 = effective height)

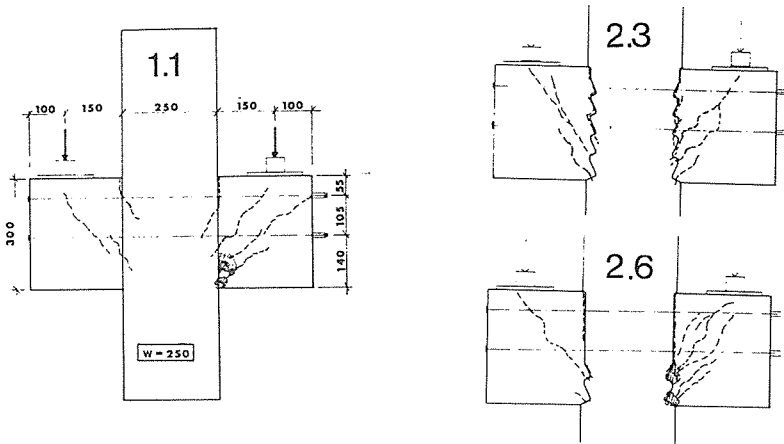
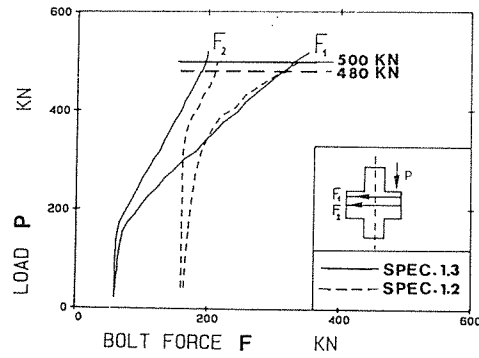
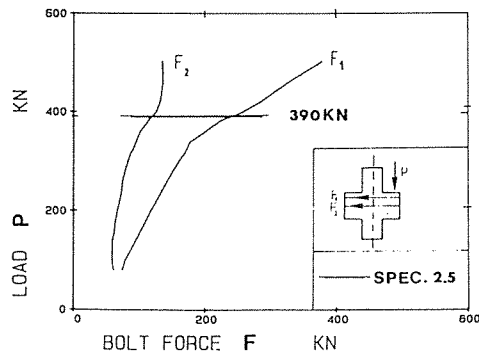


Figure 6. Typical crack pattern at failure.



7 a) Comparison of two specimens with different prestressing.



7 b) Specimen loaded beyond defined failure load.

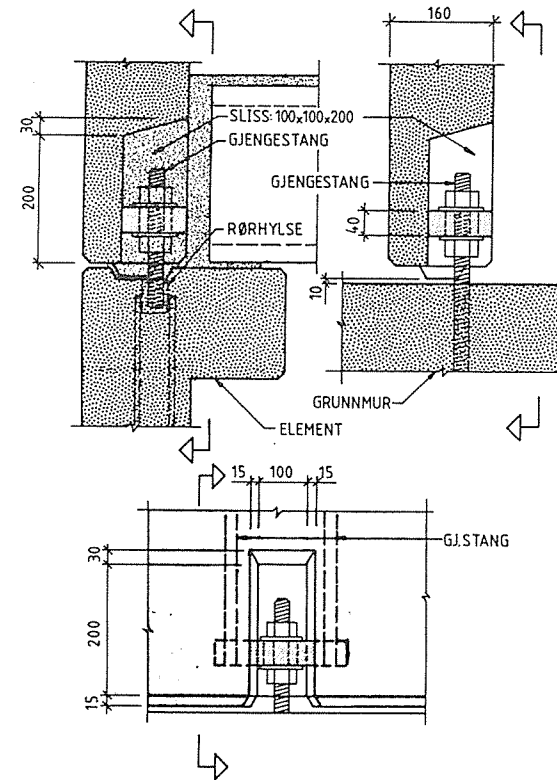


Fig. 14. Forankring av skivelementer /4/.

Figure 7. Bolt forces versus load.

$$\varphi \epsilon_s + \sigma_n = 1,05 \cdot 10^{-3} \cdot 556 + 0,45 = \underline{1,03 \text{ MPa}}$$

$$0,3 f_c = 0,3 \cdot 10,7 = 3,21 < \underline{1,03}$$

$$0,02 f_c = 0,02 \cdot 10,7 = \underline{0,21} < \underline{1,03}$$

$$V_d = t' \cdot d (v_c + \mu (\varphi \epsilon_s + \sigma_n))$$

$$= 150 \cdot 8700 (0,06 \cdot 10,7 + 0,7 \cdot 3,21)$$

$$= \underline{1780 \text{ kN}}$$

$$V_g = \underline{450 \text{ kN}} \ll V_d$$

1.7 Kommentarer

Beregningsmodellene foran er slik de utføres ved Østlandske Spennbetong A/S og representerer et resultat av litteraturgranskning og egenutvikling. Forfatteren føler at det er ønskelig med ytterligere forsøk for å komme fram til en sikrere beregningsmodell. Dette gjelder spesielt for skjær i fuger og lastfordeling til vegger med store åpninger.

LITTERATURHENVISNINGER

1. CPCI metric design manual. Canadian Prestressed Concrete Institute.
2. Plant precast and prestressed concrete - seismic systems. 2nd ed. Prestressed Concrete Manufacturers Association of California.
3. Krokstrand, Ole H. Stabilitet konstruksjonshåndbok, Betongelementer. NBIF.
4. Konstruksjonsdetaljer. Hønefoss 1983, Østlandske Spennbetong A/S.
5. DS 411. Betongkonstruksjoner. Dansk Ingeniørforening, 1984. Dansk Standard.

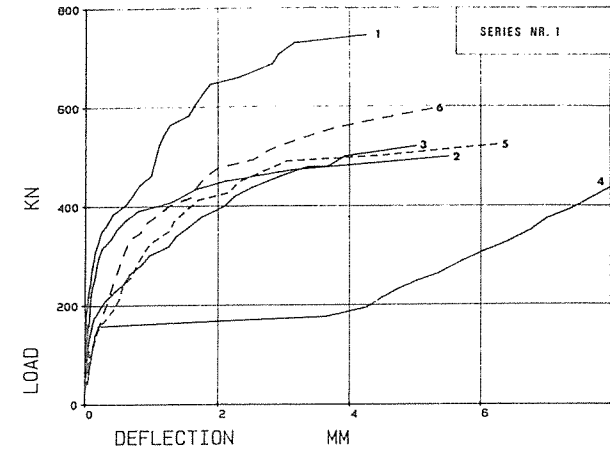


Figure 4. Vertical deflection of corbels with plane or simple recess contact surface. (Series 1.)

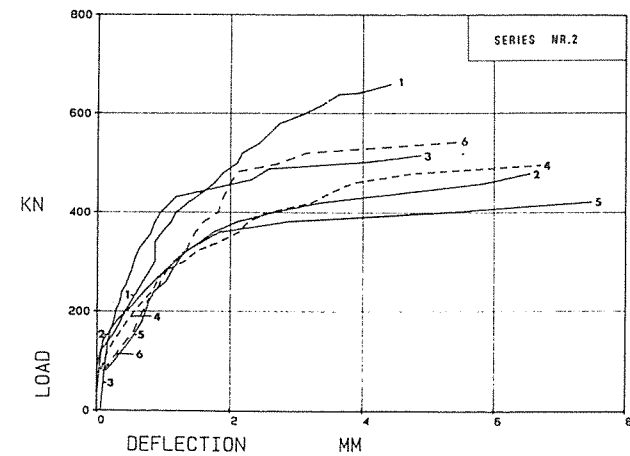


Figure 5. Vertical deflection of corbels with indented surface. (Series 2.)

crack initiated at the corbel/column corner propagating gradually downwards in the column, could be observed.

At intermediate loads diagonal cracking occurred.

At high loads close to the termination of the test, concrete crushing failure was more or less pronounced in the lower parts of the corbel.

The deflection of the two twin corbels were usually different due to small deviations from ideally symmetric loading and the use of unbonded steel bolts.

Usually the corbel with the longer deflection in early loading stages was also the one that finally failed.

In figure 4 and 5 the general behaviour of the corbels are characterized by the vertical deflection of the top surface measured 150 mm from the column face on the side with the larger deflection.

Small irregularities of the curves are mainly caused by redistribution of the deflection between the two twin corbels.

It can be seen on figure 4 that specimen 1.1 (Type P,E,P85 C40/25) and 1.2 (P,E,P85,C25) with high prestressing have very small deflections for moderate loads.

Specimen 1.4 (P,C,P30,C25) behaved differently with a considerable sudden deflection at 160 kN load. Further deflection was then restrained by dowel action of the bolts.

Figure 5 shows the behaviour of series 2 with indented joint. Slightly larger deflection for moderate loads were found for specimen 2.5 and 2.6 with two teeth dry joint.

ANSLUTNINGAR AV HÄLDÄCKSPLOTTAKONSTRUKTIONER

Arto Suikka
Oy Partek Ab
Helsingfors, Finland

Jag granskar i det följande några centrala anslutningar av häldäcksplattor på basen av de provresultat, som har erhållits med Variax häldäcksplattor antingen hos VTT (Statens tekniska forskningscentral) eller i Parteks forskningscentral. Jag koncentrerar mig i den här framställningen närmast på tre saker - plattornas uppläggning, plattornas kantförbindningar samt samverkan mellan häldäcksplattan och pågjutningen.

1 UPPLAG AV PLATTAN PÅ VÄGGEN

Häldäcksplattans minimumupplagslängd varierar i olika länder. I tabell 1 har framställts några värden.

Tabell 1. Häldäcksplattans minimumupplagslängder i olika länder.

Land	Plattans höjd (mm)		
	150...250	250...320	> 320
Finland			
- planering	65	65	105 (65)
- efter montage	40	40	80 (40)
Sverige, Variax	60	70	110
Västtyskland, Variax	70	70	-
FIP, Preliminary recommendations	50	50	-

Inverkan av upplagslängden på plattornas bärförmåga har undersökts bl.a. i Finland och Norge. I proven har man konstaterat, att större upplagslängden har icke särskilt stor inverkan på plattans bärförmåga.

I tabell 2 har framställts resultaten av en testserie (rapport BET 42819)¹⁾ (1. Som platta användes en 400 mm hög Variax-platta. Plattorna 1 - 4 var spända med 4 Ø 12,5 mm:s spännlinor och plattorna 5 - 12 med 8 Ø 12,5 mm:s spännlinor.

Tabell 2. Resultaten av en testserie. (1)

Platta nr	Stödets bredd	Avstånd från ändan av plattan till stödets kant	f _{uQ}
1	40	40	2,61
2	40	40	2,95
3	40	300	2,97
4	40	300	3,57
5	80	80	2,77
6	80	80	2,77
7	80	200	2,91
8	80	200	2,90
9	80	300	3,00
10	80	300	2,94
11	80	400	3,06
12	80	400	3,09

1) Tukipinnan leveyden vaikutus Variax 3-ontelolaatan leikkaukskapasiteettiin. Esbo 1984. Statens tekniska forskningscentral. Betong- och silikattekniska laboratoriet. Forskningsrapport BET42819. 19 s. + bil. 36 s.

Med γ_{uQ} avses säkerhetskoefficienten mot skärkraftskapacitet jämförd med den beräknade kapaciteten. Med undantag av platta 4 inträffade i alla plattor ett skärbrutt genom spännlinornas gliding. I platta 4 brast spännlinorna.

Ifrågaom håldäcksplattorna användes på plattornas stödområde tilläggsarmering, vilken placeras i fogarna mellan plattorna eller/och i eftergjutningarna in i hålen. I Finland placeras armeringen i fogarna, då stålets förankringslängd är 1 meter. Under gjorda prov förankrade sig ett \emptyset 10 mm:s kamstål redan på 200 mm:s förankringslängd i foggjutningen med 48 kN:s kraft, vilket är större än stålets beräknade draghållfasthet. Fogbetongens tryckhållfasthet var K20...23. Plattans kant var endast antingen räfflad i längdriktningen eller hade skjuvdubbar på tvären. Dessa skjuvdubbar hade ingen märkbar inverkan på stålets förankring, eftersom stängen i alla fall antingen ged ut ur fogen eller brast.

I provet använde man sig av ett bjälklag, som bestod av 5 plattor, på vilken inverkade en 150 kN:s vågrät punktlast så, att stängen, som skulle dras ut, befann sig på bjälklagets dragna kant (rapport B 9285/77)(1).

I Finland har man avgivit regler om fogarmeringens mängd, som grundar sig på att förhindra ett kontinuerligt ras/1/. I tabell 3 har framställts en 1,2 m:s bred plattas fogarmering (A400H, \emptyset) för plattans olika spännvidder, då stomkonstruktionen består av bärande väggar och håldäcksplattor.

Tabell 3. Fogarmeringen i Finland / 1/.

Byggnad	L		4,8	6,0	7,2	8,4	9,6	10,8
	B							
<u>3-4 våningar</u> - i plattornas längdsgående. Fogar vid upplaget - väggarnas vågräta fogar	2,4		10	10	10	12	12	12
	2,4		10	12	12	2x10	2x10	2x10
<u>5-8 våningar</u> - i plattornas längdsgående. Fogar vid upplaget - väggarnas vågräta fogar	3,6		10	10	12	12	2x10	16
	3,6		12	16	16	16	2x12	16+10
<u>över 8 våningar</u> - i plattornas längdsgående. Fogar vid upplaget - väggarnas vågräta fogar	4,8		10	10	12	2x10	10+12	16
	4,8		2x10	16	2x12	2+16	2+16	2x16

I tabellen är L = den långa plattans spännvidd och B = väggens antagna bredd

1) Saumaterästen ulosvetokoe ontelolaattojen pitkittäissaumasta. Esbo 1977. Statens tekniska forskningscentral. Betong- och silikattekniska laboratoriet. Forskningsrapport B 9285/77. 5 s. + bil. 1 s.

2.6 Test rig and measurements

The specimens were mounted in a simple steel frame and loaded with two similar jacks connected to the same manual pump. The column position was secured by a center-bolt at the top.

The load was distributed from the spherical jackhead to the corbel by a steel prism 50x50x250 mm laying on a steel plate 15x150x250 mm with two layers of 3 mm teflon sheets between the steel parts. This arrangement is not ideal, but reduces possible horizontal components of the load to acceptable small values.

Loads were measured with loadcells on the jacks. Likewise the bolt tension were measured with specially made cylindrical loadcells with strain gauges mounted on each bolt head.

Vertical deflection of the corbels were measured with inductive deflectometers and dial gauges relative to the unloaded upper part of the column.

In addition strains on concrete surface were measured with demountable ekstensometer with 100 mm gauge length. Due to large strain gradients, these measurements cannot give detailed information on the local concrete strain. The strain measurement will therefore not be presented here.

3 TEST RESULTS

3.1 General behaviour

All corbels (except 1.4) behaved more or less in the same manner. At low loads only a gradual opening of the joint at the top or, in some of the glued connections, a single

Enligt de finska betongnormerna / 2/ bör vägg-platta-fogens armeringskapacitet vara minst plattans stödreaktion/m, dock minst 20 kN/m.

Plattornas fogarmering monteras i fogens nedre del, eftersom deras uppgift är att ta emot endast dragpåkänningar och icke t.ex. stödmoment. Förutom stålen i tabell 3 bör bjälklagen omges med en s.k. ringarmering, vilken bör ha en beräknad kapacitet t.ex. i våningshus på minst 45 kN.

I fogen mellan väggelementen och håldäcksplattorna monteras ofta el-röranläggningar. För detta ändamål utfördes jämförande laboratorieprov, i vilka testades

- a) fem fogar utan el-röranläggningar sammanfogade på ett normalt sätt
- b) tre fogar, i vilka monterades fyra 15 mm:s el-rör av plast. Härvid göts fogen först till hälften och lätades, varefter rören placerades i fogens övre del och varefter resten av fogen göts ut
- c) tre fogar, där utrymmet mellan plattändorna lämnades helt utan foggjutning.

I provet belastades håldäcksplattan med en brukslast och väggelementet genom att öka på lasten stegvis. På basen av resultaten kan man i fogen placera 4 st el-rör, ifall fogmassans tätning göres mycket omsorgsfullt (rapport B 8805/78) (1).

Håldäcksplattornas förankring vid upplaget växlar för närvarande mycket i olika länder. I några fall bör tillägsarmeringen placeras t.o.m. i tre hål förutom fogarna. I något land, såsom t.ex. i Västtyskland, förutsättes alltid användning av spännlinor i överkanten, så att bjälklaget garanteras en viss seghet mot ett eventuellt uppkommande stödmoment. Det finska förfarandet är enkelt att utföra och i praktiken har inga skador påträffats. Ifall man börjar öppna plattans hål på grund av stödarmring, bör man göra det möjligast begränsat och helst genom att göra ett hål på 0,5 m räknat från plattans ända, varigenom man inte försvagar plattändans tvärgående draghållfasthet. I bild 1 visas lösningar från olika publikationer.

2 UPPLÄGGNING AV PLATTAN PÅ EN BALK

När man lägger plattan på en balk kan man följa bl.a. ifråga om upplagslängden och plattornas fogarmering samma regler som i väggkopplingen. I bild 2 visas några alternativ för att placera fogarmeringen. Diametern på fogarmeringen varierar normalt mellan $\varnothing 12... \varnothing 20$ mm och längden mellan 2000 - 2900 mm.

Placerandet av fogstålen vid pelarna är något besvärligare. I pelaren lämnas antingen ett hål, genom vilket fogstålet föres eller i pelaren gjutes en påfästningsskiva, på vilken fogstålet svetsas (bild 3).

1) Variax-elementtien poikittaissauman puristuskokeet. Esbo 1978. Statens tekniska forskningscentral. Betong- och silikattekniska laboratoriet. Forskningsrapport BET 8805/78. 8 s. + bil. 4 s.

2.5 Test plan

The types of specimens tested can be summarized in the following tables:

Table 1. Test plan with measured concrete strength. SERIES 1.

Number	1.1	1.2	1.3	1.4	1.5	1.6
Contact surface	P	P	P	P	R	R
Adhesive	E	E	E	C	DE	DE
Prestress	P85	P85	P30	P30	P30	P30
Concrete	C40/25	C25	C25	C25	C25	C40
Age at test	17	15	15	14	15	14
Ref. strength (N/mm ²)	40,9 26,5	23,7	25,9	25,3	25,5	38,7

Table 2. Test plan with measured concrete strength. SERIES 2.

Number	2.1	2.2	2.3	2.4	2.5	2.6
Contact surface	I ₂	I ₂	I ₅	I ₅	I ₂	I ₂
Adhesive	E	E	DE	D	D	D
Prestress	P35	P35	P35	P35	P35	P35
Concrete	C40/25	C25	C25	C25	C25	C40
Age at test	16	14	14	13	14	13
Ref. strength (N/mm ²)	40,5 26,3	23,5	25,6	25,0	25,2	38,3

Vid trappöppningarna avbrytes plattorna ofta helt. Därvid är stödprincipen för plattorna följande:

- a) De avbrutna plattorna bindes till en skiva med hjälp av en ändbalk, som gjutes i öppningens kant och genom bjälklagets ringarmering
- b) Balken dimensioneras för de laster, som kommer från hälften av de avbrutna plattorna
- c) De avbrutna plattornas laster överflyttas till de bredvidliggande plattorna genom fogens skärkapacitet
- d) Ändbalkens armering förankras i de bredvidliggande plattorna.

3 FÖRBINDNINGAR I KANTEN AV PLATTAN

Sandwich-väggelementen fästes ofta för vindbelastningar i håldäckplattans kant. Även balkongelementens vågräta krafter måste förankras i plattans kant. Partek har gjort flere testserier med håldäckplattornas kantförbindningar. Vid ett prov (rapport UCMM 115/82) göts plattstålet efteråt i kanthålet på en 265 mm hög håldäcksplatta. Eftergjutningens längd var c. 250 mm och stålet hade placerats antingen vågrätt, i en 37°:s vinkel uppåt eller i en 39...45°:s vinkel nedåt. I alla fall då stålet drogs ut, var brottet en plötslig spjälkning av håldäcksplattans kant. Förbindningarnas bråttbelastningar har framställts i tabell 4.

Tabell 4. Förbindningarnas bråttbelastningar. (1)

Platttyp	Stålet vågrätt	Stålet i 37° uppåt	Stålet i 39...45° nedåt
utan kant-spännlinor	81,0 78,8	55,5 58,5	83,8 >89,0
med kant-spännlinor	> 86,2 88,5	65,0 50,0	86,0 118,3

Vid tillämpning av resultaten bör man ta i beaktande, att vid provarrangemangen dragdomkraften hade stötts på 1 meters avstånd på vardera sidan av den förankrade stängen. Bl.a. bör man granska som en helhet belastningen, som förorsakats av flere förbindningar på samma plattas kant. Motsvarande praktiska planeringsdirektiv har presenterats i bild 4.

4 PAGJUTNINGENS VIDHÄFTNING MED HÅLDÄCKSPLOTTAN

Om håldäcksplattan dimensioneras med ytbetongen som en sammansatt konstruktion, är ytbetongens goda vidhäftning till sitt underlag mycket viktigt. Partek har gjort statistiska och dynamiska böjningstester med sammanverkande Variax-plattor samt vidhäftningstester med ytbetongen.

1) BES-liitoskoe. Tartuntojen ulosvetokoe. Pargas 1982.
Oy Partek Ab. Kehityskeskus. Rapport UCMM 115/82. 29 s.

d) Concrete strength.

Two different concrete qualities were used.
C40 with strength of \emptyset 150 x 300 (mm) cylinders approx 40 MPa.
C25 with cylinder strength ca 25 N/mm².
Specimen no. 1 in both series were made with concrete C40 in the corbels and C25 in the column (C40/25)

2.4 Materials and curing of specimens

Reinforcement: Ks 400 deformed bars (yield strength 400 MPa)
Steel bolts: \emptyset 25 high strength quality 8.8. (Ultimate strength more than 300 kN pr bolt.)

Concrete: Modified Portland Cement (With fly ash)
Natural sand, crushed stone (D_{max} 16 mm)

The reference strength were measured on \emptyset 150 x 300 (mm) cylinders cured and tested together with the specimens. Also 100 mm cubes cured in water were tested after 7 and 28 days.

Specimens with equal number in the two series are made from the same concrete batch. The specimens were cured under moist conditions in 10-12 days and further 4 days in dry air. The age at testing was 14-16 days.

The corbels were usually mounted after 1 day of drying. The epoxy resin was 3 days old at testing. Specimen 1.4 with cement paste on concrete surface was mounted after 7 days. The cement paste had 5 days moist curing and 2 days dry curing before testing.

Specimens in series 1 were tested 1 day after the corresponding specimen in series 2. The reference cylinders were tested on one of these days. The results are corrected for the strength development +/- 1 day, approx. 1 % judged from the strength development of the corresponding cubes.

I tabell 5 har framställts i en test erhållna vidhäftningsdraghållfastheter för ytbetongen vid plattans olika ytbehandlings- (rapport BET 010210))⁽¹⁾.

Tabell 5. Vidhäftningsdraghållfasthet vid olika ytbehandlings- (1)

Håldäcksplattans yta	Vidhäftningsdraghållfasthet (MPa)
- torr	2.06
- Tarra Povix-dispersions-behandling	2.38
- fuktig	2.53
- våt	2.29
- smutsig (med sågspån)	2.50
- fuktig (massan ovibrerat)	0.93

I tabell 6 har framställts resultaten av en annan testserie. I denna har vidhäftningsdraghållfastheten undersökts efter en dynamisk belastning av plattorna ($N = 10^5$) (rapport BET 22229)⁽¹⁾. En 60 mm:s ytbetong gjöts med en normal massa, max. ballaststorlek # 16 mm, genom stavvibration. En 30 mm:s ytbetong gjöts av flytbetong utan vibration då max. ballaststorlek var # 10 mm. Ytbetongens nominella hållfasthet var K 30.

Tabell 6. Vidhäftningen efter dynamisk belastning. 2)

Provkroppans nummer	Pågjutning 60 mm		Pågjutning 30 mm	
	Vidhäftningsdraghållfasthet MN/m ²	Brott-punkt	Vidhäftningsdraghållfasthet MN/m ²	Brott-punkt
1	2,18	Delvis på sidan av pågjutningen	2,42	i fogen
2	2,48	- " -	2,86	- " -
3	2,69	- " -	2,33	- " -
4	2,23	- " -	1,49	- " -
Medeltal MN/m ²	2,40		2,28	

På grund av de utförda testerna har man beslutat rekommendera användningen av flytbetong, en lätt vibrering av betongytan, ett fukligt underlag, ytans rengöring för gjutningen och ett omsorgsfullt arbetsutförande.

1) Variax 8- ja Variax-laattojen ja päällevalun yhteistoimintaa selvittävät kokeet. Esbo 1980. Statens tekniska forskningscentral. Betong- och silikattekniska laboratoriet. Forskningsrapport BET 010210. 12 s. + liitt. 6 s.

2) Päällevalulla varustetun Variax 8-ontelolaatan toiminnan selvitys liittorakenteena dynaamisessa kuormituksessa ja Variax 5-ontelolaattojen väsytyskuormituskokeiden tulosten vertailu laskennallisiin tuloksiin. Esbo 1982. Statens tekniska forskningscentral. Betong- och silikattekniska laboratoriet. Forskningsrapport BET22229. 7 s. + liitt. 32 s.

2.3 Test variables

All specimens had the same general geometry as shown in figure 2. The distance from the column face to the load axis was constant $a = 150$ mm.

A total of 12 specimens were tested in two parallel series of 6 specimens each.

a) Contact surface geometry.

In series 1 the contact surface was either plane (type P) or with a simple recess (type R). See fig. 3. The moulds were made of plywood.

Series 2 had indented surface with 5 teeth distributed over the whole corbel height (Type I₅) or with only two teeth at the lower part (Type I₂). The indentation was made by casting against carefully machined 25 mm thick steel plates mounted into the column and corbel molds. The top and bottom of the indentation were leveled differently to avoid contact between column and corbel at the top of the teeth. (Fig. 3)

b) Adhesive material.

Four types were used:

Type D: Dry surface without any treatment.

Type E: Glued with epoxy resin (Rescon Epox L)

Type DE: With epoxy only as a stressdistributing layer on the compression faces of indentations or the sloped edge of the recess.

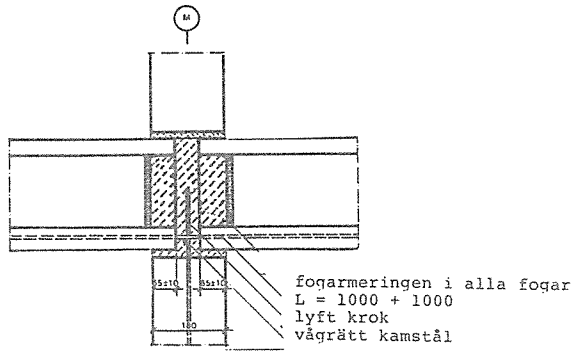
Type C: With cement paste (Specimen 1.4)

c) Prestressing.

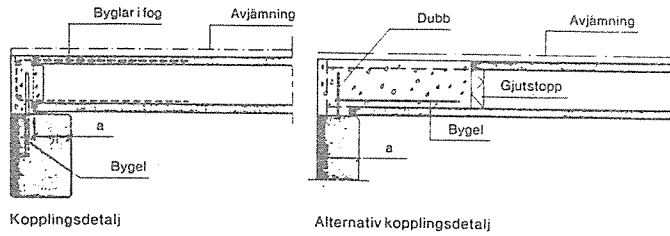
Type P 85: Specimen 1.1 and 1.2 were prestressed with approx. 85 kN pr. bolt. Total prestress 340 kN.

Type P 30 (35). All other specimens were mounted with a practical minimum force, approx 30-35 kN pr bolt.

FINLAND



SVERIGE



FIP (Utkast)

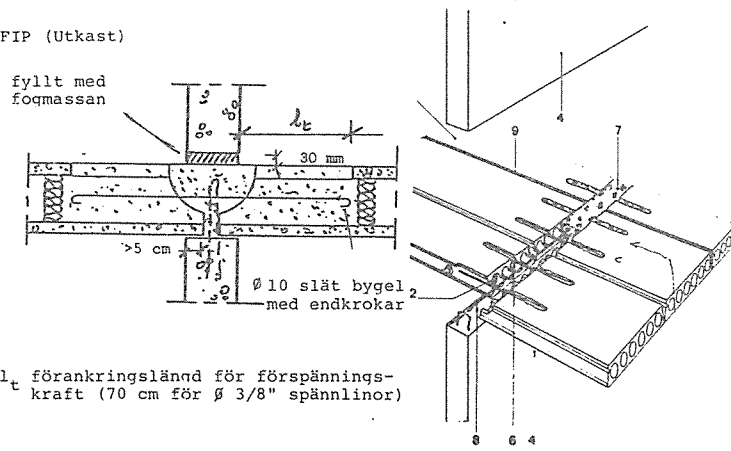
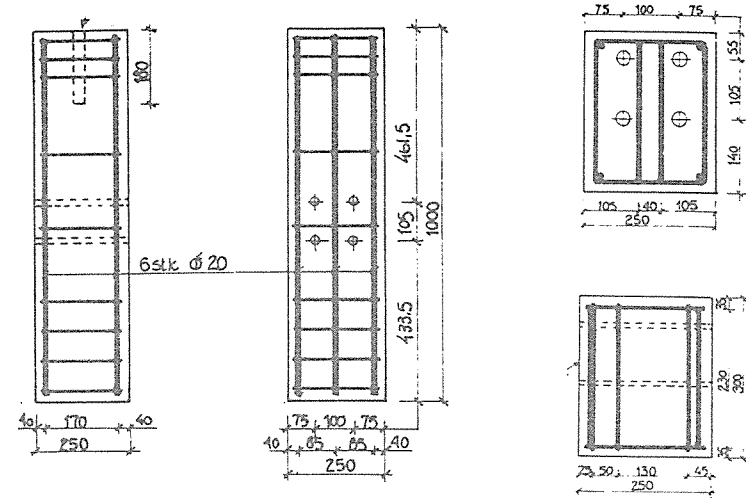


Bild 1. Fogarmeringsdetaljer.



a) Column (side and front) b) Corbel (vertical sections)
 Figure 1. Specimens. Geometry and reinforcement.

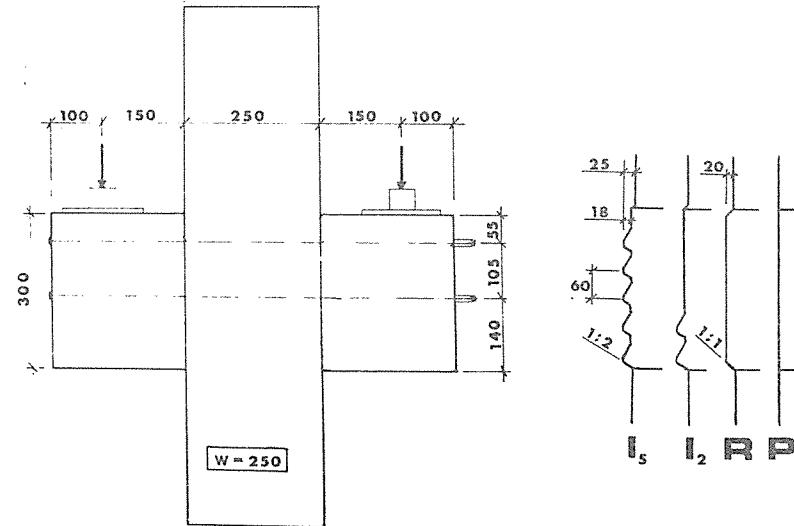


Figure 2. Mounted specimen.

Figure 3. Contact surface.

The corbel dimensions should be typical of corbels used in beam-column connections in ordinary building structures. The detailing of the contact surface between corbel and column should not interfere seriously with the column mold or the ordinary reinforcement in the column.

The test result should serve as a basis for future choice of practical design of mountable concrete corbels. The final evaluation of design strength should be based on supplementary tests of corbels with the chosen design.

2.2 Test specimens

In ordinary storey buildings with moderate height, columns with cross-section 300x300 mm with corbels $w/h/l = 300/300/200$ (mm) are often used. Dependent on the detailing the load will act at a distance from the column face of about 120-170 mm.

Practical considerations of the test set-up led to the following choice of test specimens:

Column: $w/h/l = 250/250/1000$ (mm)

Corbels: $w/h/l = 250/300/250$ (mm)

Twin corbels were mounted on two opposite sides of the column with 4 through-going $\varnothing 25$ mm steel bolts. To avoid dowel action of the bolts at early stages the bolt holes were formed by plastic tubes with internal diameter 28 mm. For the same reason mortar injection of bolt holes was omitted.

The specimens are reinforced with deformed bars Ks 400.
 Column: $2 \times 3 = 6 \varnothing 20$ mm longitudinal bars + $\varnothing 8$ mm stirrups.
 Corbel: $\varnothing 10$ mm stirrups + $\varnothing 10$ mm corner bars.
 Reinforcement detailing and geometry are shown in figure 1.
 The general geometry of mounted specimens: See figure 2.

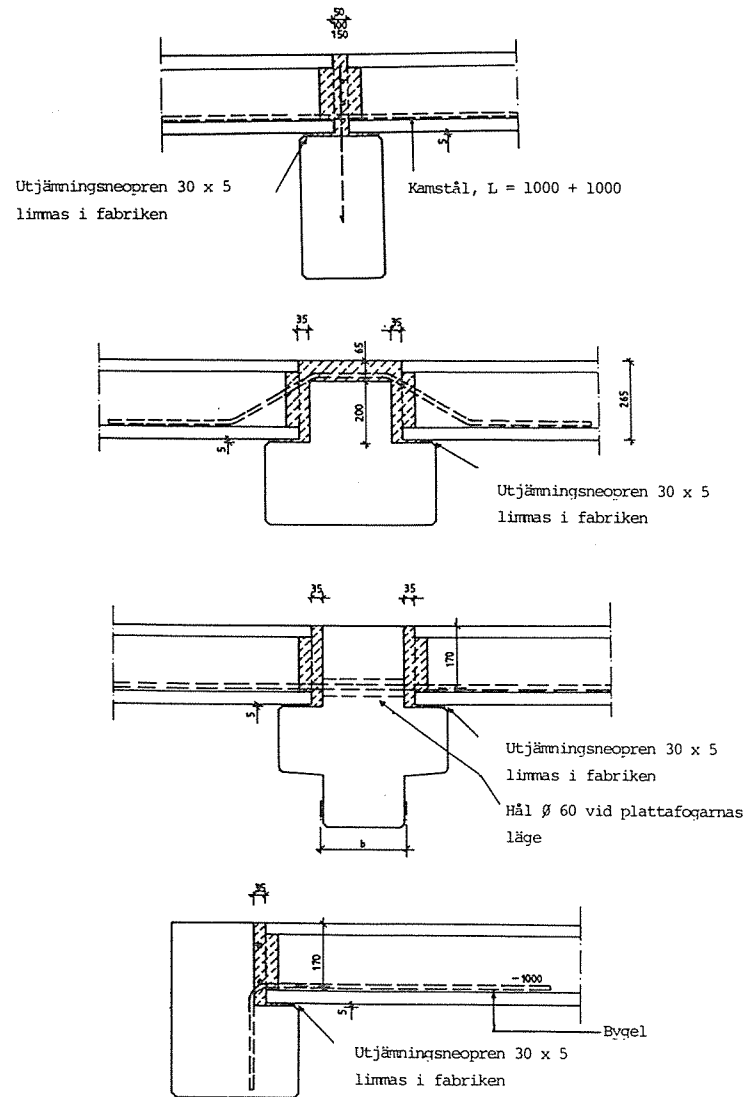


Bild 2. Alternativ för fogarmeringens placering.

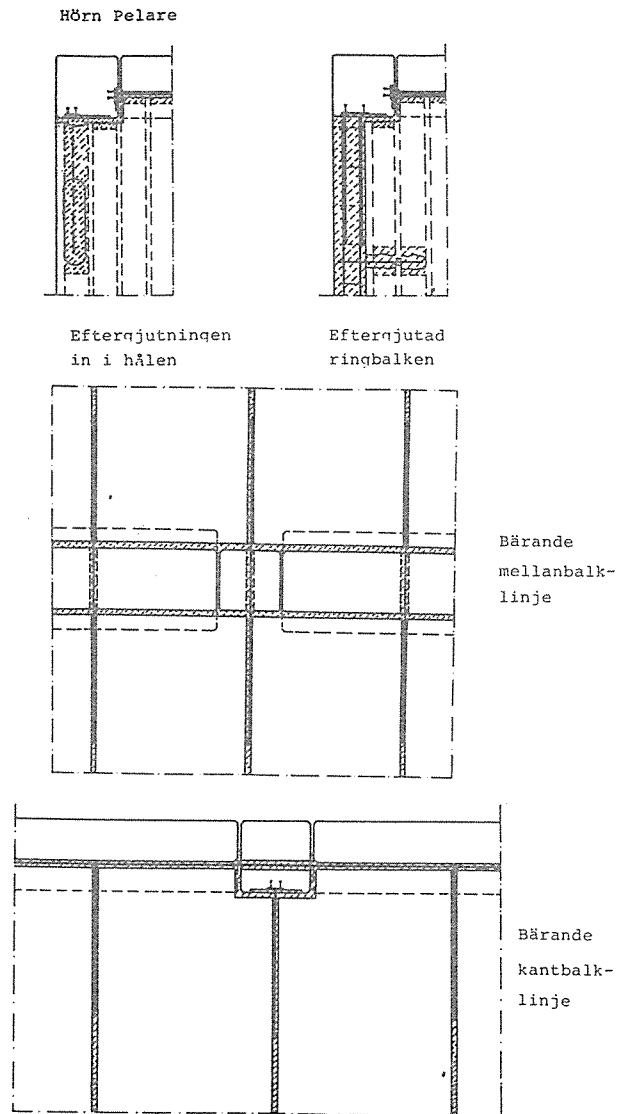


Bild 3. Placerandet av fogarmeringen vid pelaren.

BEHAVIOUR OF MOUNTED CONCRETE CORBELS

Erik Thorenfeldt
 M.Sc. Ass. Professor, Norwegian University
 of Technology, Division of Concrete Structures,
 Trondheim, Norway.
 Research Ass., SINTEF - Division FCB

1 INTRODUCTION

Precast concrete columns are usually equipped with corbels for beam support etc. The presence of corbels make the relatively simple column mold more complicated and labour-consuming. Production cost increases further when corbels are required on more than two opposite sides of the column.

The manufacture of precast columns can be simplified and more standardized if a safe and simple system for mounting of prefabricated corbels at a later stage is at hand.

Bolted or welded steel brackets are sometimes used, but have their disadvantages, among other things, the need for extra protection against corrosion and fire exposure.

Also bolted concrete corbels have been used for special structures, but the knowledge of how the detailed condition of the contact surface influences the behaviour and load-bearing capacity of such corbels is limited.

On this background it was decided to test two series of precast corbels mounted on columns by steel bolts. The tests were carried out by four graduate students at The Norwegian University of Technology, Division of Concrete Structures, under the supervision of the author (Ref. 1, 2). The project is sponsored by the Norwegian precast industry.

2 TEST PROGRAMME

2.1 Objective

The intention of the test programme is to compare the behaviour of mounted concrete corbels with different detailing of the contact surface, adhesive material, prestressing and concrete strength.

Table 5. Bæreevne af samling. Forsøgsemner med armeret fugemørtel.
 $A_m/A_c = 0,53$.

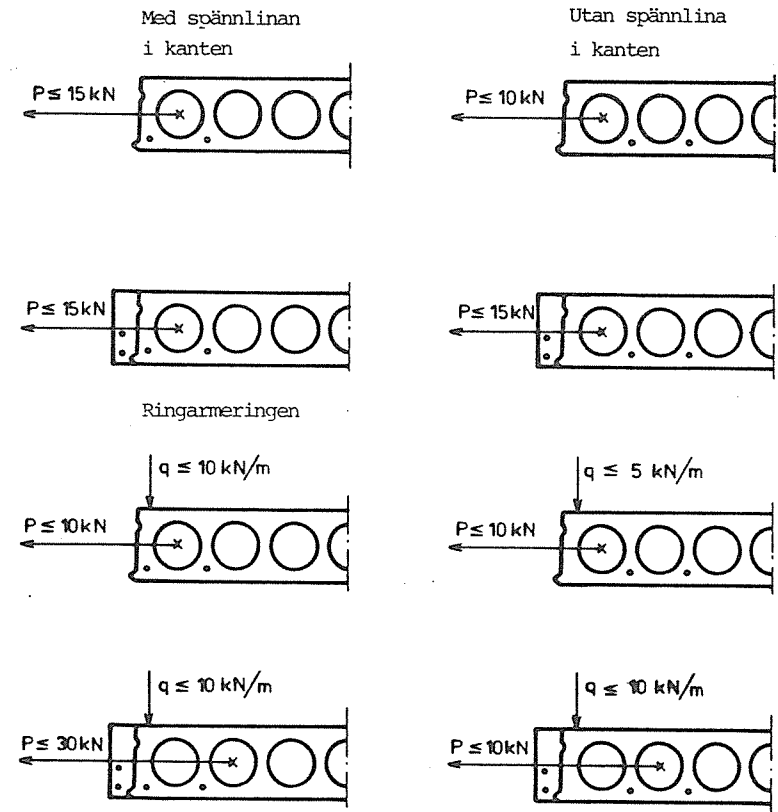
$\frac{h}{b}$	$\frac{f_m}{f_c}$	γ_m	α	$\frac{A_r}{A_c}$	$N_{J,u}^{obs}$	$N_{J,u}^{obs}$	$N_{J,u}^{cal}$	$N_{J,u}^{obs}$
					$A_m \cdot f_m$	$A_c \cdot f_c$	$A_c \cdot f_c$	$N_{J,u}^{cal}$
0,12	0,58	0,26	4,10	0,45	2,50	0,77	0,86	0,90
					2,42	0,74		0,87
0,16	0,44	0,19	4,32	0,45	3,34	0,78	0,48	1,62
					3,34	0,78		1,62
	0,58	0,23	3,10	0,45	2,66	0,82	0,70	1,17
					2,55	0,79		1,13
0,20	0,66	0,26	3,08	0,45	2,14	0,75	0,90	0,83
					2,34	0,82		0,91
	0,45	0,19	4,47	0,44	3,27	0,78	0,48	1,62
					3,27	0,78		1,62
	0,58	0,23	3,21	0,44	2,52	0,78	0,69	1,13
					2,70	0,83		1,20
0,58	0,26	3,66	0,44	2,66	0,82	0,81	1,01	
				2,67	0,82		1,01	

$N_{J,u}^{obs}$: Samlingens bæreevne, forsøsværdi

$N_{J,u}^{cal}$: Samlingens bæreevne, beregnet værdi

Litteraturhenvisning

Larsen, Henning. Bæreevne af mørtelfuger mellem betonsøjleelementer. Lyngby 1983, Danmarks tekniske Højskole, Institutet for Husbygning, Rapport nr. 165.



Siffrorna är lämpliga för plattor högre än 200 mm.
 Med lägre plattor de måste delas med 2.

Bild 4. Planeringsdirektiv för ändringarna i plattans kant.

LITTERATUR

1. BES-järjestelmän rakenteita koskeva suositus 1979. Helsinki 1979. Suomen Betoniteollisuuden Keskusjärjestö, Julkaisu 15. 68 s.
2. Betonirakenteet. Ohjeet 1981. Suomen rakentamismääräyskokoelma, Osa B 4. Helsinki, Sisäasiainministeriö, 1981. 60 s.

De i resultatbehandlingen benyttede værdier for E_c og E_m er haldningen af sekanten til punktet på arbejdskurven, hvor spændingen er 90% af styrken. Noget tilsvarende gælder for v -værdierne.

Der er her betragtet en udformning af samlingen med en mørtelfuge liggende imellem to ens betonsøjleelementer. Og belastningen er her regnet centralt virkende på samlingen.

Table 4. Bæreevne af samling. Forsøgsemner med uarmeret fugemørtel. $A_m/A_c = 1$.

$\frac{h}{b}$	$\frac{f_m}{f_c}$	$\frac{E_m}{E_c}$	γ_m	β	α	$\frac{A_r}{A_c}$	$\frac{N_{J,u}^{obs}}{A_m \cdot f_m}$	$\frac{N_{J,u}^{obs}}{A_c \cdot f_c}$	$\frac{N_{J,u}^{cal}}{A_c \cdot f_c}$	$\frac{N_{J,u}^{obs}}{N_{J,u}^{cal}}$	
0,12	1,03	0,62	0,24	0,12	1,55	0,85	0,95	0,98	0,97	1,01	
0,16	1,12	0,56	0,29	0,19	1,56	0,81	0,97	1,01	0,95	1,04	
							0,90	1,01	0,95	1,06	
0,20	0,49	0,41	0,29	0,21	1,68	0,81	0,90	0,77	0,86	0,90	
							1,56	0,82	0,95	0,95	
	0,31	0,24	0,31	0,27	2,19	0,81	1,56	0,77	0,66	0,90	
							2,13	0,66	0,66	1,00	
							2,20	0,68		1,03	
							2,15	0,66		1,00	
	0,31	0,24	0,31	0,27	2,19	0,81	2,44	0,76	0,66	1,15	
							2,29	0,71		1,08	
							2,28	0,71		1,08	
							2,16	0,62	0,40	1,55	
0,24	0,29	0,27	0,19	0,14	2,55	0,81	1,87	0,59	0,44	1,34	
							0,32	0,62	0,44	1,41	
	0,46	0,74	0,40	0,26	0,47	0,74	1,97	0,62	0,44	1,41	
							1,75	0,80	0,89	0,90	
	0,20	0,48	0,41	0,29	0,21	1,05	0,85	1,68	0,77	0,89	0,87
								1,72	0,79	0,89	0,89
		0,49	0,41	0,29	0,21	1,34	0,81	1,44	0,68	0,83	0,82
								1,70	0,80	0,96	0,96
		0,95	0,56	0,29	0,19	1,25	0,81	1,54	0,76	0,75	1,01
								1,50	0,74	0,98	0,98
0,43		0,74	0,40	0,26	0,61	0,68	1,51	0,74	0,94	0,99	
							1,14	1,08	0,94	1,15	
	1,05						1,00	1,06	1,06		
	1,93						0,83	0,74	1,12		
0,24	0,57	0,47	0,30	0,22	1,23	0,81	1,84	0,79	0,74	1,07	
							1,92	0,82	0,79	1,11	
							1,04	0,60	0,79	0,76	
							1,14	0,66	0,79	0,84	

$N_{J,u}^{obs}$: Samlingens bæreevne, forsøgs værdi

$N_{J,u}^{cal}$: Samlingens bæreevne, beregnet værdi

For forsøgsemnerne med uarmeret fugemørtel gælder, at forsøgsresultaterne i gennemsnit ligger tæt ved de teoretisk beregnede bæreevner. Men spredningen er stor.

For forsøgsemnerne med armeret fugemørtel ligger forsøgsresultaterne stort set over de teoretisk beregnede bæreevner, i gennemsnit ca. 30% over, - også med stor spredning.

I tabel 4 er vist resultater for forsøg med forsøgsemner med uarmeret fugemørtel og samme kvadratiske tværsnit i mørtlen som i søjleelementet.

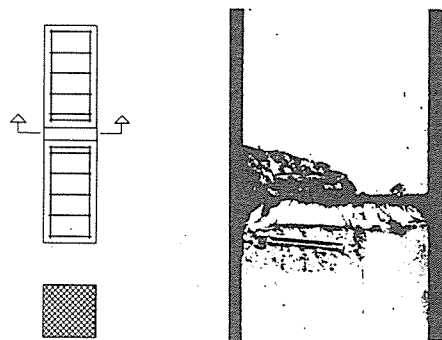


Fig. 2. Uarmeret fugemørtel. $A_m/A_c = 1$.

I tabel 5 er vist resultater for forsøg med forsøgsemner med armeret (ringarmering) fugemørtel og et tværsnit (ottekantet) i mørtlen på 53% af søjleelementets tværsnit (kvadratisk).

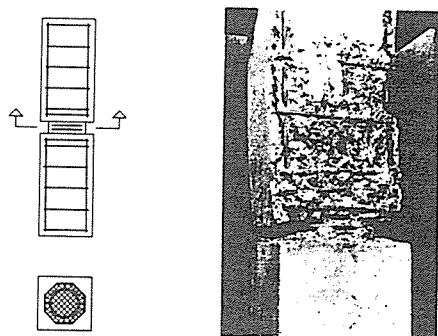


Fig. 3. Armeret fugemørtel. $A_m/A_c = 0,53$.

DIAPHRAGM ACTION IN PRECAST FLOOR SLABS - A pilot test series on precast hollow core slabs

Steve Svensson,
Chalmers University of Technology,
Division of Concrete Structures,
Göteborg, Sweden

INTRODUCTION

This paper gives a summary of a series of full-scale tests on precast slab fields. The tests were carried out in 1984 at Chalmers University of Technology, Division of Concrete Structures /1/.

Professor Krister Cederwall, Head of the Division, is responsible for the project and the tests have been performed under his guidance. Research Assistant Björn Engström has taken very active part in the planning of the tests.

The aim of the test series was to study the capacity of slab fields when loaded in in-plane bending (diaphragm action). It was of essential interest to study the importance of having the joint surfaces provided with shear keys or indentations with respect to shear force transfer between the slab panels. The influence of the boundary conditions have also been studied in some detail. Some of the slabs have thus been surrounded by conventionally in situ concreted tie beams while others have been more loosely connected through dowels to the support beams.

DESCRIPTION OF THE TESTS

The test series included six tests. Each slab field consisted of seven hollow core slab panels, see Fig. 1. The joints between the slab panels were grouted and the outermost panels were connected to edge beams by stirrups. In the tests, the edge beams were simulating stabilizing walls.

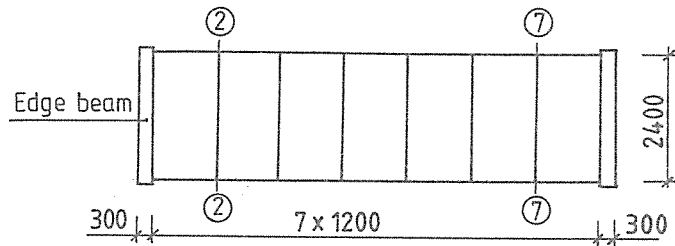


Fig. 1. The slab field.

In each test, except one, initial cracks with a width of 0,5 mm were produced in two of the joints, the joints next to the edge beams according to Fig. 1.

In two of the tests the slab panels were provided with shear keys with a depth of 3-4 mm. In the other tests the joint surfaces were unindentated.

Two different arrangements were used for the slab fields, type A and type B. Fig. 2 shows a longitudinal section of the slab fields type A.

Med armeret mørtel fås bæreevnen - efter en række forenkende tilnærmelser - som funktion af mørtelfugens effektive areal A_r med tværmål b_r , hvor b_r bestemmes som den mindste af: tværmålet for bøjlerne i mørtelfugen $b_{r,st,fug}$ og tværmålet for bøjlerne i søjleelementenden $b_{r,st,søj}$, mørtelstyrken f_m , mørtlens tværuddvidelseskoefficient v_m og en dimensionsløs størrelse α - tilsvarende ovenfor under uarmeret mørtel, men med b_r bestemt for armeret mørtel og med A_{st} også indeholdende armeringen i mørtelfugen.

For en samling med ringarmering af fugemørtlen, kan bæreevnekraften $N_{j,u,r}$ (i brudtilfælde revnet søjle) findes af tabel 3.

Tabel 3. Bæreevne $N_{j,u,r}/(A_r \cdot f_m)$ for en armeret mørtelfuge.

v_m	α					
	1	2	3	4	5	
0,35	2,68	3,76	4,54	5,12	5,57	
0,30	2,34	3,09	3,58	3,92	4,18	
0,25	2,05	2,56	2,88	3,09	3,24	
0,20	1,80	2,14	2,34	2,47	2,56	
$\alpha = \frac{A_{st} \cdot E_{st}}{b_r \cdot h \cdot E_m}$		$b_r \leq \frac{b_{r,st,fug}}{b_{r,st,søj}}$				

For brud i søjleelementenderne uden brud i mørtelfugen beregnes bæreevnen som funktion af søjlens (beton) tværsnitsareal A_c , betonstyrken f_c , mørtelfugens højde/bredde forhold h/b , forholdet mellem elasticitetskoefficienterne E_m/E_c og den dimensionsløse størrelse β (se ovenfor under brudtilfælde urevnet søjle).

Søjleelementendens bæreevne $N_{j,u,c}$ kan findes af $N_{j,u,c} = A_c \cdot f_{c,3}$, hvor $f_{c,3}$ er en reduceret betonstyrke som følge af tværtrækspændinger i søjleelementenden og bestemt for den aktuelle værdi af de forekommende tværspændinger.

Forsøg

Udførte forsøg med mørtelfuger mellem betonsøjlelementer har godtgjort, at de opstillede bæreevneformler er brugbare til beregning af bæreevnen.

Tabel 1. Bæreevne $N_{j,u,m}/(A_m \cdot f_m)$.

h/b	B				
	0,10	0,15	0,20	0,25	0,30
0,12	1,34	1,60	1,92	2,33	2,88
0,16	1,23	1,44	1,68	1,98	2,36
0,20	1,14	1,30	1,49	1,71	1,98
0,24	1,06	1,19	1,33	1,49	1,69
0,30	1,00	1,05	1,15	1,26	1,38

$$\beta = v_m \cdot \left(1 - \frac{v_c}{v_m} \cdot \frac{E_m}{E_c}\right)$$

mørtelstyrken f_m , mørtlens tværuddvidelseskoefficient v_m , mørtel-fugens højde/bredde forhold h/b_r og en dimensionsløs størrelse α , hvori indgår tværarmeringsarealet A_{st} , armeringens elasticitets-koefficient E_{st} , mørtlens elasticitetskoefficient E_m , fugens højde h og effektive bredde b_r .

Tabel 2 viser bæreevnen $N_{j,u,r}/(A_r \cdot f_m)$ med $v_m = 0,3$ som eksempel. Heraf kan bæreevnekraften $N_{j,u,r}$ i brudtilfælde revnet søjle for en samling med uarmeret fugemørtel findes. Der er forudsat en friktionskoefficient på 0,75 imellem fugemørtlen og søjleelement-endepladen.

Tabel 2. Bæreevne $N_{j,u,r}/(A_r \cdot f_m)$ for en uarmeret mørtelfuge for $v_m = 0,3$.

h/b _r	α				
	1,0	1,5	2,0	2,5	3,0
0,12	1,76	1,97	2,11	2,22	2,31
0,16	1,61	1,76	1,87	1,95	2,02
0,20	1,47	1,59	1,67	1,73	1,77
0,24	1,35	1,44	1,50	1,54	1,57
0,30	1,19	1,25	1,29	1,31	1,33

$$\alpha = \frac{A_{st} \cdot E_{st}}{b_r \cdot h \cdot E_m}$$

$$b_r \leq \begin{cases} b \\ b_{r,st,søj} \end{cases}$$

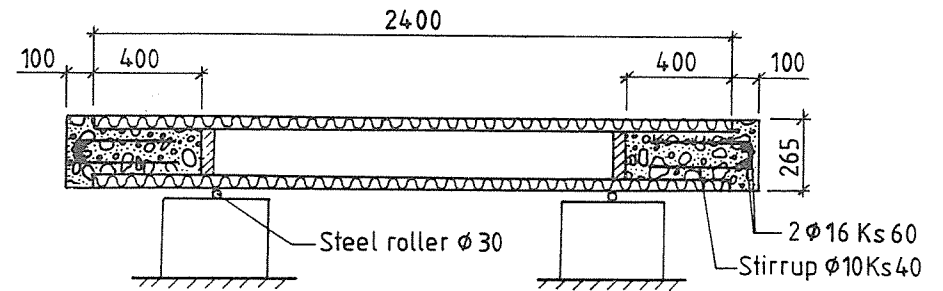


Fig. 2. Longitudinal section of the slab fields type A.

As illustrated in Fig. 2 the chord reinforcement (2φ16) was placed in a tie beam. At the ends the bars were anchored in the outermost cores. The chord reinforcement was also connected to the slab by stirrups placed in every middle core of the panels.

In the type B slab fields the panels were connected to the support beams by dowels (φ20), see Fig. 3.

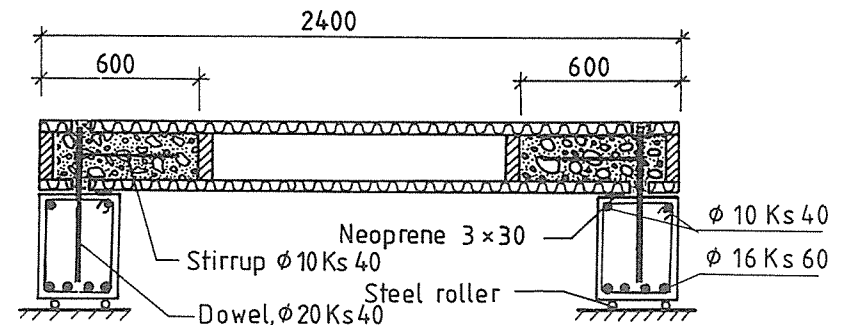


Fig. 3. Longitudinal section of the slab fields type B.

The following concrete qualities were used:

The hollow core slabs: K55

The edge beams and the support beams: K40

The tie beams, the casting around dowels etc: K25

The joint grout: K25

The different load arrangements which were used in the test series are shown in Fig. 4.

In all the tests, the slab field was loaded by two equal point loads. With respect to in-plane loading, the slab fields were indirectly supported through the edge beams. In one test the edge beams were prevented from rotating (type A:2), in order to produce restraining effects at the edges. In the other tests the edge beams were simply supported (A:1, B).

Som "modhold" for tværtrykket i mørtelfugen antages i brudsituationen dannet en trykbue i randzonen af mørtlen, gående fra søjleelement til søjleelement.

Forskydningskræfterne imellem fugemørtlen og søjleelementet regnes i brudsituationen alene overført ved friktion i randzonen.

Anbringes en armering, f.x. en ringarmering, i mørtelfugen (i randzonen), vil denne kunne udgøre modholdet for tværtrykket i mørtlen.

I søjleelementenden kommer der tvær-træk-spændinger som reaktion for de udadrettede kræfter fra trykbuen i fugemørtlen.

Trækspændingerne vinkelret på længdeaksen i søjleelementenden forårsager en reduktion af søjleelementendens bæreevne.

I brudtilfælde urevnet søjle med brud i mørtelfugen uden søjleelementenderne er revnede forinden, er opstillet et formelsæt, der - med en række forenklede tilnærmelser - giver bæreevnen som funktion af mørteltværsnittets areal A_m , mørtelstyrken f_m , mørtelfugens højde/bredde forhold h/b , forholdet mellem elasticitetskoefficienterne E_m/E_c og en dimensionsløs størrelse β , hvor i indgår tværuddvidelseskoefficienterne v_m og v_c for henholdsvis mørtel og beton samt elasticitetskoefficienterne E_m og E_c for henholdsvis mørtel og beton.

Bæreevnekraften $N_{j,u,m}$ for en samling med uarmeret fugemørtel i brudtilfælde urevnet søjle kan findes af tabel 1, hvor der er forudsat en friktionskoefficient på 0,75 imellem fugemørtlen og søjleelementendefladen. Tabellen giver bæreevnen $N_{j,u,m}/(A_m \cdot f_m)$ for $E_m/E_c = 0,5$.

I brudtilfælde revnet søjle med brud i mørtelfugen efter at søjleelementenderne er revnede, er opstillet 2 forskellige formelsæt til beregning af bæreevnen: 1 for en samling med uarmeret mørtel og 1 for en samling med armeret mørtel.

Med uarmeret mørtel fås bæreevnen - efter en række forenklede tilnærmelser - som funktion af mørtelfugens effektive areal A_r med tværmål b_r , hvor b_r bestemmes som den mindste af: fugens tværmål b og tværmålet for bøjlerne i søjleelementenden $b_{r,st,søj}$.

En given samlings teoretisk beregnede bæreevne er den største af værdierne i de to første tilfælde: brudtilfælde urevnet søjle og brudtilfælde revnet søjle, idet dog bæreevnen ikke kan være højere end værdien i det tredje tilfælde: brud i søjleende.

Det skal bemærkes, at betegnelsen brudtilfælde urevnet søjle refererer til søjleelementendens tilstand umiddelbart inden brud; i forbindelse med selve bruddet kan der ske det, at søjlen revner.

Bæreevneteorien er opstillet på grundlag af en model, som beskrevet i det følgende.

Med forskellig elasticitetskoefficient og forskellig tværuvidelseskoefficient for mørtlen og betonen vil der, når samlingen belastes, komme tværtøjninger, der er forskellige i mørtelfugen og i betonsøjleelementet, hvis intet hindrer disse deformationer.

Sammenhængen i konstruktionen bevirker, at der kommer modsatte tværsøjninger i mørtelfugen og i søjleelementenden, og forskydningskræfter i skillefladen mellem fugemørtlen og søjleelementenden.

Idet det forudsættes, at mørtlens elasticitetskoefficient E_m er mindre end betonens E_c , og at mørtlens tværuvidelseskoefficient ν_m er større end betonens ν_c , vil mørtlen blive presset udad i forhold til betonen, når samlingen belastes med en axial-trykkraft, og der kommer tvær-tryk-spændinger i mørtlen.

I mørtelfugen forudsættes deformationsforholdene i et plan vinkelret på længdeaksen at være sådan, at tøjningen er den samme og ens i alle retninger; den resulterende flytning er i ethvert punkt rettet radiært væk fra længdeaksen.

I søjleelementenderne antages tilsvarende deformationsforhold.

I en treakset trykspændingstilstand med tværtrykspændingen σ_x har mørtlen en forøget trykstyrke $f_{m,3}$ i forhold til den énaksede trykstyrke f_m .

Der benyttes en let modificeret udgave af Coulombs brudhypotese

$$f_{m,3} = f_m + 4 \cdot \sigma_x \text{ til beregning af den forøgede trykstyrke.}$$

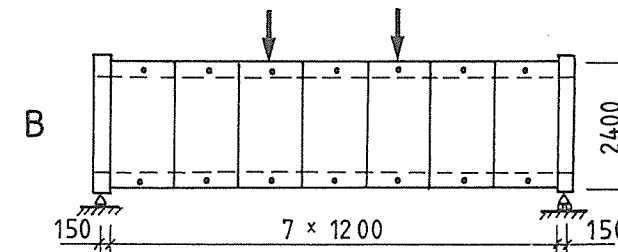
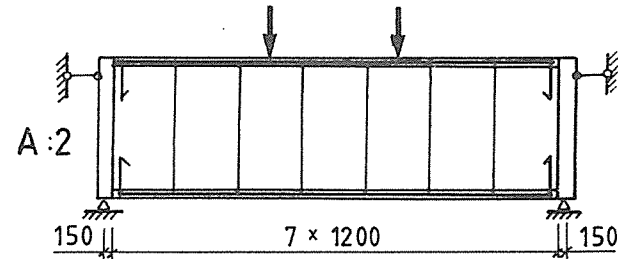
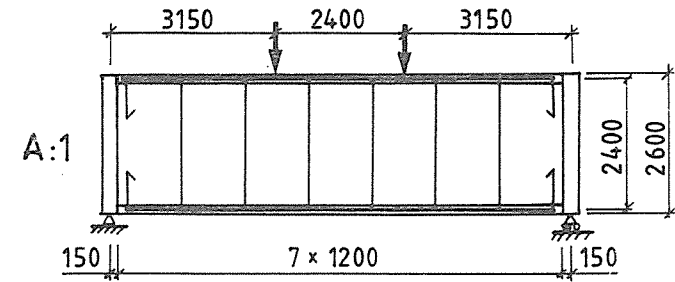


Fig. 4. The load arrangements.

The test programme is presented in Table 1.

Table 1. The test programme.

Test No.	Arrangement	Shear keys	Precracked joints
1	A:1	No	No
2	A:1	No	Yes
3	A:2	No	"
4	A:1	Yes	"
5	B	No	"
6	B	Yes	"

TEST RESULTS

Slab fields type A (test No. 1-4)

The primary shear failure at a joint was indicated by failures in the tie beams. After these primary shear failures the load capacity increased up to a maximum level. The load increase led to large relative displacements along the joints. The final decrease in load capacity was caused by failure in the compression zone of a slab panel.

Fig. 5 shows a slab field after the test has been finished.

Teori

Det særlige ved samlingen - i bæreevnmæssig henseende - er, at det er en konstruktion med to forskellige materialer, betinget af udformning og udførelse af samlingen:

dels en elementsøjle af beton, fremstillet under gode produktionsforhold på fabrik,

dels en mørtelfuge, hvor materialet er bestemt af, at det skal kunne anbringes i en fuge med forholdsvis små dimensioner, - og udført på byggeplads under forhold, der kan gøre det vanskeligt at opnå en god kvalitet af mørtlen i fugen.

Med forskellig elasticitetskoefficient og tværuvidelseskoefficient i betonen og i mørtlen - hvilket typisk vil være tilfældet (selv med samme trykstyrke for beton og mørtel) - fremkommer modsat rettede tværspændinger i mørtlen og betonen.

Disse tværspændinger vil have en væsentlig indflydelse på samlingens bæreevne.

Det vil typisk være sådan, at de tværspændinger, der optræder i mørtelfugen, er trykspændinger, når samlingen udsættes for en last fra søjlen, der giver tryk over tværnittet.

Disse tværtrykspændinger betyder, at fugemørtlen får en forøget bæreevne i forhold til den normale trykstyrke, som i praksis vil være lavere end betonens trykstyrke.

Samlingens største bæreevne nås efter flydning i mørtlen og omfordeling af forskydningskræfterne i skillefladen mellem fugemørtlen og søjleelement og af tværspændingerne i mørtlen. Denne største bæreevne af mørtelfugen fås med mest muligt af mørtlen i fugen under størst muligt tværtryk.

Der antages følgende mulige brudsituationer:

- brudtilfælde 1) Brud i mørtelfugen, uden søjleelementenderne er urevnet revnede forinden. Denne situation er benævnt søjle "brudtilfælde urevnet søjle".
- brudtilfælde 2) Brud i mørtelfugen, efter at søjleelementenderne er revnede. Denne situation er benævnt "brudtilfælde revnet søjle".
- søjleleende 3) Brud i søjleelementenderne, uden brud i mørtelfugens brudbæreevne fugen.

BÆREEVNE AF MØRTELFUGER MELLEM BETONSØJLEELEMENTER

Henning Larsen
Danmarks tekniske Højskole
Lyngby, Danmark

I præfabrikerede fleretages bygninger med betonsøjler som bærende, lodrette bygningsdele ses dels hushøje søjleelementer, gående i én længde igennem alle etagerne (maksimalt omkring 4-5 etager), dels etagehøje søjleelementer med en samling for hver etage, udformet ofte som en mørtelfuge.

Denne samling behandles her.

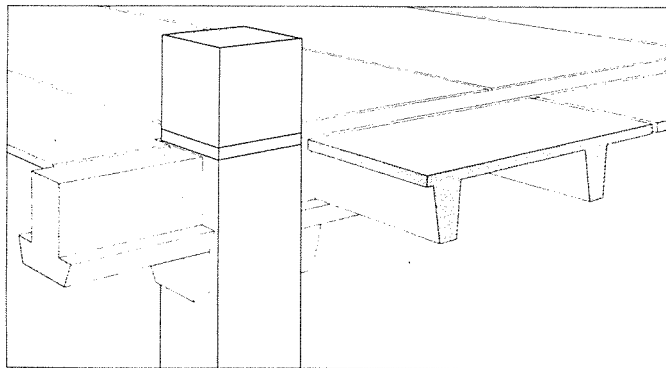


Fig. 1. Mørtelfugen imellem søjleelementerne.

I tilfældet etagehøje søjleelementer skal lasten fra det område, søjlen dækker i etagerne op igennem bygningen, overføres gennem samlingen (mørtelfugen) imellem søjleelementerne, - på et areal, der er lig med søjletværsnittet eller mindre.

I mange tilfælde har man behov for optimal udnyttelse af bæreevnen af denne samling.

Der præsenteres her (brud) bæreevneformler, opstillet på teoretisk grundlag, omend med mange tilnærmelser (Fig. 1).

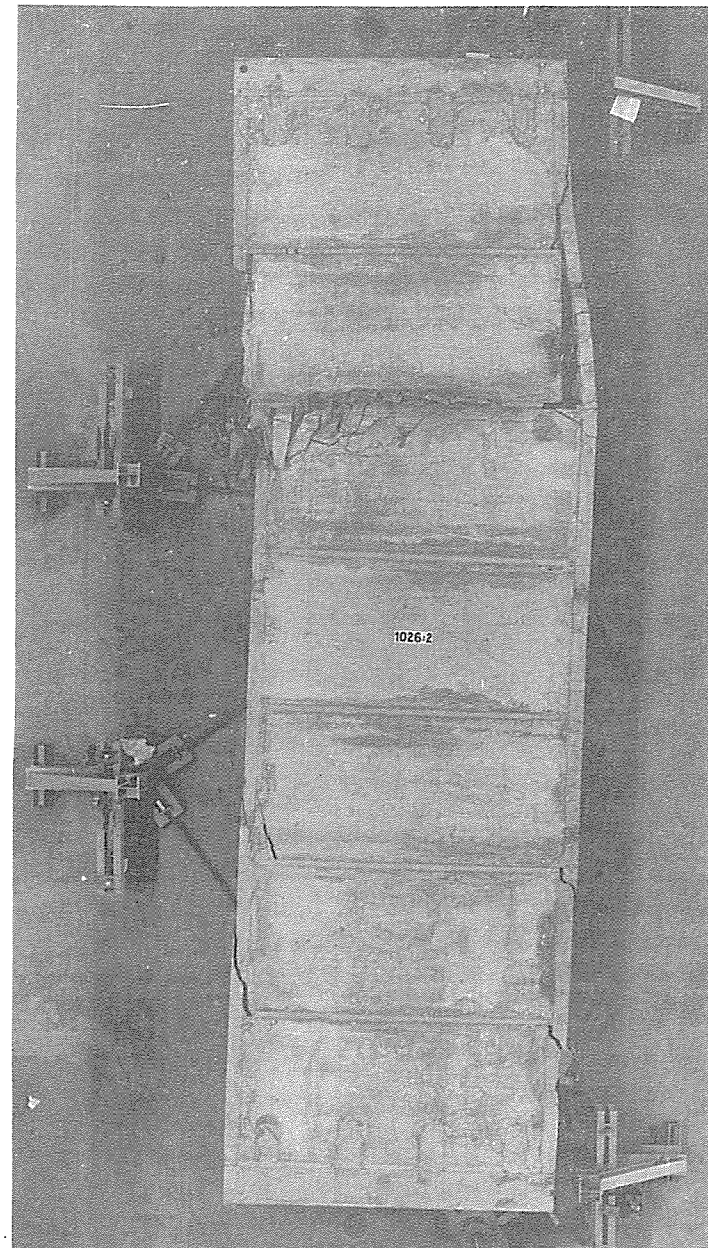


Fig. 5 Slab field after the test has been finished (test No. 2).

Table 2 gives the primary shear failure levels. The numbers in the parenthesis indicate in what sequence the failures occurred. The chord reinforcement reached the yield point stress after these primary shear failures.

The table also gives the maximum load capacity of the slab fields. (The load capacity means the sum of the two point loads.)

Table 2. Primary shear failure levels.

Test No.	Primary shear failure level [kN]				Maximum load Capacity of the slab field [kN]
	Joint No.				
	2	3	6	7	
1	-	198 (2)	183 (1)	146 (3)	488
2	93 (1)	170 (3)	169 (4)	100 (2)	435
3	81 (1)	202 (3)	369 (4)	86 (2)	727
4	230 (2)	230 (2)	222 (1)	-	469

The test results proved that

- When two of the joints were precracked the first joint failure occurred at a much lower level of the shear force.
- The restraining of the edge beams had a small influence of the primary shear failure level in the precracked joints (joint No. 2 and No. 7) but led to a marked increase of the shear failure level in joint number three and joint number six.

The restraining of the edge beams also led to a large increase of the maximum load capacity.

- When the panels were provided with shear keys the primary shear failure level was increased. This increase of the failure level was most obvious in the precracked joints (see Fig. 6).

11. StBK-N3. Skruvförbandsnorm. (Code for bolted connections. In Swedish.) Statens Stålbyggnadskommitté, Svensk Byggtjänst, 1976. 80 pp.
12. Verzeichnis der allgemein bauaufsichtlich zugelassenen Dübel und Ankerschienen. Gruppe 7. Verbundanker. Institut für Bautechnik in Berlin. Stand: 1.4.1983.

4. Anchorage to concrete. ACI Annual Conventions in January 1982, March 1983 and March 1984. To be published as ACI-Special Publications. Summaries Concrete International, 5 (1983) 7, pp. 114-116, 6 (1984) 6, pp. 107-108.
5. Paterson, W. S. Fixings in concrete. Concrete 16 (1982) 10, pp. 51 - 54.
6. Elfgren, Lennart & Eriksson, Anders. Adhesive anchors. Progress Report, June 1984. Borås 1983. The National Swedish Testing Institute, Building Technology, Work Report SP-A 83-14. 35 pp.
7. Elfgren, Lennart. Förankringar i betongkonstruktioner. Byggnadsteknikdag vid Statens Provningsanstalt, Borås den 10 okt. 1984. (Fixings in concrete structures. Paper presented at a Building Technology Day at the National Swedish Testing Institute, Borås, October 10, 1984. In Swedish). Luleå 1984, Luleå University of Technology, Division of Structural Engineering, Paper 84:08. 12 pp.
8. Granlund, Stig-Ola & Marklund, Arne. Kemankare. Finit elementmodellering av last-deformationsegenskaper vid monotont ökande last. (Adhesive anchors. Finite element modelling of load-deformation relationships for monotonically increasing loads. In Swedish). Luleå 1984, Luleå University of Technology, Division of Structural Engineering, Paper 84:04. 16 pp.
9. Helgevold, Hakån jr & Kirknes, Svein. Klebeankere i betong. Samband mellom laster og deformasjoner for forskjellige innlimingslengder. (Adhesive anchors in concrete structures. Load-deformation relationships for various bond lengths. In Norwegian). Luleå 1984, Luleå University of Technology, Division of Structural Engineering, Diploma Work 1984:17E. 74 pp.
10. Enroth, Lars & Jansson, Lars. Infästningar i betongkonstruktioner. Förankringskapacitet hos ingjutna och fastlimmade stänger. (Anchor bolts in concrete structures. Load-carrying capacity for embedded bolts and adhesive anchors. In Swedish). Luleå 1984, Luleå University of Technology, Division of Structural Engineering, Diploma Work 1984: 87E. 92 pp.

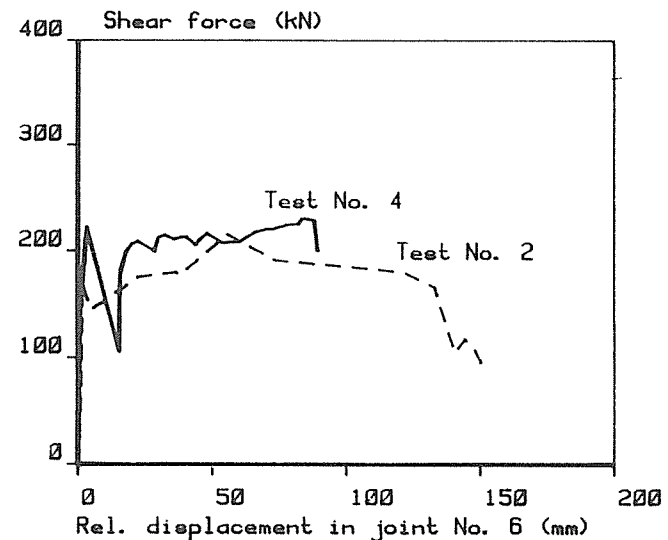
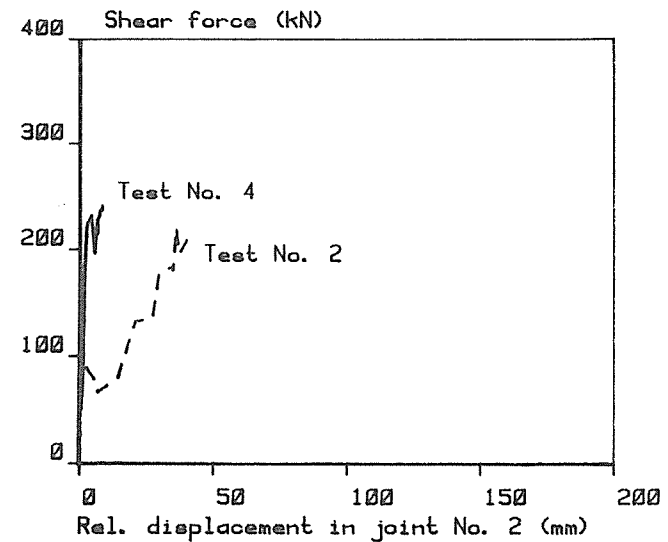


Fig. 6. Examples showing the relations between the relative displacement in a joint and the shear force in the joint. In test No. 4 the slab panels were provided with shear keys.

Slab fields type B

Fig. 7 shows the relation between the mid span deformation and the load capacity for the slab fields type B.

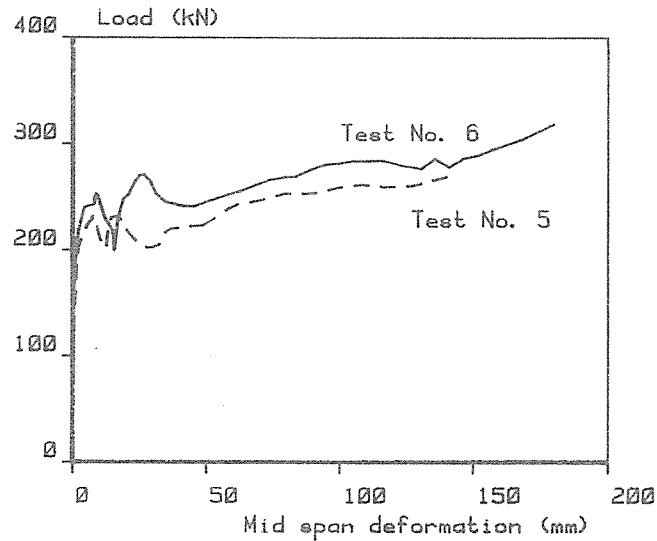


Fig. 7. The relation between the mid span deformation and the load capacity.

At a load level of about 200 kN the first bending crack in a joint was observed. Then, after a small increase of the load, there was a relative displacement in one of the precracked joints. Gradually there were relative displacements also in the other joints. At the maximum load level a longitudinal crack in the outermost panel led to an abrupt failure. This crack appeared between the edge beam and the middle of the panel.

The influence of the shear keys (test No. 6) was negligible.

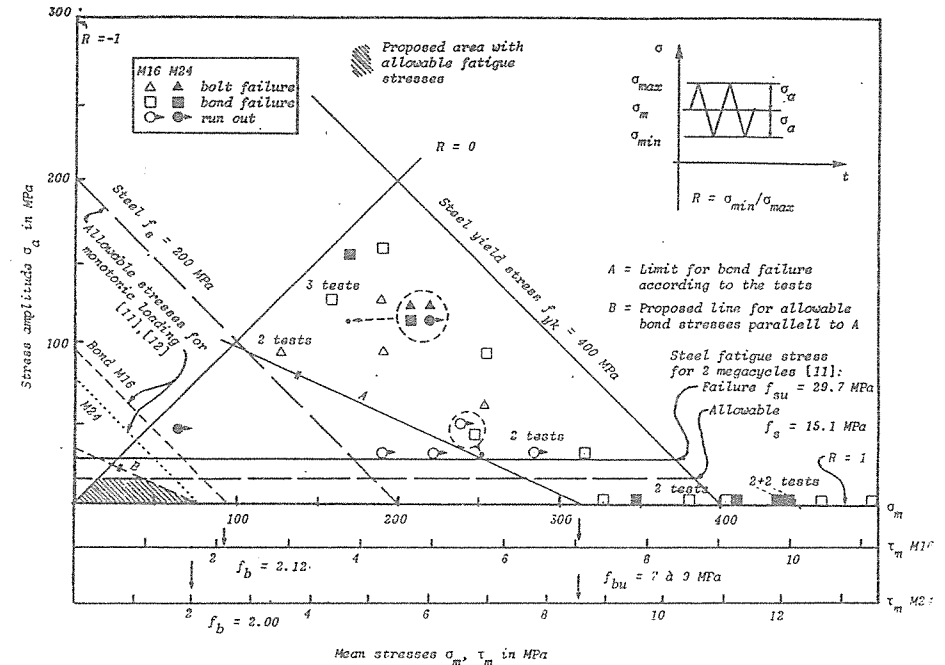


Fig 6. Haigh diagram. The shaded area in the lower left corner of the diagram indicates a proposed area with allowable fatigue stresses for a concrete compressive strength f_{cc} of 22 MPa.

REFERENCES

1. Pusill-Wachtsmuth, Peter & Eligehausen, Rolf. Stand der Befestigungstechnik im Stahlbetonbau. Zürich 1982, IABSE Surveys S-19/82, 32 pp.
2. Seghezzi, Hans Dieter. Wirtschaftliche und sichere befestigungssysteme für die Baupraxis. Betonwerk + Fertigteil-Technik, 49 (1983) 1, pp. 41 - 45, Heft 49 (1983) 2, pp. 117 - 123.
3. Jokela, Jukka & Rämä, Markku. Behaviour, use and safety of fixings in concrete. In: Nordic Concrete Research 1983. Oslo 1983, The Nordic Concrete Federation, Publication 2. Pp. 125 - 136.

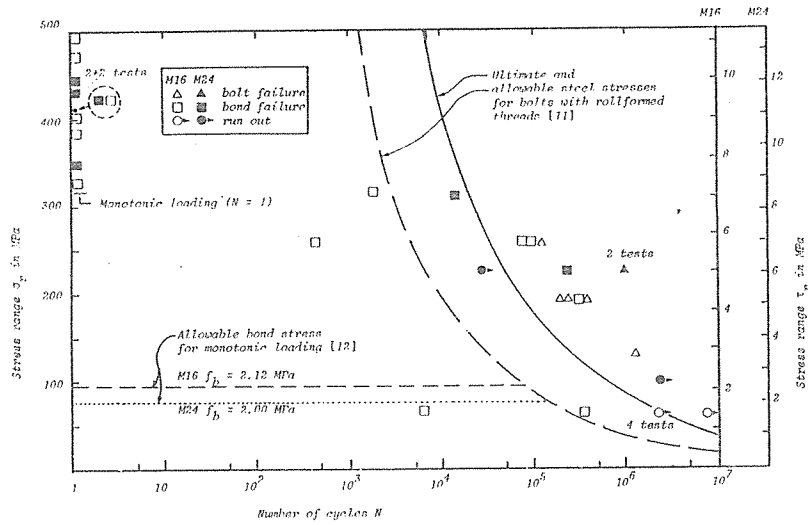


Fig 5. Wöhler diagram for M16 and M24 bolts. The stress areas used for calculating the tensile stresses are 157 mm² and 353 mm² and the stress areas used for calculating the bond stresses are $\pi \cdot 18 \cdot 125 = 7070 \text{ mm}^2$ and $\pi \cdot 28 \cdot 210 = 18472 \text{ mm}^2$. (A and C bolts).

A comparison between the test results of the slab fields type A and the slab fields type B shows:

- The first joint failure occurred at a lower load level in the slab fields type A.
- The maximum load capacity was higher in the slab fields type A.

This is illustrated in Fig. 8.

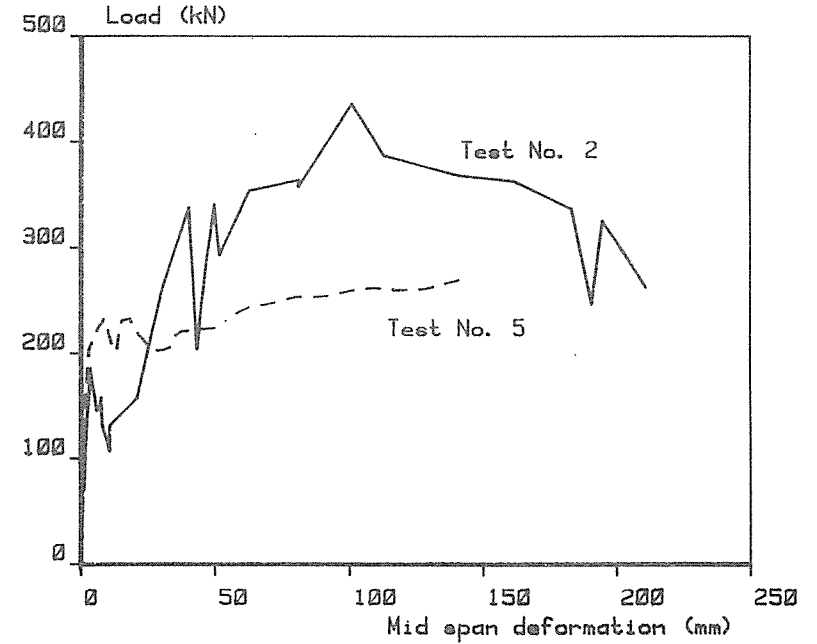


Fig. 8. The relation between the mid span deformation and the load capacity for test No. 2 (slab field type A) and test No. 5 (slab field type B).

REFERENCE

Svensson, Steve. Skivverkan i elementbjälklag. En serie pilotförsök. Göteborg 1985, Chalmers tekniska högskola, Avd. Betongbyggnad, Rapport 85:2.

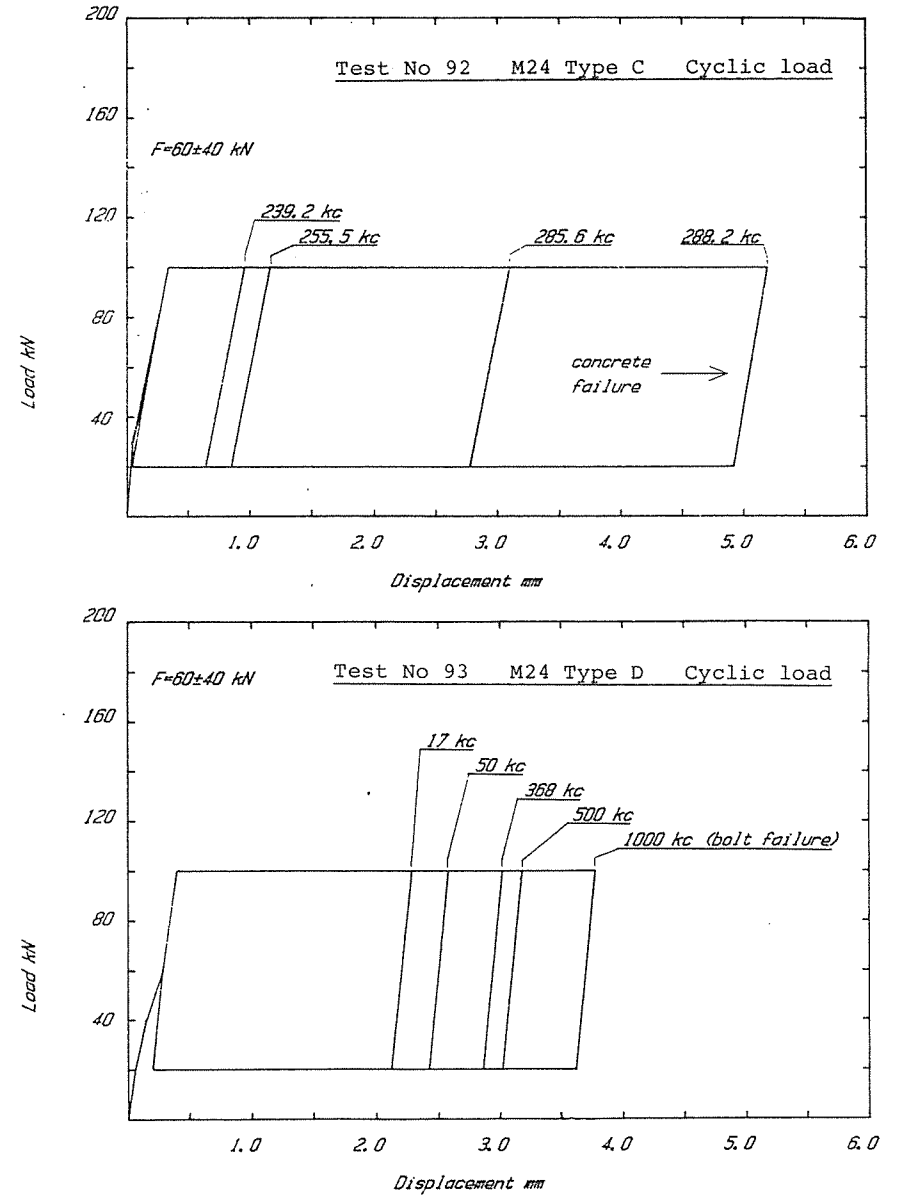


Fig 4. Load-displacement diagrams for cyclic loading of M24 bolts.

RESISTANCE OF LOCALLY DAMAGED PRECAST BUILDINGS - INFLUENCE OF THE STRUCTURAL CONNECTIONS

Björn Engström, M.Sc., Research Ass.
Chalmers University of Technology, Division of Concrete Structures,
Göteborg, Sweden

PREFACE

This paper is based on a study carried out at Chalmers University of Technology, Division of Concrete Structures. The study is part of an extensive research project entitled "Structural Connections in Precast Buildings" which is still, since 1982, under realization. The project is financially supported equally by the "Swedish Council for Building Research" and the "Swedish Foundation for Concrete Research" and is supervised by the Head of the Division of Concrete Structures, Professor Krister Cederwall.

The results of this specific study will be more comprehensively presented in /1/.

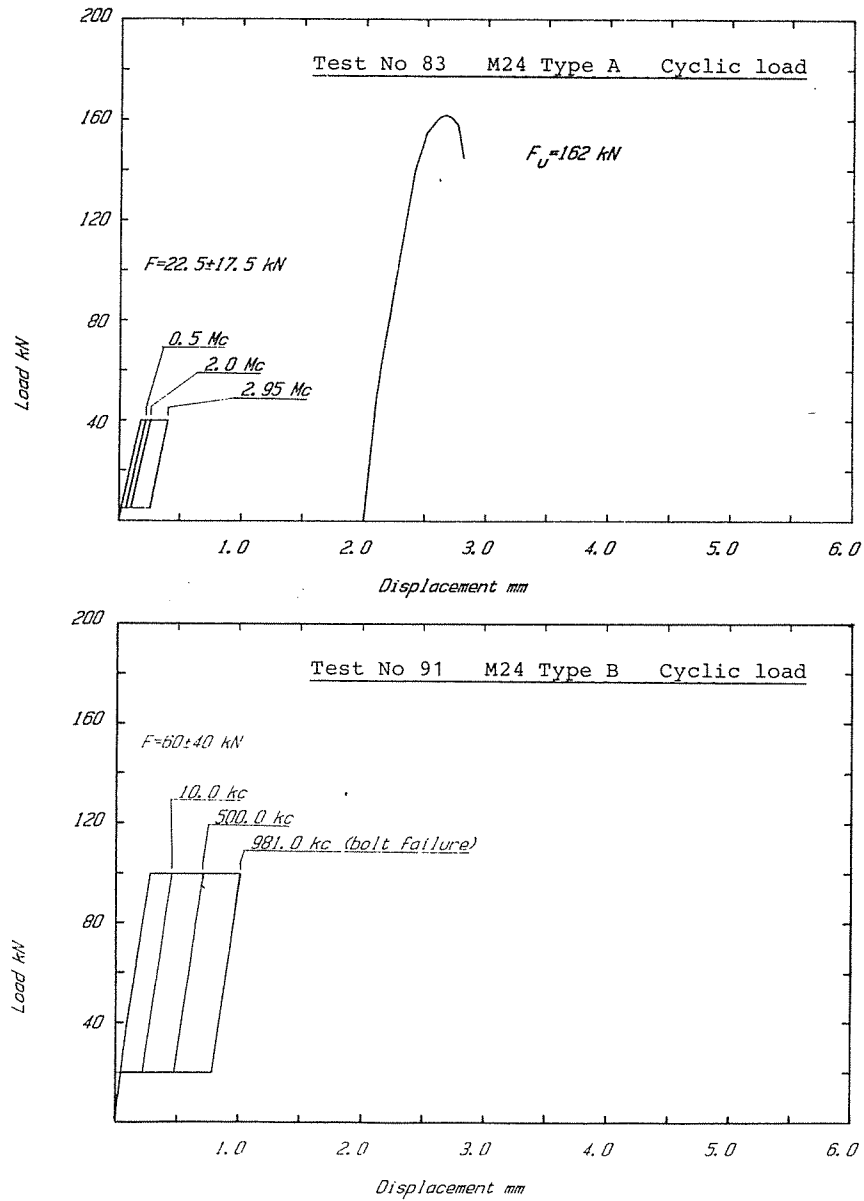


Fig 3. Load-displacements diagrams for cyclic loading of M24 bolts.

1 ALTERNATIVE LOAD-BEARING SYSTEMS IN COLLAPSE SITUATIONS

Even if accidental loading results in damage and failure of vital structural members, a progressive collapse must be prevented. Consequently, the damaged part of the structure should be bridged over by inbuilt alternative load-bearing systems. It is especially important to prevent the structural components immediately around the damaged area from falling. Otherwise, they in turn may initiate a progressive collapse.

The behaviour of a precast concrete structure is to a great extent depending on the properties of the structural connections. To get sufficient tensile strength, the connections must be provided with tie bars or other connecting arrangements from steel.

Immediately after the occurrence of a local damage, the adjacent structural members will start to deflect, be displaced, or even fall. Initially, the resistance against displacements in a possible new mode of action is small. Consequently, the structural connections around the damaged area may be overloaded and, for instance, yielding may be achieved. Hence, in order to analyse the collapse situation, it is necessary to consider the behaviour of the connections in the post-yield and ultimate states. Normally, the load-bearing capacity will vary with the deflections and displacements of the structural members constituting the new load-bearing system. In a dynamic analysis, it is essential to consider this development of the load-bearing capacity.

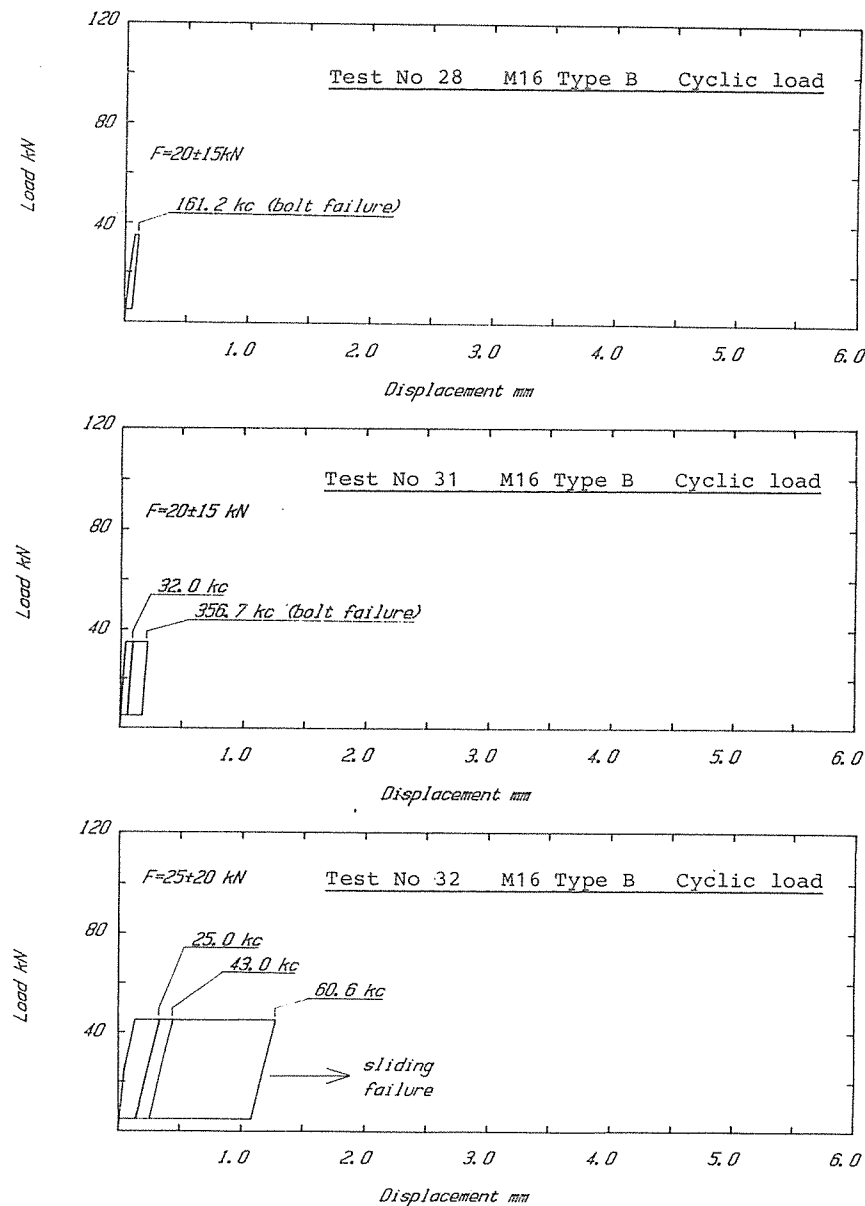


Fig 2. Load-displacement diagrams for cyclic loading of M16 bolts.

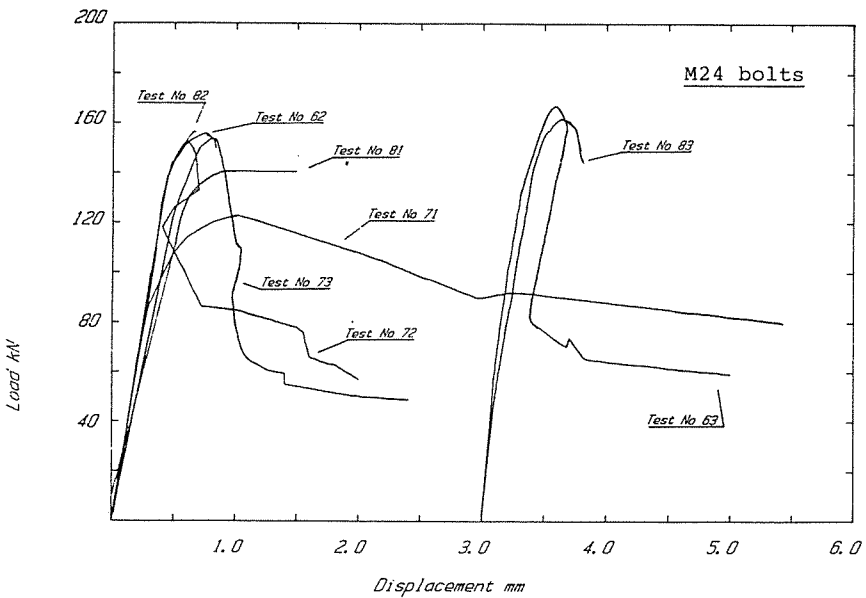
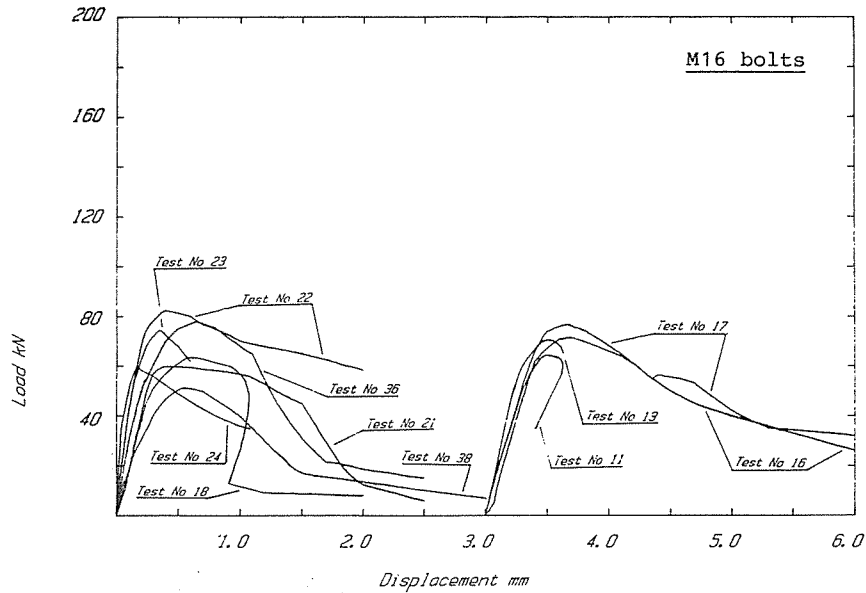


Fig 1. Load-displacement curves for monotonic loading.

2 LOAD-DISPLACEMENT CHARACTERISTICS FOR TIE CONNECTIONS

2.1 Tests on simple tie connections loaded to failure

The most simple type of a tie connection between two precast units consists of a reinforcement bar directly embedded and anchored in the connected components, which are separated only by one weak joint section or a transverse crack, see Fig. 1a. If the tensile strength of the precast units is high enough to prevent transverse cracking, the elongation of the connection will be concentrated to the joint section when the precast units are forced apart. This condition is normally valid in precast large-panel structures, as the reinforcement content is small in the connections compared with the cross-sections of the precast units.

In order to study the basic behaviour of tie connections when exposed to large displacements, especially within the plastic range, as well as to find out how to improve the ductility, several test series have been executed at Chalmers University of Technology /2/. Various simple types of tie connections were loaded in pure tension, pure bending or combined normal and transverse loading.

The test methods and the results from the tests are further discussed in /2/, where also methods for estimation of the ultimate deformations of tie connections with different types of tie bars are suggested. Tie bars from ribbed hot-rolled bars anchored by bond, smooth hot-rolled bars anchored by end-hooks, prestressing strands anchored by end-hooks in combination with bond, and prestressing wires with intentionally slipping end-anchors were examined in the tests.

The tensile tests, for instance, were executed on simplified tie connections according to Fig. 1a. Typical load-displacement relationships received in the tests are presented in Fig. 1b for connections provided with ribbed hot-rolled tie bars. The anchorage length was sufficient to enable anchorage of the fractural load of the tie bars. The elongation at fracture, δ_u , was depending on the properties of the steel, the size of the tie bar and the anchorage conditions. In Fig. 1b, the positive effect on the ductility of increased size of the tie bar and of decreased concrete strength in the anchorage zone is illustrated.

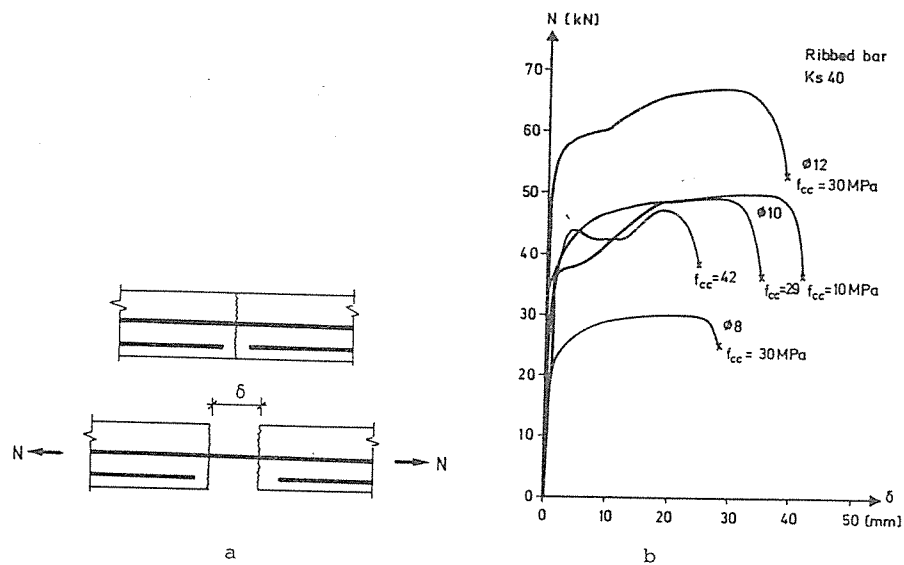


Fig. 1. Tensile tests on simplified tie connections
 a. Tie connection exposed to longitudinal tensile loading
 b. Received relationships between the tensile force N and the elongation δ for tie connections provided with ribbed hot-rolled tie bars. The test results illustrate the influence of the size of the bar and the concrete strength.

Table 4. Results from tests with M24 bolts.

Anchor size M24. Hole depth 210 mm. Hole diameter 28 mm (A,C), 32 mm (B,D).

Test No	Type	Load level	Number of cycles	Ultimate load	Type failure
		F \pm Δ F kN	kilocycles	F _u kN	
61	A	60 \pm 55	16,2	-	Sliding
62	A	Monotonic	-	154	
63	A	60 \pm 40	30,0	167	
71	B	Monotonic	-	123	
72	B	Monotonic	-	153	
73	C	Monotonic	-	156	
81	D	Monotonic	-	144	
82	B	Monotonic	-	>156	(a)
83	A	22,5 \pm 17,5	>2950	162	
91	B	60 \pm 40	981,0	-	Bolt failure
92	C	60 \pm 40	288,2	-	Concrete failure
93	D	60 \pm 40	>1000	-	Bolt failure

(a) old capsule

ACKNOWLEDGEMENT

The tests presented here have been planned and carried out by the authors under the supervision of Lennart Ågårdh. In the laboratory work valuable assistance has been given by Kjell Demker, Per-Anders Johansson, Sven-Agne Nilsson and Dan Sellman. The drawings have been made by Lars Jansson.

Table 3. Results from tests with M16 bolts.

Anchor size M16. Hole depth 125 mm. Hole diameter 18 mm.

Test No	Type	Load level	Number of cycles	Ultimate load	Type of failure
		F±ΔF kN	kilocycles	F _u kN	
11	A	30±5	>2000	64,5	
12	A	40±5	280	-	Sliding
13	A	35±5	>2000	70,5	
14	A	40±5	>2000	-	(a)
15	A	50±5	6,6	-	Sliding
16	A	45±5	>2000	71,5	
17	A	45±5	>8000	77,0	
18	A	Monotonic	-	63,5	
21	B	Monotonic	-	60,0	
22	B	Monotonic	-	82,5	
23	A	Monotonic	-	74,4	
24	A	Monotonic	-	60,1	
25	B	30±25	1,8	-	Sliding
26	B	25±20	0,4	-	Sliding
27	B	25±20	79,0	-	Sliding+bolt
28	B	20±15	161,2	-	Bolt failure
31	B	20±15	356,7	-	Bolt failure
32	B	25±20	60,6	-	Sliding (b)
33	B	30±15	231,7	-	Bolt failure
34	B	40±10	1166,0	-	Bolt failure
35	C	30±20	119,4	-	Bolt failure
36	C	Monotonic	-	77,8	
37	C	40±15	290,2	-	Sliding
38	C	Monotonic	-	51,5	

(a) Interruption in electric power supply

(b) The bolt had been hit by sudden load peak with a maximum value of 80 kN

2.2 The characteristic behaviour of tie connections loaded in tension

Tie connections with entirely anchored tie bars, by bond or end-anchors, can be characterized by simplified relationships between the tensile force and the elongation. In Fig. 2 such schematic relationships, based on test results, are presented for tie connections provided with a) ribbed bars of hot-rolled steel anchored by bond and b) end-anchored prestressing strands.

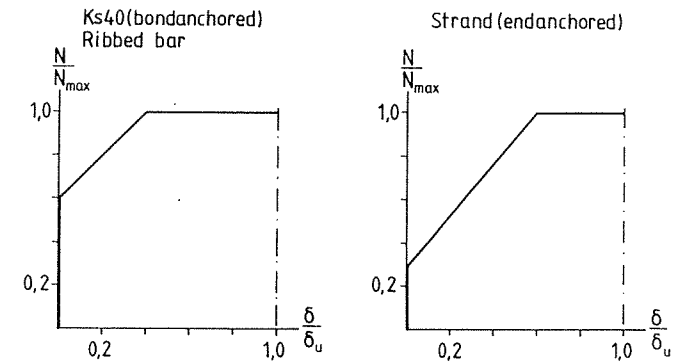


Fig. 2. Schematic relationships between the tensile force N and the elongation δ for connections with tie bars from a) hot-rolled ribbed bars anchored by bond and b) end-anchored prestressing strands.

The area, which is bounded by the tensile force curve in the load-elongation relationship represents the strain energy W_{int} . In order to describe the efficiency of a tie connection, an efficiency factor η_{ef} is introduced, defined as the ratio between the total strain energy for a certain value of the elongation $W_{int}(\delta)$ and the formal product $N_{max} \delta_u$. The strain energy developments, for the tie connections characterized by the schematic load-displacement relationships above, are presented in

Fig. 3.

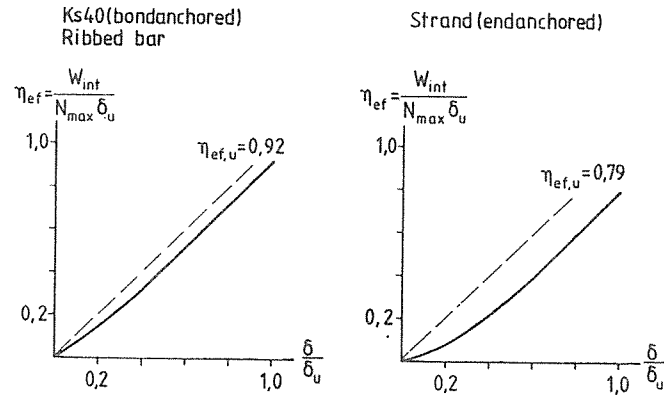


Fig. 3. Strain-energy developments, based on the schematic load-elongation relationships in Fig. 2, for connections with tie bars from a) hot-rolled ribbed bars anchored by bond and b) end-anchored prestressing strands. For comparison, the strain energy developments for ideally plastic tie connections are indicated with dotted lines.

the bolts tested with cyclic loading the test was stopped after two million load cycles. A loading to failure with a monotonically increasing load was then performed.

Load-displacement diagrams for the tests with monotonically increasing loads are shown in Figure 1. The maximum load was usually registered for a displacement of about 1 mm. After the maximum load the bolts mostly have a considerable rest load capacity due to friction.

In Figures 2 - 4 examples are given of load-displacement curves from the cyclic tests. It should be noted that the allowable static load for M16 bolts is 15 kN and for M24 bolts 37 kN according to the rules in the Federal Republic of Germany [12]. The Swedish rules have approximately the same values. The applied loads are considerably higher.

The cyclic tests are also illustrated in a Wöhler diagram in Figure 5 and in a Haigh diagram in Figure 6. The Wöhler diagram shows the influence of the stress range on the fatigue capacity. Different mean stresses have been used for different bolts, which must be born in mind when the diagram is interpreted. The Haigh diagram shows the influence of the mean stress σ_m and the stress amplitude σ_a .

Ultimate and allowable steel stresses for bolts with roll-formed threads are given in the figures according to [11] for both monotonic loading and fatigue loading. Allowable bond stresses for monotonic loading are given according to [12]. Although the number of tests is very limited the tendency is quite clear. Adhesive anchors seem to have a good capacity to withstand cyclic loading. No bond failure occurred for fatigue stresses $\sigma_m \pm \sigma_a$ giving bond stresses under the inclined line A in Figure 6. With a safety factor of three this leads to proposed allowable bond stresses as indicated with a shaded area in the lower left corner of Figure 6.

Table 1. Test program for M16 bolts. The table indicates how many tests that were performed with each type of anchor A, B or C.

Mean Load Level kN	Load Amplitude				
	kN				
	±5	±10	±15	±20	±25
20			2B		
25				3B	
30	2		B	C	B
35	A				
40	2A	B	C		
45	2A				
50	A				

Table 2. Test program for M24 bolts. The table indicates how many tests that were performed with each type of anchor A, B, C or D.

Mean Load Level kN	Load Amplitude		
	kN		
	±17.5	±40	±55
22.5	A		
60		A,B,C,D	A

TEST RESULTS

The test results are summarized in Tables 3 and 4 and in Figures 1 - 5.

In the tables the number of load cycles and the type of failure are given for each individual bolt. For some of

3 AN APPROACH FOR DYNAMIC ANALYSES OF COLLAPSE SITUATIONS

3.1 Presumptions for the analysis

A method for analyses of collapse situations in precast buildings will be presented in the following as it is applied on a simple example. In the example a wall panel at the corner of a building has lost the edge support according to Fig. 4a. The method, however, is generally applicable and will be used in the following chapter for analyses of different collapse situations.

If a structural load-bearing member is damaged or totally destroyed due to accidental loading, the load which was carried by the actual member must be transferred to the remaining parts of the structure. The precast units immediately above and around the damaged area may in this situations form an alternative load-bearing system.

In the actual example the edge support of the wall-panel is assumed to be totally out of order. An alternative load-bearing system can be formed by the wall panel acting as a cantilever. Any resistance against vertical loads will depend on the location and behaviour of possible tie connections. In the example, tie bars are placed vertically at point 1 and horizontally at point 2, see Fig. 4a.

In a simplified analysis it is assumed that the precast components are rigid and thus, all deformations will be concentrated to the connections.

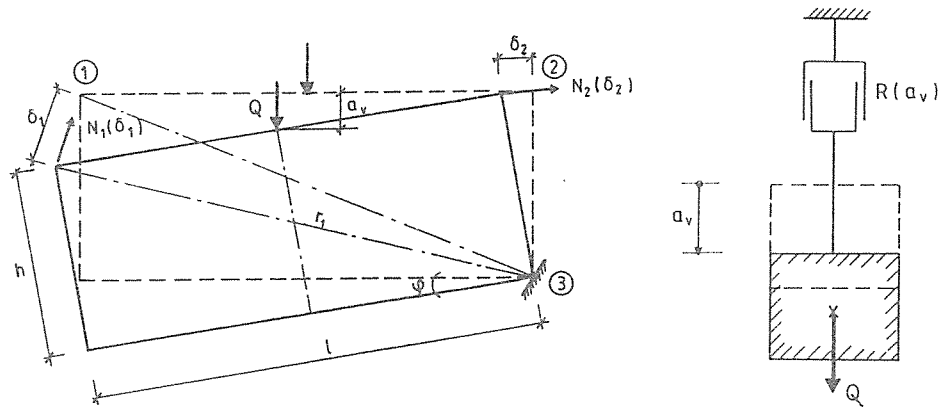


Fig. 4. Example of application - collapse situation in a precast wall
 a. Assumed load-bearing system
 b. Corresponding one-degree-freedom system.

After the loss of the edge support, the wall panel will tend to deflect because of the weight of the panel and the load on the wall. The panel will start to rotate on the remaining support at point 3. During the deflection course the tie bars will be elongated as indicated in Fig. 4a. For a certain rotation ϕ , the tie bars at point 1 and 2 will reach the following elongations respectively

$$\delta_1 = \sqrt{l^2 + h^2} \cdot \phi \quad \text{and} \quad \delta_2 = h\phi \quad (1)$$

where h is height of the panel,
 l length of the panel.

The wall load and the weight of the panel are now represented by a driving force Q acting vertically. The driving force is assumed to be placed at the mid point of the top edge of the wall panel. The driving force can be placed anywhere along an initially vertical line through the center of gravity of the wall panel without influencing the result of the analysis.

The use of adhesive anchors has expanded rapidly. In 1984 about half a million anchors were placed in Sweden and that is three times as many anchors as were placed in 1979. The most common dimensions are ϕ 10, ϕ 12 and ϕ 16 mm. They are used for installations, to support brick and other facade elements and for fixings of different components in prefabricated buildings. Larger dimensions such as ϕ 20, ϕ 24, ϕ 27 and ϕ 32 mm are finding increasing applications for the connections of structural loadbearing components such as columns and beams.

In order to study the functions of adhesive anchors a joint project is undertaken by Luleå University of Technology and the National Swedish Testing Institute in Borås. The project is supported by the Swedish Council for Building Research and by producers and suppliers of adhesive anchors. Preliminary results have earlier been reported in [6] - [10].

In this paper tests with fatigue loading are reported. The tests were carried out in 1983 and 1984 at the National Swedish Testing Laboratory in Borås.

TEST PROGRAM

In all 36 bolts have been tested. Two bolt dimensions have been used, M16 and M24. The bolts were supplied by four different manufacturers A, B, C and D. Seventeen M16 bolts and six M24 bolts were tested with different cyclic loads according to Tables 1 and 2. Seven M16 bolts and six M24 bolts were tested with monotonically increasing loads to obtain reference values of the static capacity.

The concrete had a compressive strength f_{cc} of 22 MPa determined on 150 mm cubes. The age of the concrete varied between 128 and 300 days when it was loaded. The bolts were usually mounted in the concrete 1 to 5 days before the testing was started.

ADHESIVE ANCHORS SUBJECTED TO FATIGUE LOADING

Lennart Elfgren

Division of Structural Engineering, Luleå University of Technology, S-951 87 LULEÅ, Sweden

Anders Eriksson

Building Department, Älvdalens kommun, S-796 01 ÄLVDALEN, Sweden

Roger Anneling

Laboratory for Building Technology, National Swedish Testing Institute, S-501 15 BORÅS, Sweden

INTRODUCTION

A common problem in building technology is the anchorage of loads and the design of anchors and other fixings and attachments to a structure. There are many solutions to this problem and several types of anchors have been developed. In Sweden approximately some 20 to 25 millions high capacity (≥ 1 kN) anchors are used every year. The total costs for these anchors are at least 300 million Swedish crowns (300 MSEK).

Internationally, research and development regarding fastening technique has increased during the last ten years and investigations are now in progress in many places in Europe and the United States [1 - 5].

An interesting type of anchor is the adhesive anchor. It consists of a threaded steel bolt which is placed in a hole drilled into a concrete structure. The anchor is there glued to the walls of the hole. The adhesive is usually built up of a two component polyester resin (based on e.g. maleic and fumaric acids, styrol, and benzoyl peroxide as hardener).

For a rotation ϕ the vertical displacement of the driving force will be

$$a_v = \frac{l}{2} \phi \tag{2}$$

However, the rotation will be counteracted by the tensile forces in the activated tie bars. The tie bar forces will act in the same direction as the connecting points 1 and 2 will be displaced. For a given state of deflection, defined by the rotation angle ϕ , the tensile forces in the tie bars $N_1(\delta_1)$ and $N_2(\delta_2)$ can be derived from the tie connection characteristics.

3.2 Static resistance of the alternative load-bearing system

For static equilibrium between the driving force Q and the counteracting forces in the tie bars $N_1(\delta)$ and $N_2(\delta)$ the following condition must be fulfilled.

$$Q \frac{l}{2} = \sqrt{l^2+h^2} \cdot N_1(\delta_1) + h \cdot N_2(\delta_2) \tag{3}$$

Now, the resistance R of the alternative load-bearing system is defined as the ability of the internal forces to statically balance a driving force placed at the mid-point on the top of the wall-panel.

The static resistance R will be a function of the elongations of the tie connections which in turn are functions of the vertical displacement a_v of the driving force

$$R(a_v) = R_1(a_v) + R_2(a_v) = \frac{2}{l} \left[\sqrt{l^2+h^2} N_1(\delta_1) + h N_2(\delta_2) \right] \tag{4}$$

where δ_1 and δ_2 are functions of a_v according to Eq. (1) and Eq. (2)

$$\delta_1 = \frac{2\sqrt{l^2+h^2}}{l} a_v$$

$$\delta_2 = \frac{2h}{l} a_v$$

The maximum possible static resistance will be

$$R_{max} = R_{1,max} + R_{2,max} = \frac{2}{l} \left[\sqrt{l^2+h^2} N_{1,max} + h N_{2,max} \right] \quad (5)$$

However, depending on the actual design of the tie connections, it may be impossible to achieve the maximum resistance. One of the ties may fracture before the tensile force capacity is reached in the other connection. In this respect it is important to consider the mutually deformability of the tie connections.

3.3 Consideration of the dynamic behaviour

For the dynamic analysis the alternative load-bearing system is represented by an one-degree-freedom system according to Fig. 4b. The driving force is regarded as a gravity force which acts constantly during the deflection course. The driving force is counteracted by the resistance $R(a_v)$ which may vary with the vertical displacement of the load-bearing system.

If the driving force Q exceeds the initial resistance $R(a_v=0)$, an immediate state of equilibrium is impossible. Accordingly, the panel begin to rotate influenced by the driving force Q . Hence, the driving force will act dynamically and will accordingly be denoted Q_{dyn} in the following.

However, the time-deflection course will be influenced by the varying resistance $R(a_v)$ of the cantilevering wall panel. The problem is now to find out wheather or not a deflected state of equilibrium is possible to reach. On the safe side, it is now assumed that the support was suddenly removed by the accidental loading. From the

REFERENCES

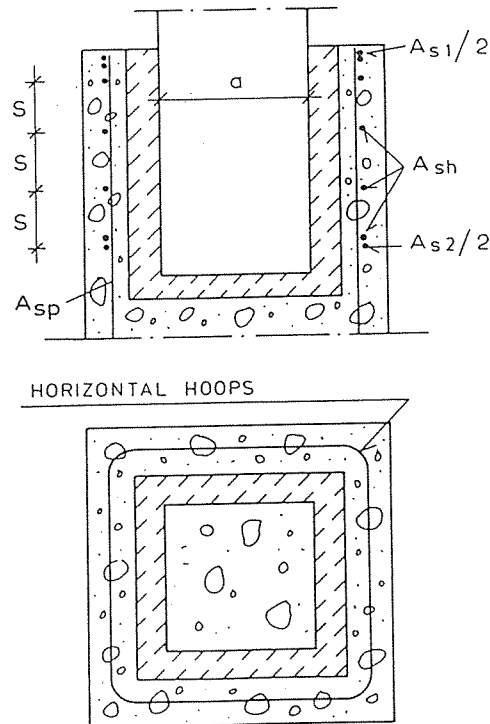
1. Betonielementtirakenteet. Helsinki 1977. Suomen Rakennusinsinöörien liitto, RIL 115. 416 pp.
2. Olin, J., Hakkarainen, T & Rämä, H. Betonielementtien liitokset ja saumat. Espoo 1984, Technical Research Centre of Finland, Research Reports 316. 146 pp. + app. 46 pp. (Connections and joints between precast concrete units. Translation will be published during 1985.)

force N is calculated from the vertical equilibrium condition of the forces as follows:

$$N = V_d - \mu \cdot H_y - V_x \quad (13)$$

The horizontal reinforcement in the middle part of the socket is calculated from formula (11).

The calculation model used previously (Fig. 1) is practicable when the eccentricity of the normal force is so great that the horizontal force H_a of the socket, calculated in conformity with the model, is positive, although the friction force at the base of the column resulting from the normal force is taken into consideration.



BET 1922

Fig. 5. Hoops and stirrups of the socket.

equation of motions, a condition for a possible deflected state of equilibrium can be derived. According to this condition, the external work, W_{ext} , of the constantly acting driving force Q_{dyn} equals the internal work, W_{int} , of the tie connection forces $N_1(\delta_1)$ and $N_2(\delta_2)$ when the downward motion totally ceases.

The downward motion ends for the vertical displacement $a_{v,max}$ of the load-bearing system. The corresponding elongation in the different tie connections i are denoted $\delta_{i,max}$. For each connection i , the following condition must be fulfilled

$$\delta_{i,max} \leq \delta_{i,u}$$

It is possible to choose the maximum elongation δ_{max} in order to achieve an acceptable safety against fracture. However, it should be noted that the elongations of the connections are mutually dependent according to the location of the tie bars within the load-bearing system.

In the actual example, for instance, the connection in point 1 will receive the largest elongation for a certain vertical displacement a_v . If the two connections have the same design and, accordingly, the same ultimate elongation δ_u , the connection in point 1 will be the critical one.

If not extra safety against fracture is aimed at, the design condition will be

$$\delta_{1,max} \leq \delta_u \quad (6)$$

The corresponding elongation $\delta_{2,max}$ of the other connection and the vertical displacement $a_{v,max}$ can be calculated using Eq. (1) and Eq. (2)

$$\delta_{2,max} = \frac{h}{\sqrt{l^2+h^2}} \delta \quad (7)$$

$$a_{v,max} = \frac{l}{2\sqrt{l^2+h^2}} \delta u \quad (8)$$

The energy equilibrium condition now gives

$$W_{ext} = W_{int}$$

$$Q_{dyn} \cdot a_{v,max} = \int_0^{\delta_{1,max}} N_1(\delta_1) d\delta_1 + \int_0^{\delta_{2,max}} N_2(\delta_2) d\delta_2 \quad (9)$$

$$Q_{dyn} \cdot a_{v,max} = W_{int,1}(\delta_{1,max}) + W_{int,2}(\delta_{2,max})$$

If the tie connection characteristics, as defined in Fig. 2 and 3, are introduced in Eq. (9), the following expression is received

$$Q_{dyn} a_{v,max} = \eta_{ef,1}(\delta_{1,max}) N_{1,max} \frac{\delta_{1,u}}{\delta_{1,max}} \delta_{1,max} + \quad (10)$$

$$+ \eta_{ef,2}(\delta_{2,max}) N_{2,max} \frac{\delta_{2,u}}{\delta_{2,max}} \delta_{2,max}$$

$$\text{where } \eta_{ef}(\delta) = \frac{W_{int}(\delta)}{N_{max} \cdot \delta_u}$$

or using Eqs. (6) - (8)

$$Q_{dyn} = \frac{2\sqrt{l^2+h^2}}{l} \eta_{ef,1}(\delta_{1,max}) \frac{\delta_{1,u}}{\delta_{1,max}} N_{1,max} + \quad (11)$$

$$+ \frac{2h}{l} \eta_{ef,2}(\delta_{2,max}) \frac{\delta_{2,u}}{\delta_{2,max}} N_{2,max}$$

Comparing Eq. (5) and Eq. (11) it is possible to recognize the dynamic effects on the possible maximum static resistance.

$$Q_{dyn} = \eta_{ef,1}(\delta_{1,max}) \frac{\delta_{1,u}}{\delta_{1,max}} R_{1,max} + \eta_{ef,2}(\delta_{2,max}) \frac{\delta_{2,u}}{\delta_{2,max}} R_{2,max} \quad (12)$$

into expression (5), the expression

$$V_x = 0.15 f_{ctd} \cdot h \cdot a \quad (10)$$

is obtained for the resultant of bond stress.

The vertical load of the column will produce a splitting force in the socket, when the joint faces are rough.

Stirrups must be placed in the socket to ensure the bond stress used in calculation. The area of horizontal reinforcement for one stirrup section shall be at least

$$A_{sh} = 0.17a \cdot s \cdot \frac{f_{ctk}}{f_{yk}}, \quad (11)$$

where a is the length of the column side (Fig. 4), s is the spacing of stirrups, f_{ctk} is the characteristic tensile strength of grout and f_{yk} is characteristic strength of the stirrups.

6 DESIGN OF THE SOCKET

For the force H_y of the upper edge of the socket (Fig. 2) in different cases, solutions (1) to (3) and (6) to (8) are presented. The hoop area A_{s1} is calculated by dividing the force H_y by the design strength of the reinforcing bar (Fig. 5). The force H_a acting on the lower edge of the socket is calculated from formula (4). Between the lower end of the column and the base of the socket a friction force acts horizontally. If the friction force is great, the force H_a will not necessarily be produced and the hoops of the lower edge are not needed. The required steel amount (Fig. 5) can thus be calculated from the formula

$$A_{s2} = \frac{H_a - \mu \cdot N}{f_{yd}}, \quad (12)$$

where N is the support force of the lower end of the column. The support

5 ROUGH JOINT FACES

When the joint faces are rough, the bond force given in expression (5), can be taken along with the moment equilibrium equation (see Fig. 2) as being formed with regard to the point of action of the force H_a . For the support force H_y of the upper edge in this case the solution reads /2/

$$H_y = \frac{M_d - 0.17a \cdot V_d + 0.9h \cdot H_d - 0.083 \cdot a \cdot V_x}{0.8h + 0.33a \cdot \mu} \quad (6)$$

The notations are given in Figs. 2 and 4.

For the coefficient of friction the value $\mu = 0.6$ representing sliding friction is used. When the value is substituted into expression (6), the expression reads

$$H_y = \frac{M_d - 0.17 a \cdot V_d + 9h \cdot H_d - 0.083a \cdot V_x}{0.8h + 0.2a} \quad (7)$$

When (7) the value $a = h/1.3$ is substituted into expression for the side measurement of the column, the formula

$$H_y = 1.05 \cdot \frac{M_d}{h} + 0.95 H_d - 0.13 V_d - 0.06 V_x \quad (8)$$

is obtained for the joint, in agreement with the recommendations.

If the insertion depth differs from the recommended value $h = 1.3a$, the force H_y is calculated from expression (7). For the bond stress the value

$$v_u = 0.3 f_{ctd} \quad (9)$$

can be used in conformity with the Finnish Building Code, where f_{ctd} is the design value of the tensile strength of grout. When it is substituted

4 EXAMPLES OF APPLICATION

4.1 A system of two perpendicular wall panels cantilevering at the corner of a building

In the following example the building has load-bearing facade walls in two directions. A support at the corner of the building is totally destroyed by accidental loading. An alternative load-bearing system consists of two wall panels placed perpendicular to each other at the corner of the building according to Fig. 5. If the floor slab is connected to the top edges of the wall panels, it can be interacting in the alternative load-bearing system.

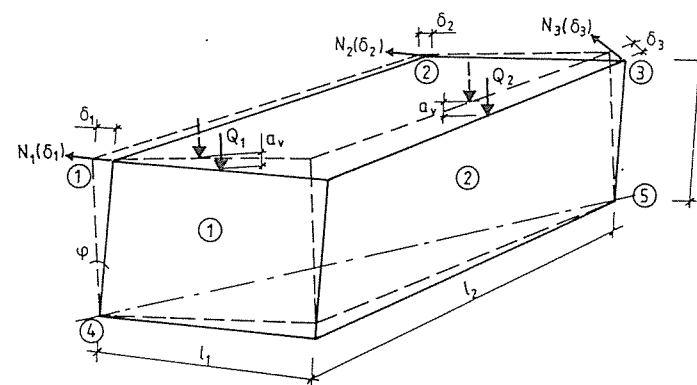


Fig. 5. An alternative load-bearing system at the corner of a building after loss of the outermost support.

After loss of the support, the composed cantilever will tend to rotate around an axis through the points 4 and 5 in Fig. 5. The resistance of the new load-bearing system will depend on the location and design of the tie connections. Tie bars are assumed to be placed in the walls at points 1 and 3. Transverse tie bars are also placed in the floor slab at point 2.

Driving forces Q_1 and Q_2 are placed at the mid-points of the top edges of the wall panels. Each driving force consists of the weight of the panel and the wall load.

For a certain rotation ϕ of the system the tie connections will have the following elongations

$$\begin{aligned} \delta_1 &= \delta_2 = h\phi \\ \delta_2 &= \sqrt{\frac{(\ell_1 \ell_2)^2}{\ell_1^2 + \ell_2^2} + h^2} \cdot \phi \end{aligned} \quad (13)$$

The vertical displacements of the driving forces will be

$$a_{v1} = a_{v2} = \frac{\ell_1 \ell_2}{2\sqrt{\ell_1^2 + \ell_2^2}} \cdot \phi \quad (14)$$

For static equilibrium, the following condition must be fulfilled

$$(Q_1 + Q_2) \frac{\ell_1 \ell_2}{2\sqrt{\ell_1^2 + \ell_2^2}} = N_1 (\delta_1) \cdot h + N_2 (\delta_2) \sqrt{\frac{(\ell_1 \ell_2)^2}{\ell_1^2 + \ell_2^2} + h^2} + N_3 (\delta_3) \cdot h \quad (15)$$

The maximum possible static resistance will be

$$\begin{aligned} R_{\max} &= R_{1,\max} + R_{2,\max} + R_{3,\max} = \\ &= \frac{2\sqrt{\ell_1^2 + \ell_2^2}}{\ell_1 \ell_2} \left[h \cdot N_{1,\max} + \sqrt{\frac{(\ell_1 \ell_2)^2}{\ell_1^2 + \ell_2^2} + h^2} \cdot N_{2,\max} + h \cdot N_{3,\max} \right] \end{aligned} \quad (16)$$

The maximum possible driving force Q_{dyn} , considering the dynamic behaviour will be, with the tie connection characteristics

$$\begin{aligned} (Q_1 + Q_2)_{\text{dyn}} &= \eta_{\text{ef},1} (\delta_{1,\max}) \frac{\delta_{1,u}}{\delta_{1,\max}} R_{1,\max} + \eta_{\text{ef},2} (\delta_{2,\max}) \frac{\delta_{2,u}}{\delta_{2,\max}} R_{2,\max} + \\ &+ \eta_{\text{ef},3} (\delta_{3,\max}) \frac{\delta_{3,u}}{\delta_{3,\max}} R_{3,\max} \end{aligned} \quad (17)$$

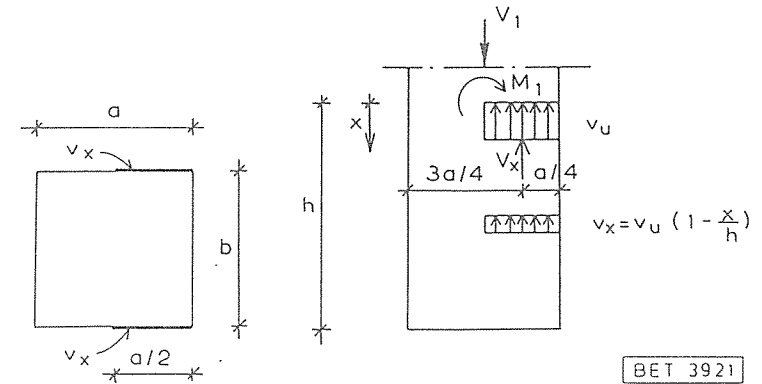


Fig. 4. Vertical bond stresses at the lateral surfaces of the column in the ultimate limit state.

The bond stress will remain unchanged, even if the connection surfaces slide with respect to one another, in other words, the joint will be ductile. The column will therefore be roughened on the surface. The lower-end-column faces will be roughened to such a depth that the bond capacity is maintained although a crevice at the joint is produced due to the shrinkage of grout. Subclause 4.2.4.11 of the National Building Code of Finland mentions that the joint is rough if the surface roughness has a depth of 2-5 mm. In this case the surface of the column and the inner surface of the socket shall be rough.

the location of the bond stress resultant V_y does not differ much from the position of the force H_y . The bond stresses reduce the support force H_y , but in principle, if account is taken of these, they do not influence the design of the socket. The performance model as regards the lower column end is quite similar to that in Fig. 2. The stress distributed along the wall of the socket requires practically the same kind of reinforcement as the concentrated support force H_y .

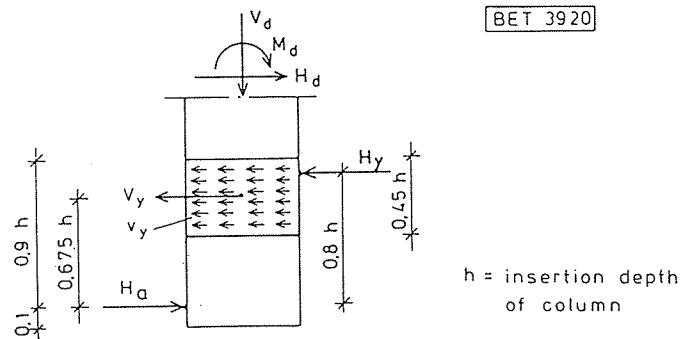


Fig. 3. Horizontal bond stress at the lateral surfaces of the column.

The magnitude of the vertical bond stresses in different parts of the joint is difficult to define accurately. When it is borne in mind that the slips are large in the ultimate limit state and that connection is ductile, the stress distribution as shown in Fig. 4 can be used in the examination. The size of the stress resultant is calculated from the expression

$$V_x = 0.5 v_u \cdot h \cdot a \cdot . \quad (5)$$

The sideways position of the resultant in the section of the column is indicated in Fig. 4.

4.2 A system of a wall panel and an interacting floor slab cantilevering at the corner of the building

In the following example the building has transverse shear walls but no longitudinal load-bearing walls. A support at the corner of the building is totally destroyed by accidental loading. The wall-panel above the damaged area will act as a cantilever in a new alternative load-bearing system. The floor slab is connected to the top edge of the wall panel and will interact in the alternative load-bearing system. After loss of the support, the composed cantilever will tend to rotate around an axis through the points 3 and 4 in Fig. 6.

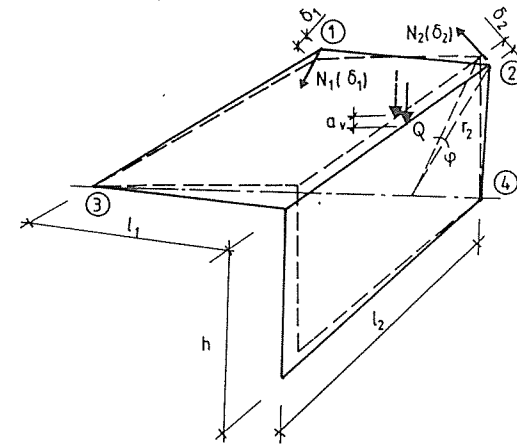


Fig. 6. An alternative load-bearing system at the corner of a shear wall building after loss of the outermost support.

The resistance of the new load-bearing system will depend on the location and design of the tie connections. Tie bars are assumed to be placed along the wall panel at point 2 in Fig. 6. Tie bars are also placed in the floor slab, across and perpendicular to the shear walls, points 1 in Fig. 6.

A driving force Q is placed at the mid-point of the top edge of the wall panel. The driving force consists of the weight of the panel and the wall load.

For a certain rotation ϕ of the system the tie connections will have the following elongations

$$\delta_1 = \frac{\ell_2 \sqrt{\ell_1^2 + h^2}}{\sqrt{\ell_1^2 + \ell_2^2 + h^2}} \phi \quad (18)$$

$$\delta_2 = \frac{h \sqrt{\ell_1^2 + \ell_2^2}}{\sqrt{\ell_1^2 + \ell_2^2 + h^2}} \phi$$

The vertical displacement of the driving force will be

$$a_v = \frac{\ell_1 \ell_2}{2 \sqrt{\ell_1^2 + \ell_2^2 + h^2}} \phi \quad (19)$$

For static equilibrium, the following condition must be fulfilled

$$Q \frac{\ell_1 \ell_2}{2} = N_1 (\delta_1) \ell_2 \sqrt{\ell_1^2 + h^2} + N_2 (\delta_2) h \sqrt{\ell_1^2 + \ell_2^2} \quad (20)$$

The maximum possible static resistance will be

$$R_{\max} = R_{1,\max} + R_{2,\max} = \frac{2}{\ell_1 \ell_2} \left[\ell_2 \sqrt{\ell_1^2 + h^2} \cdot N_{1,\max} + h \sqrt{\ell_1^2 + \ell_2^2} \cdot N_{2,\max} \right] \quad (21)$$

The maximum possible driving force Q_{dyn} , considering the dynamic behaviour will be, with the tie connection characteristics

$$Q_{\text{dyn}} = \eta_{\text{ef},1} (\delta_{1,\max}) \frac{\delta_{1,u}}{\delta_{1,\max}} R_{1,\max} + \eta_{\text{ef},2} (\delta_{2,\max}) \frac{\delta_{2,u}}{\delta_{2,\max}} R_{2,\max} \quad (22)$$

For the actual collapse situation, the influence of different tie connection characteristics is further exemplified in /3/.

about 1.3 x the side measurement of the column. When $a = h/1.3$ is substituted into expression (2), the formula appropriate to the connection agreeing with the recommendations reads

$$H_y = 1.14 \cdot \frac{M_d}{h} + 1.03 H_d - 0.15 V_d \quad (3)$$

The prerequisite for the use of formula (3) is that the insertion depth of the column be about 1.3 x the maximum side measurement of the column.

When the equilibrium equation of forces in the horizontal direction is drawn up, for the force H_a the expression reads

$$H_a = H_y - H_d \quad (4)$$

The shear force of the column end in the socket is equal to H_a .

4 SHEAR STRESSES IN JOINT FACES

At the column/grout interface shear stresses are produced due to friction and bond. Friction is formed at the surfaces where compression is produced owing to external loads. This is taken into consideration by using the coefficient of friction corresponding to the quality of the surfaces. In the lateral surfaces of the column, where no horizontal forces are produced by the external forces shear stresses are being developed as a result of the bond.

The direction and magnitude of the bond stresses are determined by the displacement of the column. In ordinary loading cases the column sinks downwards and at the same time moves sideways. The bond stresses of the lateral surfaces can be divided into the horizontal and vertical components.

The horizontal component of the bond stress is examined on the basis of Fig. 3. The slip between the surfaces in the ultimate limit state is of such magnitude that it can be assumed that the bond stress v_y is distributed uniformly in the area depicted in Fig. 3. As shown in the figure,

In conjunction with this research project separate instructions for the design of socket connection have been prepared.

2 DISTRIBUTION OF THE SUPPORT REACTION OF THE LOWER END OF THE COLUMN

In the ultimate limit state the column turns within the socket and the resultant of the support reaction at the lower end of the column is transmitted from the centre line towards the edge. Its position is dependent on several factors, such as the size of the loads and the dimensions of the socket. In the case of ordinary moment-resisting columns the value $a/6$ can be used as the distance of the resultant of the support reaction from the centre line of the column (Fig. 2). Friction forces acting at the lower end of the column are not taken into consideration, since a full friction force will not necessarily be developed there.

When the moment equilibrium equation with regard to the point of action of the force H_a is formulated, for the force H_y the expression reads /2/

$$H_y = \frac{M_d - 0.17a \cdot V_d + 0.9h \cdot H_d}{0.8h + 0.33a \cdot \mu} \quad (1)$$

The notations are illustrated in Fig. 2. The coefficient μ is the coefficient of friction.

3 SMOOTH JOINT FACES

When the surface of the column is smooth, the value $\mu = 0.3$ which represents sliding friction is used for the coefficient of friction. When this is substituted into expression (1), a simplified expression reads /2/

$$H_y = \frac{M_d - 0.17a \cdot V_d + 0.9h \cdot H_d}{0.8h + 0.1a} \quad (2)$$

It is recommended that the height of the socket be 1.5 x the maximum side measurement of the column. The insertion depth in this case is about

4.3 Catenary action of a longitudinal strip of a floor slab

A strip of a floor slab consists of floor panels placed after each other according to Fig. 7. An internal support is totally destroyed by accidental loading. After loss of the support the floor panels begin to rotate at the remaining supports. For a vertical mid displacement of twice the height of the slab, a catenary will be formed. The resistance of the new load-bearing system will depend on the tie connections between the floor panels. The floor slab in the example is provided with longitudinal tie bars placed mid-depth.

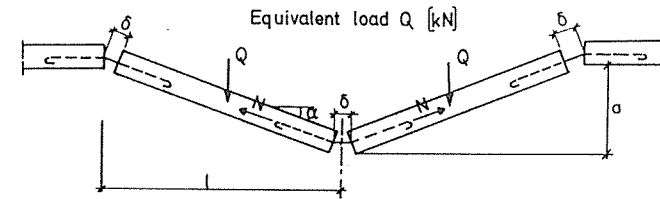


Fig. 7. Catenary action of a longitudinal strip of a floor slab after loss of an internal support.

Equal driving forces Q are placed at the centers of gravity of the rotating floor panels. The driving force consists of the weight of the panel and dead load on the slab.

The elongation of the tie connections are now assumed to reach the same value δ in all the three connections. For a certain vertical mid-displacement a , according to Fig. 7, the elongation of the connections will be

$$\delta = \frac{a^2}{3l} \quad (23)$$

The vertical displacement of the driving forces will be

$$a_v = \frac{a}{2} \quad (24)$$

For static equilibrium in a deflected state, the following condition must be fulfilled

$$Q = 2N \frac{a}{l} \quad (25)$$

The maximum static resistance will be, using Eq. (23)

$$R_{\max} = 2N \frac{a_{\max}}{l} = 2N \sqrt{\frac{3\delta_{\max}}{l}} \quad (26)$$

where $\delta_{\max} \leq \delta_u$

The maximum possible driving force Q_{dyn} , considering the dynamic behaviour, can be derived from an energy equilibrium condition according to Eq. (9)

$$\int_0^{a_{v,\max}} 2Q_{\text{dyn}} da_v = 3 \int_0^{\delta_{\max}} N(\delta) d\delta \quad (27)$$

$$2Q_{\text{dyn}} \frac{a_{\max}}{2} = 3\eta_{\text{ef}}(\delta_{\max}) N_{\max} \frac{\delta_u}{\delta_{\max}} \delta_{\max}$$

using Eq. (23)

$$Q_{\text{dyn}} = \eta_{\text{ef}}(\delta_{\max}) N_{\max} \frac{\delta_u}{\delta_{\max}} \frac{a_{\max}}{l} \quad (28)$$

and with Eq. (26)

$$Q_{\text{dyn}} = \frac{1}{2} \eta_{\text{ef}}(\delta_{\max}) \frac{\delta_u}{\delta_{\max}} R_{\max} \quad (29)$$

COLUMN-TO-BASE CONNECTION IN A SOCKET

Tapani Hakkarainen
 Technical Research Centre of Finland
 Concrete and Silicate Laboratory
 Espoo, Finland

1 GENERAL

The performance model of the connection and the calculation method have been presented in several manuals (Fig. 1). The actual capacity of the connection has been verified as being clearly greater in some cases than the capacity given by the above-mentioned calculation method. Extra capacity results from the bond stresses in joints and from the displacement of the support reaction of the lower end of the column (Fig. 2).

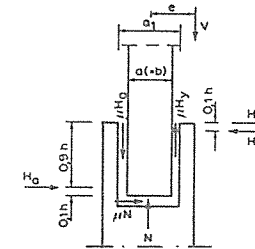


Fig. 1. Performance model of socket connection used previously /1/.

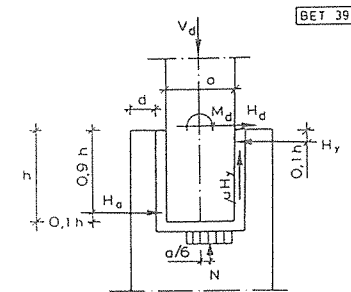


Fig. 2. Forces acting in the column-to-base connection within a socket.

Although the construction of low heavily reinforced corbels has been made possible one should avoid using of them. If they are applied it must be made sure that the tensile stress of the main reinforcement does not exceed the design value and that the corbels are not subjected to any vertical or horizontal loading greater than the design loads.

REFERENCES

1. Sarja, A. Analysis of nonlinear statical properties of reinforced concrete slabs. Espoo 1979, Technical Research Centre of Finland, Building Technology and Community Development, Publ. 16. Pp. 23 - 26.
2. Olin, J., Hakkarainen, T. & Rämä, M. Betonielementtien liitokset ja saumat. Espoo 1984, Technical Research Centre of Finland, Research Reports 316. 146 pp. + app. 46 pp. (Connections and joints between precast concrete units. Translation will be published during 1985.)
3. Ojala, A. Teräsbetoniulokkeen kapasiteetista. Diplomityö. Tampere 1982, Tampereen teknillinen korkeakoulu, rakennustekniikan osasto. 45 pp. (Capacity of reinforced concrete corbels. Master's thesis. Tampere University of Technology.)

REFERENCES

1. Engström, Björn. Utformning och placering av förbindningar i elementbyggda betongstommar med hänsyn till funktionen i rassituationer, (Design and location of tie bars in precast concrete structures with regard to the behaviour in collapse situations). Göteborg, Chalmers tekniska högskola, avd Betongbyggnad, Rapport 85:3. (Ännu ej publicerad.)
2. Engström, Björn. Ductility of tie connections for concrete components in precast structures. Göteborg 1983, Chalmers University of Technology, Division of Concrete Structures, Publikation 83:1.
3. Engström, Björn. Resistance of locally damaged precast walls - influence of tie connection behaviour. CIB-Symposium on Wall-Structures. Warsaw, June 1984. Göteborg 1984, Chalmers University of Technology, Division of Concrete Structures, Publikation 84:1.

DESIGN OF PLAIN ELASTOMERIC BEARING PADS IN PRECAST CONCRETE STRUCTURES

Leidulv Vinje
Chairman Technical Committee,
The Norwegian Precast Concrete Federation,
Chief Structural Engineer,
Nordenfjeldske Spennbetong A/S
Trondheim, Norway

INTRODUCTION

The Norwegian Building Research Institute (NBI) recently conducted a laboratory test program on plain elastomeric bearing pads.

The test program was assigned by The Norwegian Precast Concrete Federation. The results are compared with those of similar German Laboratory studies. Recommended tentative design specifications for plain elastomeric bearing pads in precast concrete structures are presented.

The factors β_1 and β_2 are given in Table 2. They are determined on the basis of the effective depth of the corbel and internal lever arm, and correspond to the 10 o/oo strain in steel in case 1° and to 1.8 o/oo in case 2°. In the latter case the factors also include an additional safety factor of 1.2.

The area of tension reinforcement is calculated from the formula

$$A_s = \frac{T_{sd}}{f_{yd}} \quad (13)$$

In formula (13) the design value for steel greater than 365 MN/m² must not be used.

Fig. 5 shows a hatched area of loading, in which the best result, both economically and technically, is achieved by ordinary corbels.

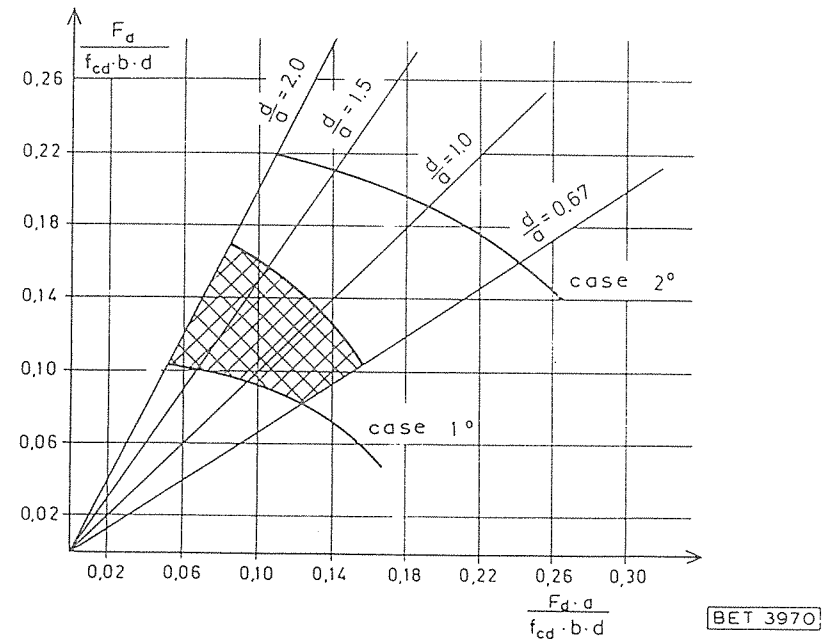


Fig. 5. Load capacities of corbels. The recommendable area of loading is shown by hatching.

4 DESIGN INSTRUCTIONS FOR CORBELS

Design instructions for corbels have been worked out on the basis of the method presented in Chapter 2. Low corbels provided with a heavy reinforcement are also allowed for design but an additional safety factor is required in this case.

In the design of the corbel two extreme cases can be distinguished. One case concerns the corbels, which satisfy the condition

$$\frac{F_d}{f_{cd} \cdot b \cdot d} \leq 0.07 + 0.02 \cdot \frac{d}{a} \quad (10) \text{ (case } 1^0\text{)}$$

The other case comprises the corbels which satisfy the condition

$$\frac{F_d}{f_{cd} \cdot b \cdot d} = 0.14 + 0.04 \cdot \frac{d}{a} \quad (11) \text{ (case } 2^0\text{)}$$

Formulae (10) and (11) hold good, when $\frac{2}{3} \leq \frac{d}{a} \leq 2$.

Cases 1^0 and 2^0 are depicted more exactly in the form of a diagram in Fig. 5. Case 2^0 forms at the same time the upper limit for the capacity of the corbel.

The design value for the tensile force of the reinforcing bars in the corbel is calculated on the basis of the extreme values from the formula

$$T_{sd} = \beta_1 \cdot \frac{F_d \cdot a}{d} + \beta_2 \cdot H_d \quad (12)$$

Table 2. The factors β_1 and β_2 . Intermediate values may be obtained by linear interpolation.

Relative shear force $\frac{F_d}{f_{cd} \cdot b \cdot d}$	β_1	β_2
$\leq 0.07 + 0.02 \cdot \frac{d}{a}$	1.15	1.20
$= 0.14 + 0.04 \cdot \frac{d}{a}$	1.65	1.55

2 TEST CARRIED OUT BY NBI

Laboratory tests of compression strain, lateral expansion, shear strain and permanent deformation of elastomeric bearing pads commonly used in precast concrete construction in Norway, were carried out by The Norwegian Building Research Institute (NBI) in Nov. 1983 /3/. The test program is presented in table 1.

The tests were carried out as described in /5/. The test results from /3/ and partly from /5/ are systematically analyzed in /2/ to obtain design data for actual types of elastomeric bearing pads.

Table 1. Test program.

Type of elastomer				
Designation	Type of material	Producer	Measured Shore A	Specified Shore A
TNTQ 7090* (TAQ 70)	Chloroprene (CR)	Continental Gummi-Werke West Germany	70	70
TPAQ 7090	"	"	60-66	65
NOKIA 64701	"	OY NOKIA AB Finland	70	70
NOKIA 64601	"	"	60-66	60
ALLPAC 1729	Natural Rubber (NR)	Trelleborg AB Sweden	71	70
ALLPAC 1729	Natural Rubber (NR) Reinforced with 2 layers of polyamide	"	73	70
TRELLPLY 400/2	Styrene Butadiene Rubber Reinforced with 2 layers of polyamide/ polyester	"	70	60

Dimensions: Thickness : t = 4, 6, 10, 15mm.
Minimum area : 25x360/120x120mm.
Maximum area : 270x360mm.
Shapefactor : S = 3 - 6.

The test samples were made with and without holes or slots for bolts.

Maximum compression stress $\sigma_m = 16 \text{ N/mm}^2$.
Maximum lateral movement $\Delta = 3 \text{ t}$.

All samples were tested against a face of concrete cast in steel formwork.

1 THE NEED FOR DESIGN SPECIFICATION

Plain elastomeric bearing pads are used extensively in precast concrete structures in Norway, especially in beam, slab and wall construction.

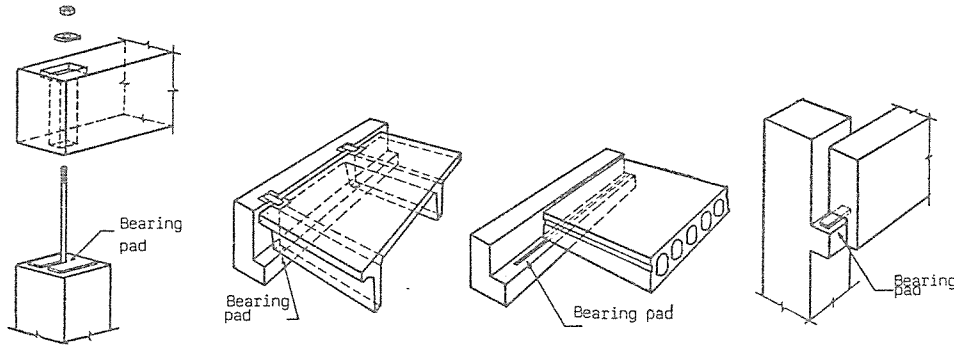


Fig.1. Beam. Fig.2. Double Tee. Fig.3. Slab. Fig.4. Wall.

The use of elastomeric bearing pads in precast concrete building construction in Norway has up to date been based on design specifications given by the bearing pad manufacturers and applicable foreign building codes.

However, these design specifications are mainly pertaining to steel reinforced elastomeric bearing pads used in bridge construction, and will normally lead to undue expensive connection design when used in normal building construction.

Conclusions drawn from field observations of plain elastomeric bearing pads in precast concrete structures in Norway confirms that when the reinforcement in the bearing area is properly designed, and when the bearing pad is withdrawn 15 - 30 mm from the concrete edges, there will be no damages from high bearing stresses.

It is of great importance however to know the accompanying lateral expansion (bulging) and the resistance force against lateral movements (shear deformation). To obtain this information, laboratory tests had to be conducted.

For more complete information read /1/.

where

$$k_{f1} = \frac{-a}{0.8k_x \cdot b \cdot d^2 \cdot (1-0.4k_x)} \quad (8)$$

$$k_{f2} = \frac{1}{0.8k_x \cdot b \cdot d} \quad (9)$$

The relative depth k_x of the compression area is calculated from formula (5).

3 COMPARISON OF CALCULATED CAPACITIES ACCORDING TO YIELD CRITERION WITH OTHER CALCULATION METHODS AND TEST RESULTS

The diagram in Fig. 4 indicates that the capacity of the corbel is great, if the steel strain and stress are small. An increase in the capacity has been verified by several tests in other research laboratories in which the corbel has been provided with heavy reinforcement. The capacities calculated in accordance with yield criterion (1) are compared with the test results given in source /2/.

In source /3/ the different design methods for the corbel are compared by means of an example. A study for engineering diploma carried out at the Tampere University of Technology, Finland, was used as a source. The results of comparison are presented in Table 1.

Table 1. Corbel capacity obtained from different methods /3/.

Method	Capacity kN
Franz-Niedenhoff	370
Swedish method	350
Glyn Jones	340
Betonkalender 1976	200
Betonkalender 1975	310
Rakentajain kalenteri	185
Yield criterion (1), plastic design	389

$$\xi = \frac{1}{d^2} = \frac{-3.885k_{d2}^2 - 0.276k_{d1} \cdot f_{cd} + \sqrt{(3.855k_{d2}^2 + 0.276k_{d1} \cdot f_{cd})^2 + 5.104k_{d1}^2 \cdot f_{cd}^2}}{2.552k_{d1}^2} \quad (2)$$

where

$$k_{d1} = \frac{-F \cdot a}{0.8k_x \cdot b \cdot (1 - 0.4k_x)} \quad (3)$$

and

$$k_{d2} = \frac{F}{0.8k_x \cdot b} \quad (4)$$

The coefficient k_x in formulae (3) and (4) is the relative depth of the compression area

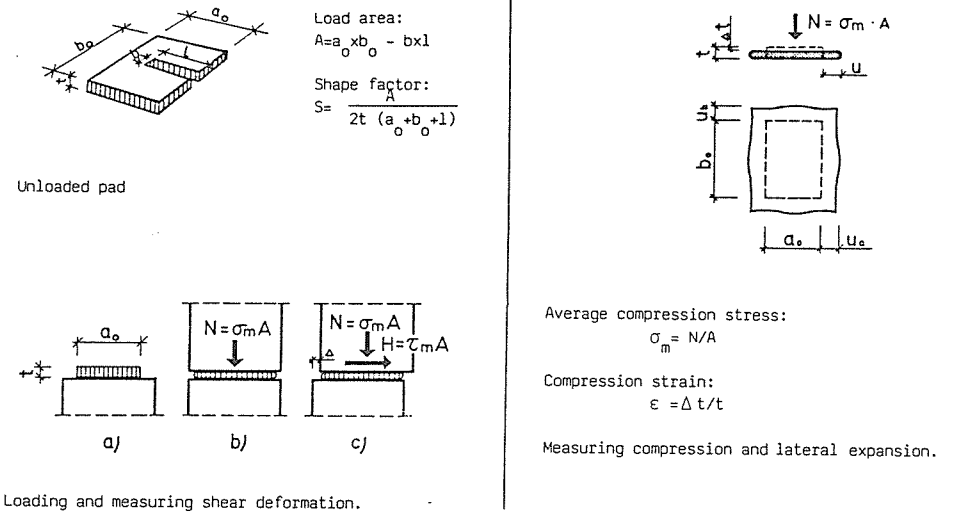
$$k_x = \frac{\epsilon_c}{\epsilon_c + \epsilon_s} \quad (5)$$

The required effective depth is obtained from the result of formula (2) as follows

$$d = \frac{1}{\sqrt{\xi}} \quad (6)$$

For the capacity of the corbel the formula in source /2/ has been derived:

$$F_u = \frac{-0.276k_{f1} \cdot f_{cd} + \sqrt{0.076 k_{f1}^2 \cdot f_{cd}^2 + (5.104k_{f1}^2 + 15.420k_{f2}^2) \cdot f_{cd}^2}}{2.552k_{f1}^2 + 7.770 k_{f2}^2} \quad (7)$$



Loading and measuring shear deformation.

Fig. 5. Definitions.

Test results

The compression strain, lateral expansion and shear deformation varies mostly with the type of elastomer. The compression strain, lateral expansion and shear deformation is only to a small extent affected by the elastomeric hardness Shore A, even for elastomer of same manufacture.

The effect of two layers with fiber reinforcement is negligible.

Elastomeric plates with thickness $t = 15\text{mm}$ showed such great lateral expansion that they were judged not fitted for use in connections shown in fig. 1 - 4.

The compression strain varies partly with the pad thickness and the shape and size of the loaded area. The variation, however, is dependent on the compression stress σ_m and the type of elastomer.

The compression strain increases as the shape factor S decreases.

The lateral expansion increases with increasing thickness - also relatively.

The lateral expansion varies partly with the shape and size of the loaded area. The variation, however, is dependent on the compression stress σ_m and the type of elastomer.

/5/ shows that the shear stiffness increases relatively with decreasing area A.

This is only partly confirmed by /3/. Besides, this relationship varies with σ_m , t and the type of elastomer.

/5/ shows that the shear stiffness increases with increasing pad thickness (for equal ratio of Δ/t). This is only partly confirmed by /3/. Also this relationship varies with σ_m and the type of elastomer.

The shear stiffness increases with increasing compression stress σ_m

The tests also shows that the resistance against lateral movements is not proportional to the ratio Δ/t . The resistance is great for small values of Δ/t and then decreases (relatively) with increasing values of Δ/t .

The test samples were also measured one month after unloading. The samples showed very small permanent deformations even for $\sigma_m = 16 \text{ N/mm}^2$ combined with $\Delta/t = 3,0$. None of the samples showed damages.

3 SUMMARY

1. Plain elastomeric plates and stripes are highly suitable as bearing pads in most types of precast construction.
Recommended thickness: $t = 4 - 10\text{mm}$.
Recommended hardness : 60 - 70 Shore A.
2. The roughness of the contact surface area and the type of elastomer affects the bearing pad behavior far more than the hardness Shore A.
3. Creep effect varies with the loading rate.
4. The compression strain increases with decreasing shape faktor S.
5. The lateral expansion increases with increasing thickness- also relatively.
6. The shear stiffness increases with increasing compression stress. The shear stiffness is not proportional to the horizontal deformation.
The shear resistance is small compared to the vertical load.
7. The elastomer may be subjected to great compression stresses and horizontal movements without being damaged.
8. Compression, rotation and edge clearances should be limited due to concrete strain consideration.
9. The maximum allowable horizontal movements should be limited due to an evaluation of thickness, compression stress, temperature movement, and deterioration consequences.
10. Design diagrams should be based upon tests of the actual type of elastomer.

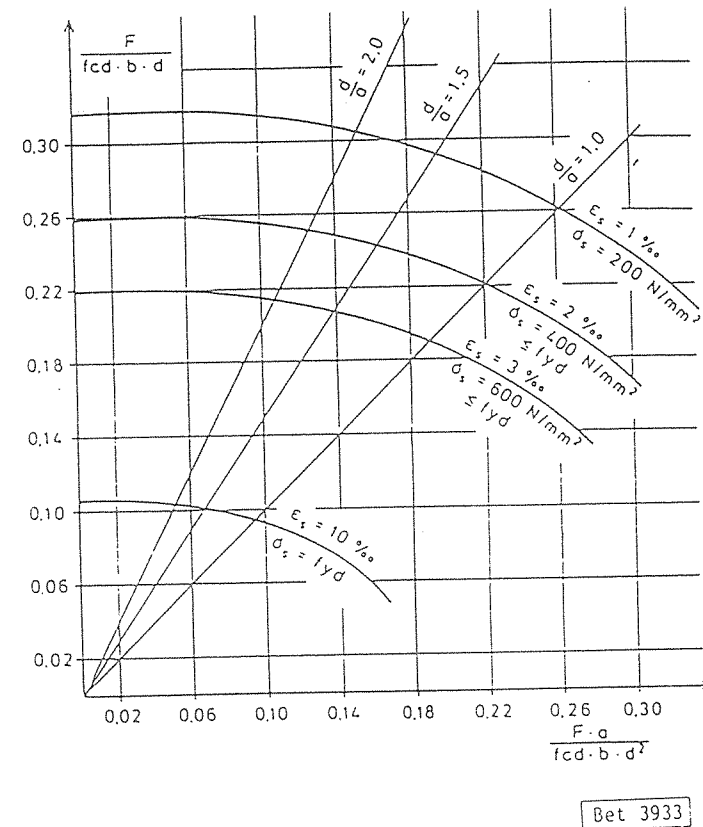


Fig. 4. Capacity diagram for corbels.

The required effective depth of the corbel or the capacity of the corbel can be solved analytically from the yield criterion. In order to calculate the effective depth d, the following formula has been derived in source /2/:

The stress are calculated in the direction of the corbel side and perpendicularly to it as shown in Fig. 3.

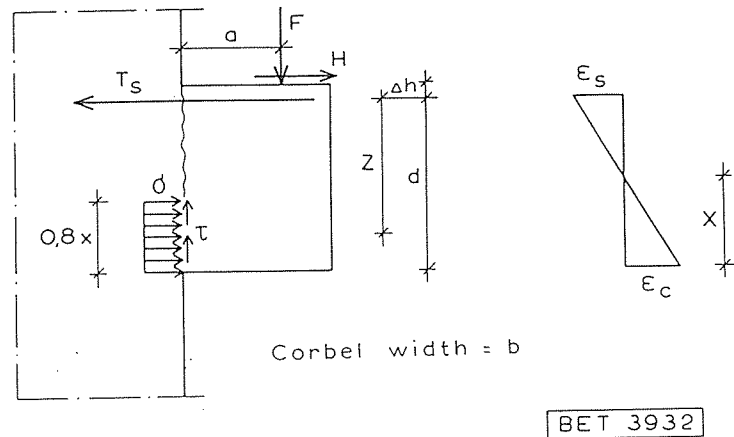


Fig. 3. Stress components at the interface of a corbel and its support.

The depth of the stress distribution area, $0,8x$, depends on the magnitude of the compressive strain, ϵ_c , and on the strain in steel bars, ϵ_s . Thus by applying the yield criterion (1) it is possible to study the effect of deformations on the capacity of the corbel. The capacity curves for the corbel calculated by means of the yield criterion (1) and the distribution of stress in accordance with Fig. 3 are plotted in Fig. 4. They indicate that the overreinforcement of the corbel ($\epsilon_s < \frac{f_{yk}}{E_s}$) considerably increases its capacity. The value $\epsilon_c = 3.5 \text{ o/oo}$ is used for strain in the extreme fibre of the compressed concrete.

4 DESIGN OF PLAIN ELASTOMERIC BEARING PADS - PROPOSAL

- Limitations:
- Type of elastomer : As described in NBI test program - see chapter 2.
 - Hardness : 60 - 73 Shore A.
 - Maximum area : $A = 300 \times 400 \text{ mm}$.
 - Shape factor : $S = 2 - 7$.
 - Thickness : $t = 4 - 10 \text{ mm}$.
 - Contact surface : Concrete.
 - Maximum 2 layers of fiber reinforcement.
- The concrete bearing zone must be designed and reinforced as advised by the NBIF Design Manual /4/.

Design loads

The elastomeric bearing pad must be designed for vertical and horizontal loads according to valid Building Code.

This includes rotation and horizontal movements from volume changes.

The performance of the bearing pads is a function of deformation characteristics under service loads. Hence, the pads must be designed using unfactored (service) loads.

Compression stress

Maximum allowable average compression stress σ_m is limited (due to concrete strain limitations) to f_c in ultimate state design according to Norwegian Code NS 3479 and NS 3473.

Transferred to design with service loads (unfactored) when the vertical load N consists of 50% dead load and 50% live load:

Concrete C35 (cube strength 35 N/mm ²) (cyl. strength 30 N/mm ²)	: $\sigma_m = 11,4 \text{ N/mm}^2$
Concrete C45 (cube strength 45 N/mm ²) (cyl. strength 40 N/mm ²)	: $\sigma_m = 13,7 \text{ N/mm}^2$
Concrete C55 (cube strength 55 N/mm ²) (cyl. strength 50 N/mm ²)	: $\sigma_m = 16,0 \text{ N/mm}^2$

Normally a limitation of compression stresses to $\sigma_m = 10 - 12 \text{ N/mm}^2$ will lead to reasonable and practical bearing connections.

Compression and rotation

Compression strain $\epsilon = \Delta t/t$ due to the average compression stress σ_m and with shape factor S , is found in fig. 6.

The compression strain includes creep due to longterm loads, except for TPAQ 7090. For this type it is advised to increase the compression strain due to longterm loads by 15%. For further information see /5/.

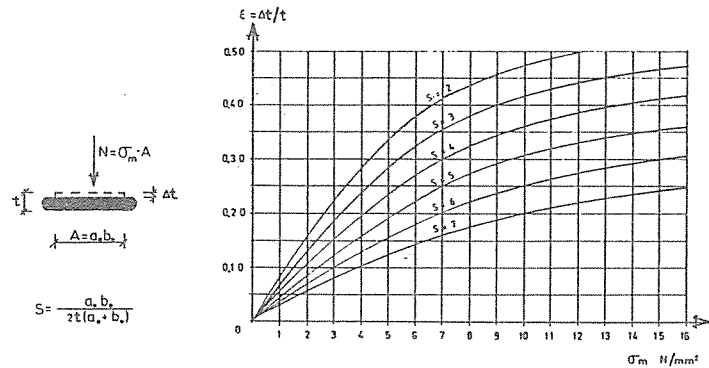


Fig. 6. Compression strain.

The thickness t should be designed so that there will be compression over the total pad face, that is $t_1 \leq t$ (see fig. 7) which leads to:

$$t \geq \frac{\theta \cdot a_0}{\epsilon \cdot 2}$$

The thickness t must be designed to prevent direct contact between the concrete elements:

$$t_2 = t - \epsilon \cdot t - \theta \cdot l$$

The lower limit for t_2 should be chosen in accordance with the calculation accuracy and erection tolerances.

As an absolute lower limit it is recommended to use $t_2 \geq 3\text{mm}$

When designing for small horizontal movements and low compression strain values it is permissible to have compression only over a part of the pad face.

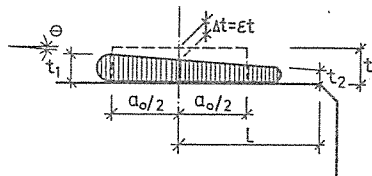


Fig. 7. Combined compression and rotation.

true to the model. The capacity of the compressed member should be sufficiently large for failure to occur in a ductile way by bending. In order to ensure the ductile mode of failure an upper limit has been set on the capacity of the compressed member, which results in rather high corbels.

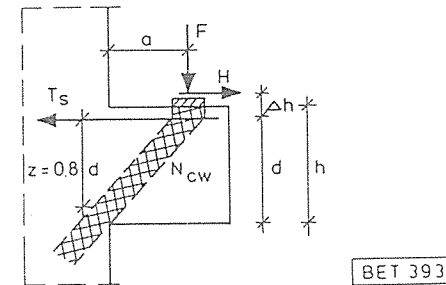


Fig. 2. Performance model for a corbel based on the direction of principal stress.

2 APPLICATION OF TWO-DIMENSIONAL YIELD CRITERION OF CONCRETE TO THE LOW COLUMN CORBEL

The capacity of the corbel is examined primarily on a basis of a yield criterion of concrete presented in the literature. The yield criterion is described in source /1/, and it reads

$$(2 - b^{-1}) \cdot \sqrt{\sigma^2 + 3 \tau^2} + (1 - b^{-1}) \cdot \sigma = f_{cd}, \quad (1)$$

where b is 1.16,
 τ the shear stress and
 σ the compressive stress at the edge of the column.

DESIGN OF COLUMN CORBELS

Tapani Hakkarainen
 Technical Research Centre of Finland
 Concrete and Silicate Laboratory
 Espoo, Finland

1 GENERAL

In buildings in which the frames are composed of prefabricated beams and columns, the floor beams are connected to the columns with corbels (Fig. 1). The corbel transmits the load from the beam to the column. It must be often built into the beam (Fig. 1) and made very low, since the overall thickness of the floor construction must be kept as small as possible.

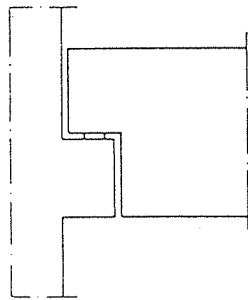


Fig. 1. Beam-to-column connection by means of a corbel.

The corbel is usually designed using the performance model shown in Fig. 2. It is assumed in the model that an inclined compressed member in the direction of the principal stress is formed in the corbel. The compression stress of concrete and the tensile force of steel bars are calculated on the basis of the equilibrium conditions of the structure

Lateral expansion

The lateral expansion u due to the average compression stress σ_m and with pad thickness t is found by fig. 8.

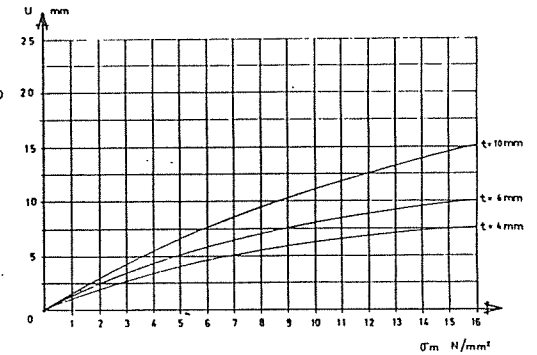
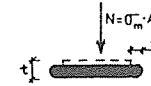


Fig. 8. Lateral expansion.

The size of the pad ($a + b$) should be limited so that the pad will not protrude from the concrete edges when subjected to loading - fig. 9.

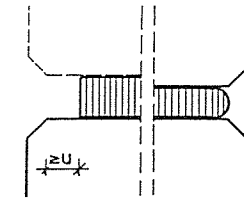


Fig. 9. Edge clearance.

Shear deformation

Maximum horizontal resistance force H against shear deformation Δ (lateral movement), dependent on the compression stress σ_m , is found by fig. 10.

If the resistance against lateral movement is needed to transfer horizontal forces, use fig. 11.

The values are valid at $+20^\circ\text{C}$.

The shear stiffness increases with low temperature. The effect of low temperatures on the friction forces between elastomer and concrete has not yet been studied. It is therefore advised to correct the shear stiffness with the factor k_T at low temperature according to fig. 12.

It is recommended to limit the maximum allowable shear deformation Δ for plain elastomeric bearing pads related to pad thickness t and compression stress σ_m as shown in fig. 13.

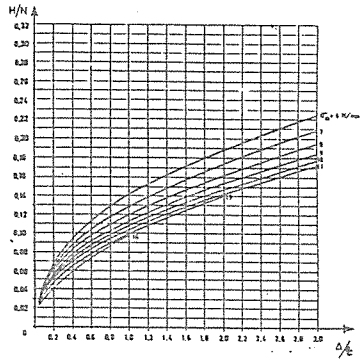


Fig. 10. Shear deformation Maximum H/N.

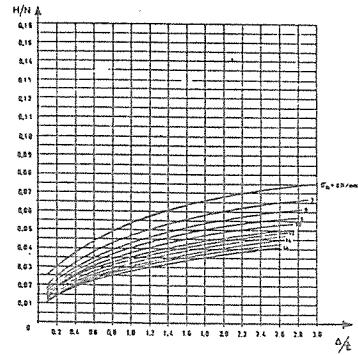
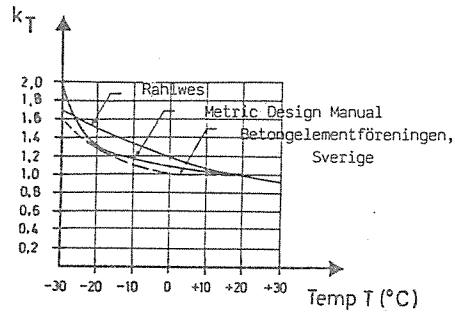
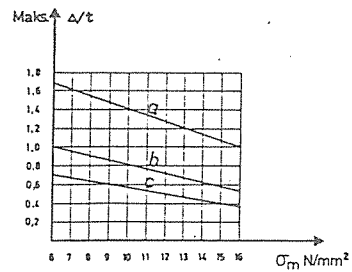


Fig. 11. Shear deformation Minimum H/N.



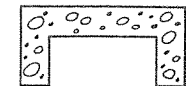
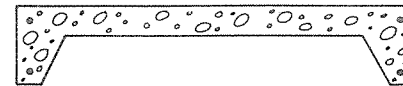
Shear modulus
 $G_T = k_T \cdot G_{20^\circ C}$

Fig. 12. Shear modulus/Temperature.

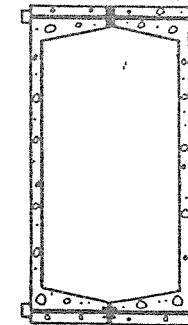
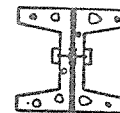
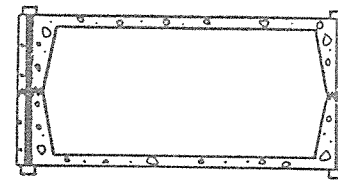


- a. Heated, indoor - static vertical load.
- b. Outdoor - static vertical load.
- c. Outdoor - dynamic vertical load.

Fig. 13. Maximum allowable shear deformation Δ for plain elastomeric bearing pads with thickness t .



a) precast sub-elements



b) composite elements

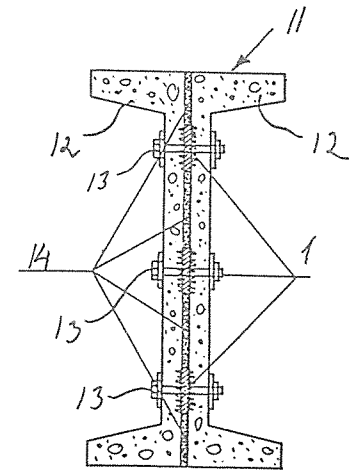


Fig. 11. Principal ideas for the composite precast concrete elements.

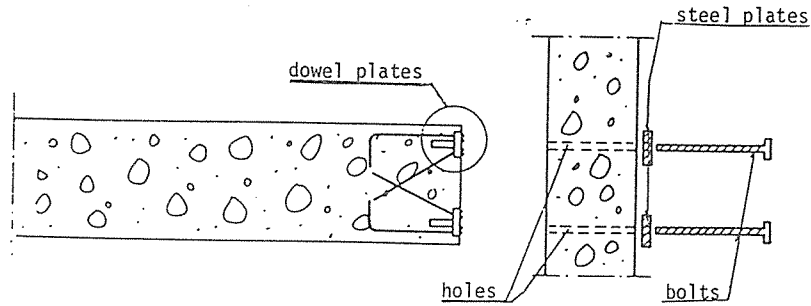


Fig. 9. Connection of the bending and shear resistant frame edge.

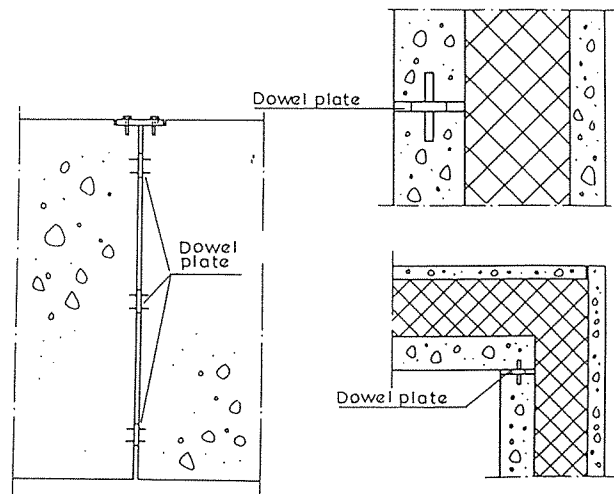


Fig. 10. Dowel plate connection of the wall elements.

Effect of environment

The environmental qualities of elastomeric bearing pads must be checked with the same thoroughness as when designing for physical loads.

Recommended types of elastomer and general qualities are given in Table 2.

Table 2. Recommended types of elastomer and general qualities.

Quality	Natural Rubber (NR)	Styrene Butadiene Rubber (SBR)	Chloroprene (CR)
Elasticity	Especially good	Good	Good
Dynamic qualities	Very good	Good	Good
Wearing strength	Very good	Especially good	Very good
Tearing strength	Good	Good	Very good
Weathering/ozone resistance	Poor	Less good	Especially good
Chemical resistance (acid, base)	Good	Good	Good
Oil resistance	Poor	Poor	Good

For outdoor unprotected use it is recommended to use Chloroprene (CR).

For outdoor protected use or indoor construction Natural Rubber (NR) and Styrene Butadiene Rubber is just as suitable as Chloroprene (CR), unless directly exposed to oil.

REFERENCES

1. Vinje, Leidulv. Design of plain elastomeric bearing pads in precast concrete structures (in Norwegian). Betongprodukter 2(1984)3.
2. Vinje, Leidulv. Elastomeric bearing pads. Report on measuring compression and shear stiffness (in Norwegian). The Norwegian Precast Federation. Betongforsk. 1984:1.
3. Measurement of shear stiffness and compression for elastomeric bearing pads (in Norwegian). Oslo 1983, The Norwegian Building Research Institute, Report 07976 and 06/17210.
4. NBIF-Design manual. Concrete elements (in Norwegian). Oslo 1985. The Norwegian Precast Concrete Federation.
5. Flohrer, Manfred. Untersuchungen über die Eignung unbewehrter Elastomerlager als Baulager. Betonstein-Zeitung 37(1971)11.

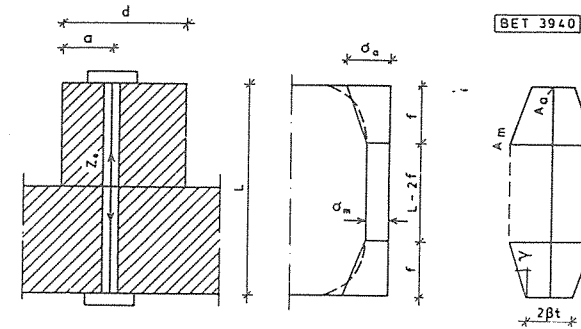


Fig. 7. Distribution of compressive stress
 a) the prestressed connection
 b) change in compressive stress
 c) change in compressed zone.

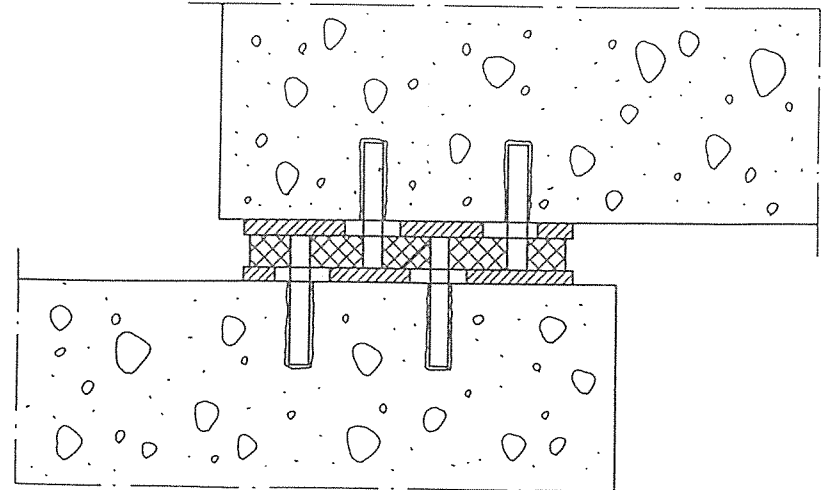


Fig. 8. Dowel plate with limited movement as the support connection of the beam.

BOLTED BEAM-COLUMN CONNECTIONS FOR PRECAST STRUCTURES

Björn Engström, M.Sc., Research Ass.

Chalmers University of Technology, Division of Concrete Structures
Göteborg, Sweden

PREFACE

This paper is based on a study carried out at Chalmers University of Technology, Division of Concrete Structures. The study is part of an extensive research project entitled "Structural Connections in Precast Buildings" which is still, since 1982, under realization. The project is financially supported equally by the "Swedish Council for Building Research" and the "Swedish Foundation for Concrete Research" and is supervised by the Head of the Division of Concrete Structures, Professor Krister Cederwall.

The results of this specific study will be more comprehensively presented in [1].

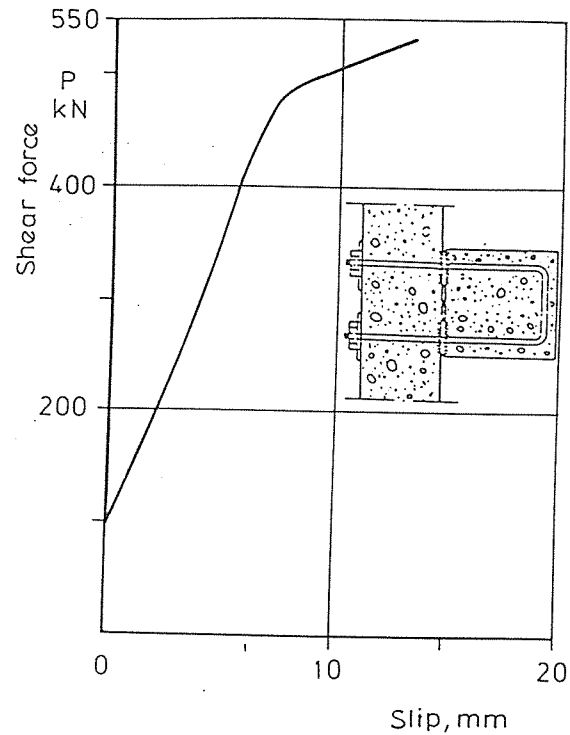


Fig. 6. Force-slip curve for the nail plate-bolt connection of the column corbel.

1 INTRODUCTION

In a precast building, the connections will normally form weak sections where structural deformations will be concentrated. Consequently, the structural behaviour will to a large extent depend on the load-displacement characteristics of the connections, at least in the ultimate state.

For instance, in a careful analysis of probable collapse mechanisms the load-displacement relationships ought to be considered. However, up to now many common types of connections have not been experimentally examined in this respect and the knowledge about the behaviour in the ultimate state is inadequate.

With this background, a test series of bolted beam-column connections was carried out at Chalmers University of Technology. The test specimens were in full scale but bounded to the connection as such with its different components. The aim was to examine the composed behaviour of the connection when it was exposed to large relative displacements and to search for indications of improved detailing with regard to ductility and residual resistance. The load-displacement relationships were to be continuously recorded during the tests and the influence of various detailing on the deformability and the strain-energy capacity should be studied.

2 DESCRIPTION OF THE TESTS

2.1 Test specimens

The test specimen was designed in order to simulate a bolted beam-column connection, for instance according to Fig. 1a. However, an idealized and somewhat simplified lay-out was used in the tests according to Fig. 1b.

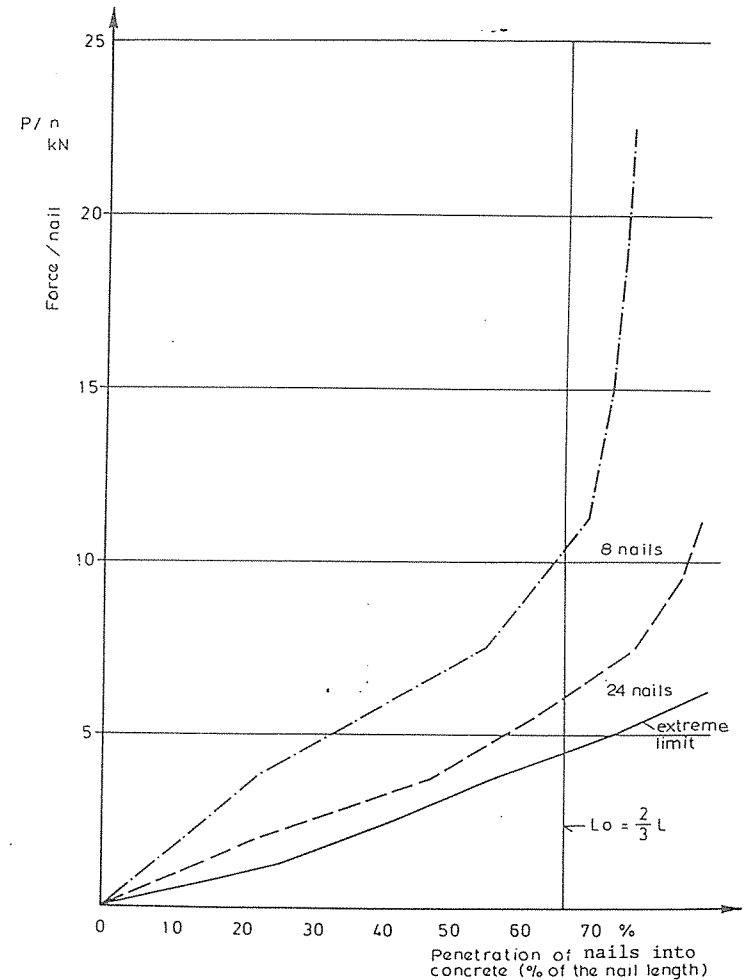


Fig. 5. Compression force-nail penetration curves for the nail plate connection.

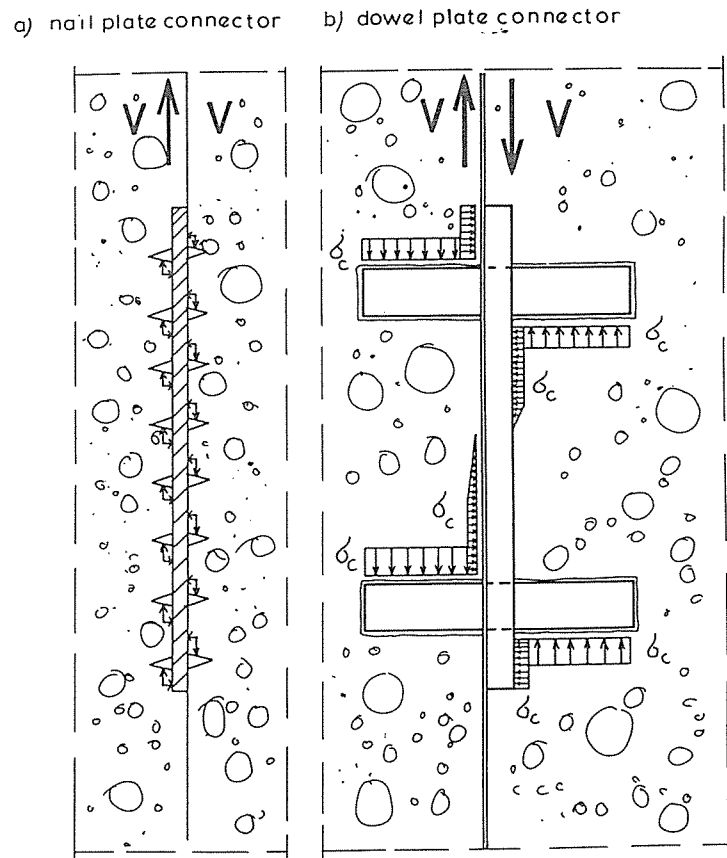


Fig. 4. Force state of the nail and dowel plate connection under shear.

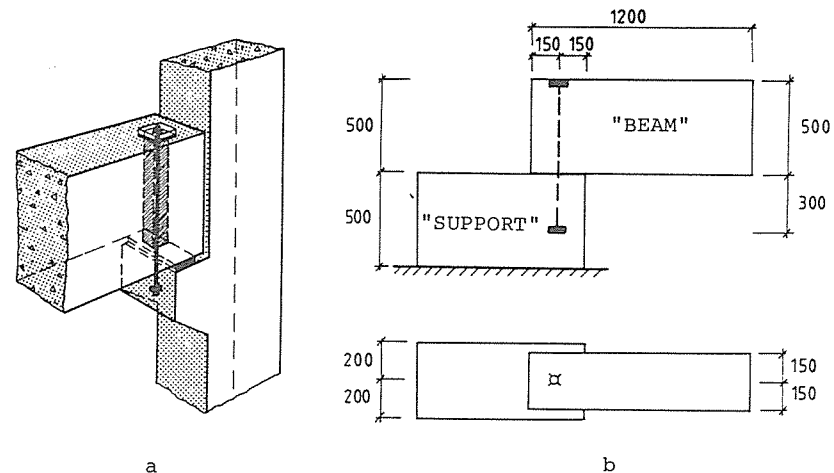


Fig. 1. Bolted beam-column connections
a. Typical solution in a precast structure
b. Test specimen used in the actual project.

Each test specimen consisted of a "support" unit, a "beam" unit and a bolt with anchorage arrangements. In some of the tests, the support was also provided with a 10 mm bearing plate from steel or neoprene.

The bolt was anchored in the "support" unit by an end-anchor, by bond, or by a threaded insert embedded at the interface. The "beam" unit was provided with a vertical bolt hole with rectangular cross-section, 40x80 mm, and threaded onto the protruding bolt. The hole was formed by a plastic tube. After mounting the "beam" unit to the support, the hole was normally grouted, but left open and ungrouted in some of the tests. The "beam" unit was normally fastened to the support by a nut, screwed on the upper end of the bolt. When the connection was provided with a top nut, the nut was always tightened

with a twisting moment of 150 Nm. However, in some of the tests the top nut was omitted and the "beam" unit was only fastened by the bond between the bolt and the grout in the bolt hole.

In all the test specimens, a concrete quality of K40 was used. The mean compressive strength measured on 150 mm cubes was about 50 MPa.

The "beam" and "support" units were reinforced with longitudinal ribbed bars $\phi 12$ Ks40 and stirrups $\phi 8$ Ks40S, see Fig. 3. In the detailing, the splitting effect from the bolt was considered. Splitting cracks, according to Fig. 2, were presupposed and the reinforcement was designed in order to safely balance the entire splitting force corresponding to the dowel capacity of the bolted connection at yielding.

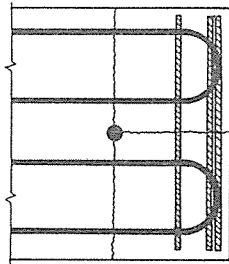


Fig. 2. Horizontal section through the "beam" unit with presupposed splitting cracks around the bolt. The detailing is performed according to alternative "A" in Fig. 3.

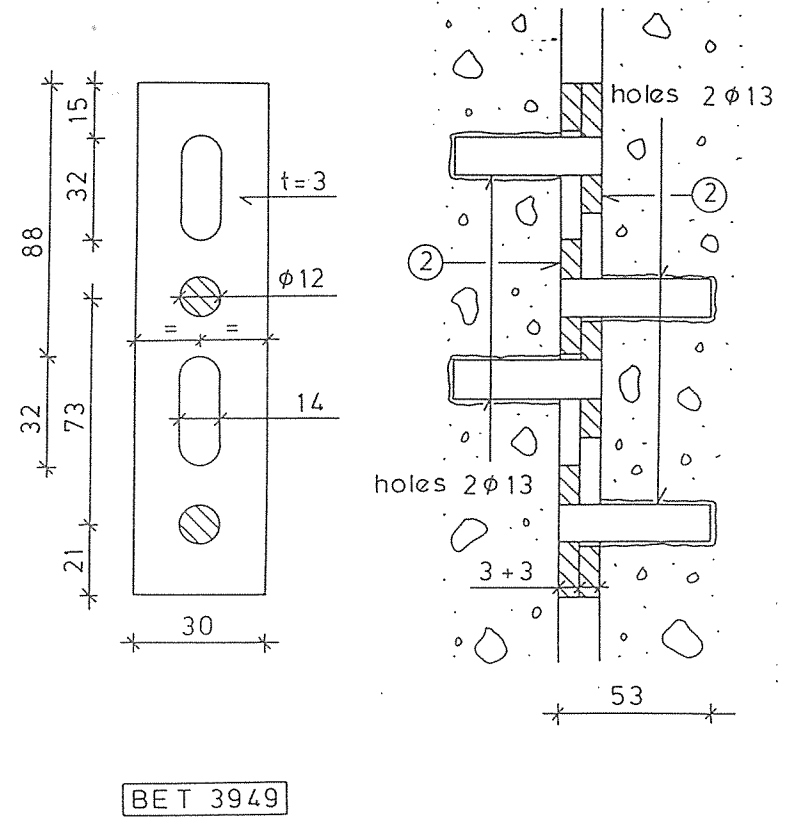


Fig. 3. Limitedly movable dowel plate connection.

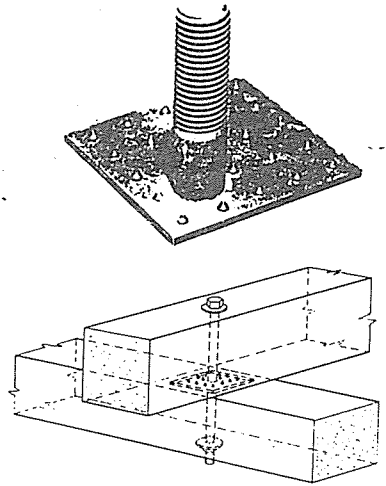


Fig. 1. Nail plate-bolt connection.

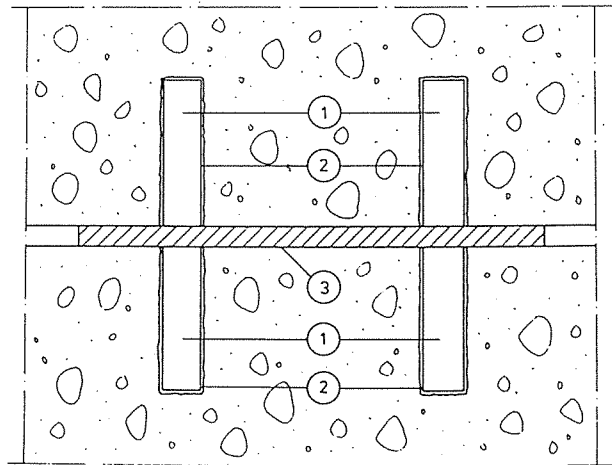
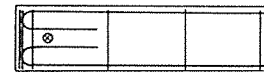
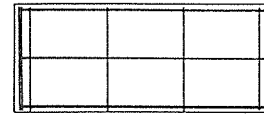


Fig. 2. Rigid dowel plate or dowel plate-bolt connection.
 1 dowel
 2 hole in concrete
 3 steel plate

In the "beam" units, two alternative reinforcement arrangements were used according to Fig. 3. They were denoted type A, "normal", and type B, "reinforced beam end".

Main reinforcement $\phi 12$ Ks40

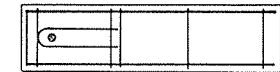
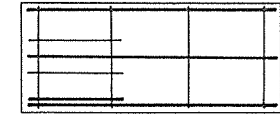
Stirrups $\phi 8$ Ks40S



a

Main reinforcement $\phi 12$ Ks40

Stirrups $\phi 8$ Ks40S



b

Fig. 3. Alternative reinforcement arrangements in the "beam" units

- a. Type A, "normal" arrangement with vertical stirrups
- b. Type B, "reinforced beam end" with horizontal stirrups.

The bolts were made from high strength structural steel, SIS 2172, either type 1 - smooth bars partial with cut threads M24, or type 2 - bars with cut threads M24 all over the length. When anchorage was to be provided by bond, the bond capacity was achieved by means of the threads. Detailed data of the bolt types appear from Table 1.

Table 1. Data of the bolts.

Type	Size [mm]	Quality	f_{sy} [MPa]	f_{stu} [MPa]	ϵ_{lim}	Threads
1	24	SIS 2172	476	674	0,212	M24
2	"	"	510	653	0,177	"

Remarks: Type 1 - partly with threads, type 2 - threads all over.

The compositions and strength of the used grouts appear from Table 2. Two types of grout were used, a normal one, type 1, and a porous one, type 2.

Table 2. Grout used for the bolt holes.

Type	Composition (0,020 m ³)				f_{cc} [MPa]	ρ [kg/m ³]
	C	S (0-4 mm)	W	Additive (Cemos)		
1	16,1 kg	16,1 kg	8,9 kg	-	~35-50	~2,1-2,2
2	"	"	"	0,48 kg	~35	~2,0

Remarks: Type 1 - "Normal", type 2 - "Porous".

2.2 Load-arrangements and measurements

Two types of loading were used.

In one test series, the connections were loaded in tension as the "beam" unit was forced to slip on the support according to Fig. 4a. The force was applied on two tie-rods from ribbed reinforcement bars $\phi 16$ Ks60 embedded in the "beam" unit. During the test procedure, the tensile force and the relative horizontal displacement between the "beam" and the "support" were measured continuously. Outermore, the relative vertical displacement between the "beam" and the "support", and the displacement between the bolt and the surrounding concrete blocks at the ends of the bolt were measured at intervals.

LITERATURE

1. Olin, J., Hakkarainen, T. & Rämä, M. Connections and joints between precast concrete units. Espoo 1984, Technical Research Centre of Finland, Research Reports 316. 146 pp. + app. 46 pp. (in Finnish with English summary).
2. Jokela, J. & Lintunen, H. Test with the nail plate and dowel plate connections. Espoo, Technical Research Centre of Finland. Research Reports of the Concrete and Silicate Laboratory, No. BET13169 and BET 62/0/81 (in Finnish).
3. Pat. Fi 64428. Sarja, A. Method for the jointing of prefabricated concrete elements or sub-elements. Appl.813921, 7.12.1981. 6 pp.+ app. 1983 (in Finnish).
4. Eibl, J. & Schürmann, U. HV-Schraubenanschlüsse für Stahlbetonkonsolen. Bauing. 57 (1982) 2, pp. 61 - 68.

Assets of nail and dowel plate connectors during use include statical safety, high safety against progressive collapse, and high safety against fire. Particularly important is the total elimination of progressive collapse, as this is often difficult when using traditional connection techniques. The bending capacity of connections also enables statically preferable multistorey framed structures to be used instead of the usual present-day cantilever column frames. This not only means considerable savings, particularly in column costs, but also some assets for the beams. The economy pertaining to columns can be significantly improved using new production techniques possible with the new types of connections.

4.2 Innovative use of connectors

Examples of use include:

- column corbels (Fig. 6),
- beam supports (Fig. 8),
- edge connections of the frames with internal threads for the bolts (Fig. 9),
- wall joints (Fig. 10).

With innovative design, most of the connection problems, particularly between one-dimensional and often between two-dimensional elements, can be solved using the nail plate of dowel plate connectors. The increase in bolted connections is an important step towards a demountable prefabricated construction technology.

In prefabrication, the necessity for highly mechanised production and flexible products gives rise to the need for an increase in building with prefabricated elements, jointing them with sub-elements. This technique makes it possible to produce a set of sub-elements, which can be joined together in the element factory for different types of elements. For such techniques bolted, shear resistant connections are needed. Some examples of the composition of elements using sub-elements are presented in Fig. 11.

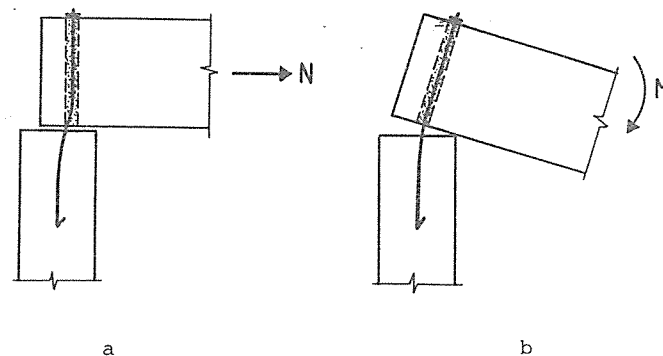


Fig. 4. Load arrangements used in the tests.
 a. Tensile tests
 b. Bending tests

In the other test series, the beam-column connections were loaded in bending. The "beam" unit was forced to rotate at the edge of the support according to Fig. 4b. The support was reinforced at the outermost corner by an embedded steel angle in order to prevent local crushing. The bending moment was created by a vertical point load acting on the "beam" unit. During the test procedure, the load and the rotation were measured continuously. Furthermore, the displacement between the bolt and the surrounding concrete blocks was measured at intervals at both ends of the bolt.

2.3 Various detailing

In both the test series, the influence of various detailing was to be studied. Reference tests were defined according to Fig. 5. In the various tests one parameter at a time diverged from the detailing in the reference tests according to Table 3 for the tensile tests and Table 4 for the bending tests.

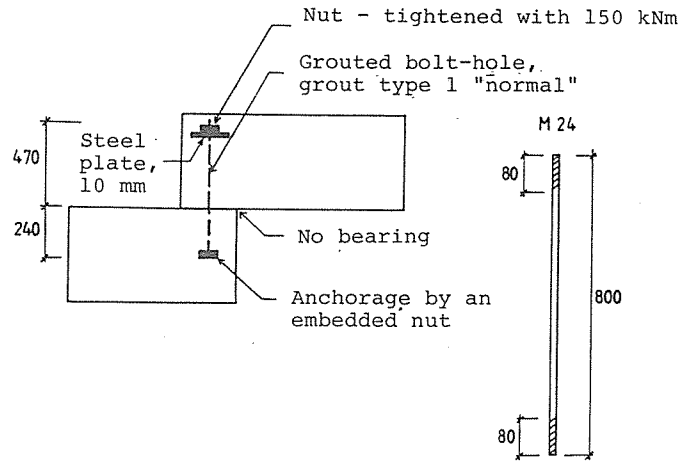


Fig. 5. The detailing of the reference tests.

Table 3. Various detailing of the tensile tests.

Test No.	Reinf. arr. type	Hole	Grout type	f_{cc} [MPa]	ρ [kg/m ³]	Bolt Anchorage/length [mm]		Bearing thickness [mm]
						type top	bottom	
2	A	Open	-	-	-	1	nut emb.nut	
5	"	Grouted	1	47,1	2,13	"	" insert	
6	"	"	"	"	"	2	nut/bond (450) bond (300)	
7	"	"	"	46,1	"	"	bond (450) "	
8	"	"	2	36,9	2,03	"	nut/bond (450) "	
9	B	"	1	51,4	2,14	1	- emb.nut	
10	"	"	"	"	"	"	nut "	Steel (10)
11	A	"	"	33,2	2,16	"	" "	
12*	"	"	"	48,1	2,15	"	" "	
13	"	"	"	46,1	2,12	"	" "	Neo-prene (10)

* Reference test

In research /4/ it is considered safe to assume the stress losses as being 25 %.

3.2 Design of the washers of prestressed bolts

Research carried out /4/ has established that the most appropriate dimensions for Fe 52 washers for minimization of the stress forces are

$$t = 20 \sqrt[3]{\frac{Z_0}{198}} \quad (6)$$

and

$$A \geq 15600 \sqrt[3]{\frac{Z_0}{198}}, \quad (7)$$

where

t is the thickness of the washer (mm)
 A the surface area of the washer (mm²) and
 Z_0 the prestressing force of the bolt (kN).

4 EXAMPLES OF THE POSSIBLE USE OF NAIL AND DOWEL PLATE CONNECTORS

4.1 Assets of nail and dowel plate connectors

Nail and dowel plate connectors are suitable for use where a high shear capacity is required. Combined with prestressed high strength bolts, the shear capacity and the service state stiffness can be improved. The bolts also make possible a high bending capacity for the connection.

Advantages in production include the possibility of prefabrication in the element factory, independently of connection detailing, easy mounting on site and easy demounting and re-use of the structures.

The compressive stress at the joint of the prestressed bolt connection as shown in Fig. 7 at the height of the bolt is

$$\sigma_m = \frac{-Z_o}{A_k} - \frac{Z_o}{I_k} \left(\frac{d}{2} - a \right)^2, \quad (3)$$

The compressive stress under the washer is

$$\sigma_a = \frac{Z_o}{A_a} \approx \frac{-Z_o}{(\beta t)^2 \pi} \quad (4)$$

In formulae (3) and (4)

- Z_o is the original compressive force
- A_k the surface area of the joint between the structural members
- I_k the moment of inertia of the joint between the structural members
- A_a distribution area of the compressive force in the washer
- t the thickness of the washer and
- $\beta \approx 3$ constant

Other quantities appear in Fig. 7.

The stress loss due to creep obtained is /4/

$$\Delta\sigma_z = \frac{E_s}{E_c} \cdot \frac{\phi}{L} \cdot [\sigma_m \cdot (L - f) + \sigma_a \cdot f] \quad (5)$$

where

- E_s is the elastic modulus of steel
- E_c the elastic modulus of concrete
- σ_m obtained from formula (3)
- σ_a obtained from formula (4)
- ϕ creep factor
- L the combined thickness of the structural members to be joined
- f the distance, within which the compressive stress changes from the value σ_a to the value σ_m , when $\tan \gamma = \frac{1}{2}$.

Table 4. Various detailing of the bending tests.

Test No.	Reinf. arr. type	Hole	Grout type	f_{cc} [MPa]	ρ [kg/m ³]	Bolt Anchorage/length [mm]			Bearing thickness [mm]
						type	top	bottom	
22*	A	Grouted	1	56,5	2,23	1	nut	emb.nut	Neo-prene (10)
23	"	"	"	50,8	2,17	"	"	bond(70)	
24	"	"	"	"	"	"	"	insert	
25	"	"	"	42,4	2,13	2	bond(450)	bond(300)	
26	"	"	"	"	"	"	nut	"	
29	"	Open	-	-	-	1	"	emb.nut	

* Reference test

3 TEST RESULTS

3.1 Tensile tests

In all the tests with grouted bolt holes, the connection had initially an elastic stiff response. All the connections did resist at least the calculated capacity in dowel action.

For bolts of type 1 this capacity was estimated to 103 kN according to the following, see [1]

$$V_{y1} = c \cdot \phi^2 \sqrt{f_{cc} f_{st}} = 1,16 \cdot 0,024^2 \sqrt{50 \cdot 10^6 \cdot 476 \cdot 10^6} = 103 \cdot 10^3 \text{ N}$$

Correspondingly, for bolts of Type 2, the capacity in dowel action was estimated to 74 kN.

$$V_{y2} = 1,16 \cdot 0,020^2 \sqrt{50 \cdot 10^6 \cdot 510 \cdot 10^6} = 74,1 \cdot 10^3 \text{ N}$$

The cross-section area is reduced with regard to the threads at the interface section.

For the connection with 10 mm bearings the calculated dowel capacity must be reduced because of the excentricity at the interface. For bolts of Type 1 the reduced dowel capacity was estimated to about 75 kN, see [1].

When the dowel capacity was reached the bolt began to yield. However, it was still possible to increase the load, but the connection was now apparently less stiff than in the initial stage. The tensile force capacity was achieved mainly by dowel action, but in the plastic state. When large displacements were forced on the connection, the splitting effects around the bolt were observable. A successively propagating vertical splitting crack occurred in the middle of the end face of the "beam" unit. The crack was prevented from opening by the stirrups. However, with increasing relative displacements, a splitting failure finally occurred which limited the maximum tensile force capacity. All the tested connections were able to resist quite large displacements before splitting failure occurred, normally about 25-30 mm. When the bolt was anchored in the support by an embedded threaded insert, the splitting failure occurred when the horizontal displacement was about 15 mm.

After the splitting failure, the connections had still a considerable tensile force capacity because of a shear-friction effect. Taking this residual resistance into account, the connections normally resisted a total relative displacement of about 120-140 mm. However, the residual capacity finally decreased either because of gradually crushing of the support interfaces, or collapse of the "beam" unit.

- γ the capacity safety factor,
- ϕ the bolt diameter,
- f_{cd} the design prism strength of concrete ($\sim 0.5 K$),
- f_{yd} the design strength of the bolt.

In the case where the length of the dowel is at least three times the diameter, the shear capacity of the dowel plate or combined dowel plate-bolt connection can be calculated using the following equation:

$$V_{ud} = 1.2 (\sum \phi_d^2 + \sum \phi_b^2) \sqrt{f_{cd} f_{yd}} \quad (2)$$

where

- ϕ_d is the diameter of the dowel,
- ϕ_b the diameter of the bolt,
- f_{cd} the prism design strength of concrete ($\sim 0.5 \cdot K$, where K is the cube strength),
- f_{yd} the design strength of the steel.

As an example, the design shear capacity of a connection with four bolts of diameter 16 mm and four dowels of diameter 12 mm, in concrete K 40 and steel quality Fe 520, is 219 kN.

3.1 Design in the serviceability limit state

In the serviceability limit state, the displacement and crack width of the connection are to be limited.

The displacement can be evaluated at the force-displace curves of each type of connection. The allowed value of displacement on the structures can be defined separately in the serviceability limit state and in the ultimate limit state.

The cracking at the connection joint can be avoided dimensioning the prestressing force to correspond the tension forces in service state. In that case, the losses of bolt forces has to be calculated.

stretched in the direction of movement. After the permitted movement has taken place, the dowel will be interlocked against the connecting steel plate, thus moving the shear force again from one concrete surface to the other. Naturally, if required, a two-dimensional movement can also be allowed.

The combined dowel plate-bolt connection is preferably also made with prestressed bolts in those cases where the connection is subjected to a combined shear force and bending moment or where a high degree of stiffness in the service state is important. The calculation of the bending capacity can then also be effected by means of usual methods as in the case of nail plate-bolt connections.

3 DESIGN OF THE BOLTED CONNECTION

The bolts in the bolted joint of the reinforced concrete elements take the tensile forces. The shear forces are transmitted from one structural member to another by means of bolts, dowel effect of bolts and, if necessary, by means of mechanical connecting parts.

The shear capacity of the nail plate-bolt connection can be calculated using the following equation:

$$V_{ud} = \frac{n \cdot f \cdot K}{\gamma \cdot K_f} + \phi^2 \sqrt{f_{cd} \cdot f_{yd}} \quad (1)$$

where

- V_{ud} is the design value of the ultimate shear capacity,
- n the number of nails,
- f the ultimate shear capacity of one nail with the calibration concrete strength,
- K the concrete cube strength,
- K_f the calibration cube strength of concrete corresponding to the value f ,

In Fig. 6 it is possible to study the influence of the reinforcement arrangement in the "beam" unit. The reference test, No. 12, was provided with the "normal" arrangement, type "A" in Fig. 3. Test No. 10, with a "reinforced beam end", type "B" in Fig. 3, had a higher residual capacity (about 130 kN). The load when the splitting failure occurred was also somewhat higher (about 160 kN) than in the reference test, and the displacement at the splitting failure was remarkable higher (about 45 mm). In the same figure it is also possible to study the effect of open, ungrouted bolt hole, test No. 2. Initially, this connection was without tensile force capacity of importance. When the "beam" was sliding on the support, the loose between the bolt and the surrounding "beam" unit in the hole was decreasing until contact. It is noticeable that the horizontal displacement was very high (about 100 mm) before splitting failure occurred.

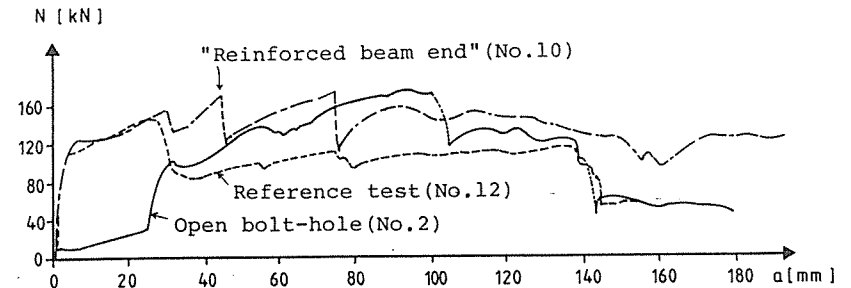


Fig. 6. Load-displacement relationships from the tensile tests. The effect of "reinforced beam end", type B and the effect of open, ungrouted bolt hole.

In one of the tensile tests, test No. 5, the bolt was anchored in the support by an embedded threaded insert. The effect of this arrangement appears from Fig. 7. The

splitting failure occurred for less horizontal displacement (about 20 mm). Otherwise, the load-displacement relationship was similar to that in the reference test.

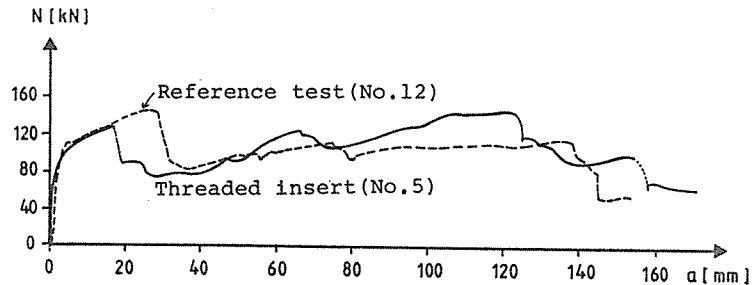


Fig. 7. Load-displacement relationships from the tensile tests. The effect of anchorage by an embedded threaded insert in the support.

The effect of anchorage by bond can be examined in Fig. 8 and Fig. 9. If the bolt at the top was anchored both by bond and a nut, and at the bottom by 300 mm bond only, the connection behaved quite similar to the reference. Compare test No. 6 with the reference, test No. 12, in Fig. 8. Thus, the anchorage in the support created by 300 mm bond only was sufficient in comparison with firm anchorage by means of an embedded nut. In another test, No. 8, the anchorage was arranged identically but the grout was of a porous type, type 2 according to Table 2. The behaviour of this connection showed up to be about the same as for the previous one. However, the splitting failure occurred for a rather big displacement, about 40 mm, see Fig. 8. When bond anchorage was arranged without providing the bolt with a nut at the top, test No. 7, the load-displacement relationship was quite different from the reference. The tensile force capacity was markedly reduced for large displacements as slipping occurred in

The test results show that a decrease in bolt prestressing force, down to the final value of 10 % of the design value, affects the ultimate capacity by no more than 15 %.

Approximately one third of the nail length can be used as an estimation of the permissible unevenness or rotation of the connection.

The toughness of the nail plate-bolt connection is good, the ultimate slip measuring many tens of a millimeter.

2.2 Dowel plate connection

The dowel plate connector is presented in Figs. 2 and 3. The principal difference in comparison with the nail plate connection is the need for drilled or cast-in holes for the dowels. Practically speaking, the steel plate in the dowel plate connection should also be thicker because of the larger bending moment due to the forces at the dowels. Typically, the thickness of the steel plate varies between 3 and 10 mm, the diameter of the dowels ranging from 12 to 16 mm. The necessary thickness of the steel plate can be calculated on the basis of the bending moment presented in Fig. 4.

The shear capacity, stiffness and toughness properties of the dowel plate connector are qualitatively of the same kind as those of the nail plate connector.

In order to avoid a change of the failure mechanism into a tension failure of the concrete cover, a necessary amount of reinforcement must be placed near the surfaces of the connecting concrete structures.

At the moving supports a limited movement in some direction is required at the connection. In that case, the dowel plate can be designed in order to allow for limited movements, as presented in Fig. 3. The holes of double steel plates are

2.1 Nail plate-bolt connection

The nail plate connection is built by means of the penetration of sharp nails into concrete, using the compression force brought about by the gravitational force of the structures or by the prestressing force of the bolts.

Several force-penetration curves are presented in Fig. 5. The required penetration limit is 2/3 of the nail length. The penetration force for each nail varies between 5 kN and 10 kN.

The increase in the number of nails decreases the penetration force for one nail.

The length of the nail may vary, the usual length being 5 mm.

The shear force-slip curve for the nail plate-bolt connection of a column corbel with four prestressed bolts 16 mm in diameter, and with four nail plates each including 24 nails, is presented in Fig. 6.

In the example presented in Fig. 6, the capacity with four bolts of diameter 24 mm and concrete strength $K = 50$ MPa corresponding to the capacity safety factor $\gamma = 1.7$ is about 310 kN.

As a rough estimation, the penetration force and the shear capacity of the nail plate connection have the same numerical value.

If the connection, as, e.g., in Fig. 6, has a bending moment, the bending moment capacity can be calculated by usual methods. The suitable prestressing force following anchorage, creep and shrinkage losses corresponds to the tensile force of the bolts under service loads.

In the tests, the sensitivity of the nail plate-bolt connection to variations in bolt prestressing force, to the rotation or unevenness of the connecting concrete surfaces, has been studied.

the bolt hole between the grout and the surrounding "beam" unit, see Fig. 8.

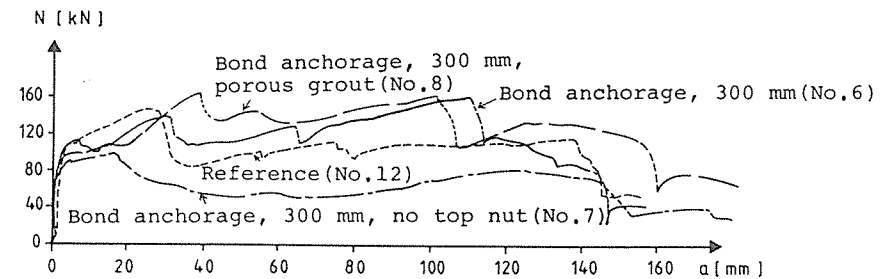


Fig. 8. Load-displacement relationships from the tensile tests. The effect of anchorage by bond.

In Fig. 9 another example of bond anchorage appears, test No. 9. The arrangement was the same as in the previous one, test No. 7, but the "beam" unit was reinforced according to type B in Fig. 3. The load-displacement relationship showed a higher residual capacity than for the test specimen with a "beam" unit of type A, test No. 7.

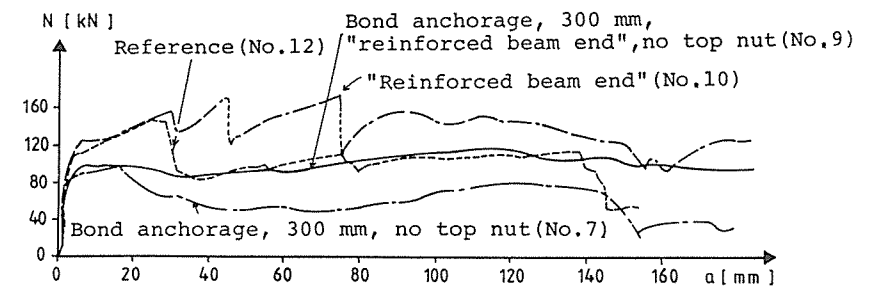


Fig. 9. Load-displacement relationships from the tensile tests. The effect of bond anchorage for a reinforced "beam" unit, type B.

The effect of bearings at the support appears from Fig. 10. Besides the reduced yield load due to the excentricity, the load-displacement relationships were similar to that in the reference test. However, when the bearing was from neoprene, test No. 13, the relationship showed up to be rather uneven in the residual stage.

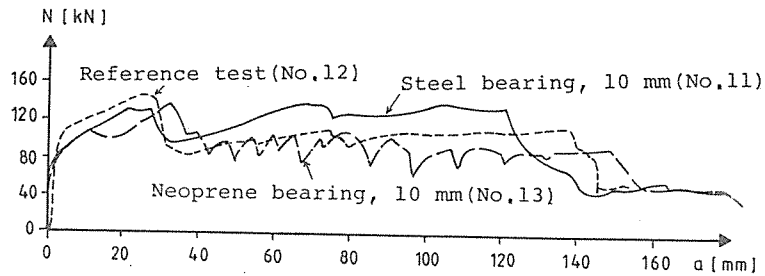


Fig. 10. Load-displacement relationships from the tensile tests. The effect of 10 mm bearings at the support.

3.2 Bending tests

Splitting failures never occurred in the bending tests and splitting cracks were never observed. The "beam" units seemed to be rotating at the support as rigid bodies. The ultimate failure was caused either by fracture of the bolt or loss of anchorage.

In the reference test, No. 22, the bolt fractured. The moment-rotation relationship appears from Fig. 11. In the same figure, it is possible to study the effect of an open, ungrouted bolt hole. In the latter case, test No. 29, the moment-rotation relationship was markedly less stiff before yielding was achieved.

2 PRINCIPLES OF THE CONNECTIONS

At the Technical Research Centre of Finland the dowel plate connection technique has been innovated and developed /1, 2, 3/. The following three types of dowel plate connection have been developed:

- Rigid nail plate-bolt connection (Fig. 1)
- Rigid dowel-plate or combined dowel plate-bolt connection (Fig. 2)
- Limited deformable dowel plate or-combined stud dowel plate-bolt connection (Fig. 3).

The functional role of the dowel plate is to take the shear force of the connection. The possible tensile forces are taken with high strength prestressed bolts. The force state at the dowel plate is presented in Fig. 4. The shear force between the concrete surfaces to be connected is moved out of the concrete surface into the steel plate, with shear nails or dowels, and again out of the steel plate into the other concrete surface. The shear force causes bending into the dowels and also through the dowels into the steel plate. The steel plate should therefore be stiff and sufficiently strong to take the integrated bending moment of the dowels.

The effectiveness of the dowel plate in comparison with the usual shear bars is based on the rigidity and moment capacity of the steel plate, which enables the effective shear resistance of the dowel connection (Fig. 4). The thickness of the steel plate depends on the forces and varies typically between 2 and 4 mm. The production advantage of this is that the structural elements can be made without any special outstanding ties or other connection details. For the dowel plate connections, the drilling of holes for bolts and duct dowels can be made as a supplementary measure after or during the hardening of concrete.

DEVELOPMENT OF DRY MECHANICAL CONNECTIONS

Asko Sarja
Technical Research Centre of Finland
Concrete and Silicate Laboratory
Espoo, Finland

1 NEED FOR DRY MECHANICAL CONNECTIONS

Winter construction together with the need for simplifying the stabilization of the structures and structural members as well as the possibility of demounting the structure without damaging structural members have all contributed to the need to develop the mechanical connections between the elements. The mechanical connection can be prepared quickly and without special workers. It is ready to function immediately once the parts are connected together, and it thus also acts as a fixing during erection. When the final connection is prepared by grouting, the use of the mechanical connection as an erection connection speeds up and facilitates the continuation of erection work.

When using the mechanical connection without grouting afterwards the demounting of the structures will be possible without damage to the elements. In the service state the mechanical connection is also flexible and allows the displacements due to the shrinkage, creep and temperature changes in elements.

During production, traditional types of connections often cause difficulties both in the element factory and on site. The main difficulties in the production by element factories are caused by connection ties and other connection details, such as column brackets. These details cause difficulties in moulding and particularly in the development of modern production such as extrusion and sliding techniques.

On site, the main disadvantage of current connections lies in the great need for labour and prolonged assembling times.

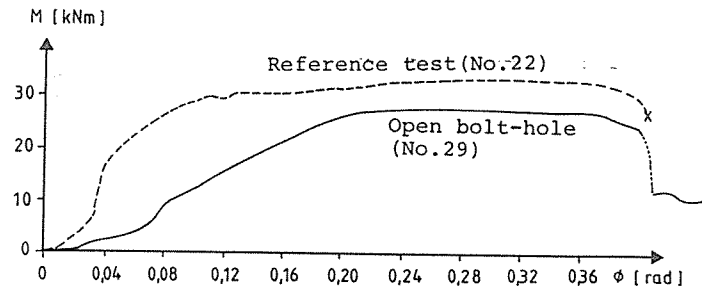


Fig. 11. Moment-rotation relationships from the bending tests. The effect of an open, ungrouted bolt hole.

In one of the bending tests the bolt was anchored in the support by an embedded threaded insert, test No. 24. This connection had apparently less deformability before the ultimate fracture of the bolt, see Fig. 12.

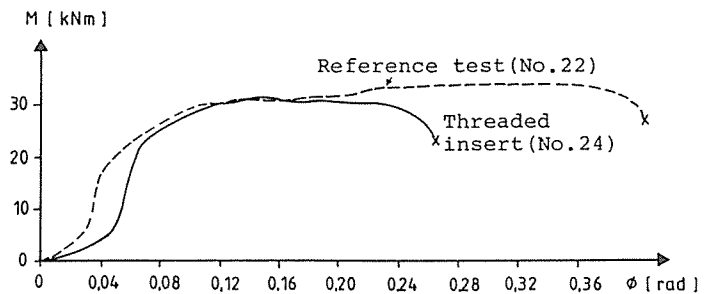


Fig. 12. Moment-rotation relationships from the bending tests. The effect of anchorage in the support by an embedded threaded insert.

The effect of anchorage by bond is illustrated in Fig. 13. In test No. 23, the bolt was anchored at the top

both by bond and a nut, and at the bottom by 70 mm bond only. The anchorage length at the bottom showed up to be insufficient and the bolt began to slip out of the support unit. However, the bolt could resist some tensile force by friction during this slippage. The friction effect decreased successively with increasing rotation. In another test, No. 25, the bolt was only anchored by bond, 450 mm at the top and 300 mm at the bottom. Now, the bolt was not provided with a nut at the top. Almost no bending moment capacity was achievable. When the rotation was forced on the connection slipping occurred in the bolt hole between the grout and the surrounding "beam" unit. The bolt with the grout was pulled out of the "beam" unit.

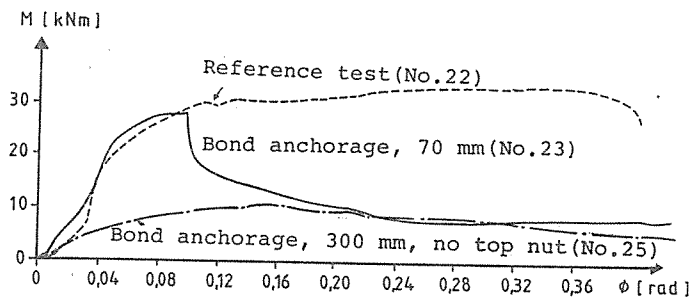


Fig. 13. Moment-rotation relationships from the bending tests. The effect of anchorage by bond.

Comparison between the reference test and a connection, test No. 26, provided with a 10 mm neoprene bearing at the support can be made in Fig. 14. For small rotations, the connection with the bearing could not transfer almost any bending moment at all. Bending moment capacity was not received until contact was established between the "beam" unit and the outermost edge of the support.

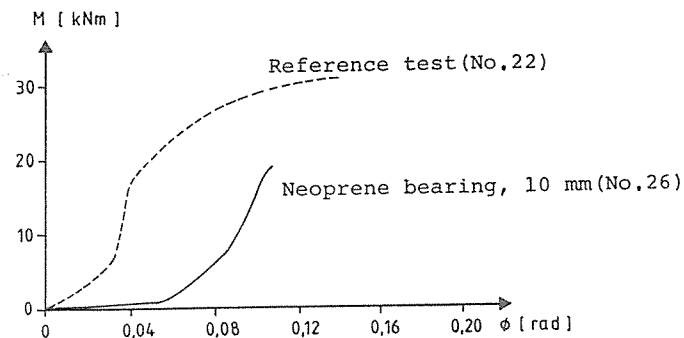


Fig. 14. Moment-rotation relationships from the bending tests. The effect of a 10 mm neoprene bearing at the support.

REFERENCE

Engström, Björn. Kraftöverförande anslutningar mellan förtillverkade betongelement - verknings-sättet hos balk-pelarslutningar med bultförbind-ning (Structural connections in precast buildings - The behaviour of bolted beam-column connections). Göteborg, Chalmers tekniska högskola, Avd. Betongbyggnad, Rapport 85:4, (ännu ej publicerad).